(41)

Evaluating and Utilizing Weak Interactions in Biologically Relevant Systems

by

Yoko Kato
B.A., Chemistry
Cornell University
Ithaca, NY

submitted to the Department of Chemistry in partial fulfillment of the requirements for the degree of

Doctor of Philosophy

at the
Massachusetts Institute of Technology
February 1996

Signature of Author.....
Department of Chemistry
January 3, 1996

Certified by.....
Professor Julius Rebek, Jr.
Thesis Supervisor

Accepted by.....
Professor Dietmar Seyferth
Chairman, Departmental Committee on Graduate Students

This doctoral thesis has been examined by a Committee of the Department of Chemistry as follows:

Professor S. Masamune .....

Chairman

Professor J. Rebek, Jr. .....

Thesis Supervisor

Professor S. L. Buchwald .....

EVALUATING AND UTILIZING WEAK INTERACTIONS IN BIOLOGICALLY RELEVANT SYSTEMS

by
Yoko Kato

Submitted to the Department of Chemistry on January 3, 1996 in Partial Fulfillment of the Requirements for the Degree of Doctor of Philosophy in Chemistry

ABSTRACT

Water soluble receptors for adenine derivatives were synthesized for the study of molecular recognition in aqueous solution. Each modular receptor makes use of hydrophobic interactions, Watson-Crick and Hoogsteen hydrogen-bonding, and phosphate-guanidinium electrostatic interaction to bind cyclic adenosine monophosphates. Association constants with adenine derivatives were measured in aqueous solution, then converted to free energies of association. Comparison of these energy values allowed evaluation of phosphate-guanidinium salt-bridge interactions, hydrogen bonding and hydrophobic interactions in aqueous media.

Binding affinities of 2',3'-cAMP and 3',5'-cAMP with the water soluble receptors were determined at 51 mM and 501 mM ionic strength (H_2O/D_2O solution at 10 °C, pH 6.0). The phosphate-guanidinium interaction in this system is estimated to contribute on average 0.6 kcal/mol (51 mM ionic strength) and 0.3 kcal/mol (501 mM ionic strength) to binding. The maximum value of a phosphate-guanidinium electrostatic interaction is estimated to be 2.4 kcal/mol in water.

Association constants between 9-ethyl adenine and *mono*(imide)carbazole, *mono*(imide)naphthalene, or *bis*(imide)carbazole receptors were measured in aqueous solution at five different temperatures from 3-27 °C (pH 6, 51 mM ionic strength). The free energy at 298 K of a single hydrogen-bond is estimated to be only 0.2 kcal/mol. The enthalpy of a single hydrogen bond in this solvent-exposed system is estimated to be at most 0.8 kcal/mol indicating that enthalpy barely compensates for the unfavorable entropy in this system. These values reflect stronger hydrophobic interactions with the more-polarizable naphthalene as well as enthalpy-entropy compensation effects.

A conformationally locked diacid and acid-amide having the ability to form normal or short hydrogen bonds were studied in non-polar organic media. NMR analysis confirmed the formation of a low-barrier hydrogen bond (LBHB) in the monodeprotonated diacid (a symmetrical carboxyate-acid pair), but showed a conventional hydrogen bond was formed in the corresponding state of the acid-amide (a carboxylate-primary amide pair). The equilibrium constants for the deprotonation of the two systems with organic bases were determined. Their comparison allowed an assessment of the extra stabilization energy arising from the formation of a LBHB: the free energy differences at 25° C were -2.4 kcal/mol in benzene and -1.4 kcal/mol in CH_2Cl_2.

Acid-imidazoles capable of forming intramolecular hydrogen bonds were synthesized. ^1H NMR analysis suggested formation of a LBHB in the acid-methylimidazole molecule. However, these systems could not be well-characterized due to complications from multiple conformations.

The design of the adenosine receptors was exploited to develop water soluble 5'-AMP and ApA binders and a library of nucleotide receptors. The limited water solubility of all receptors prevented thorough analysis of these systems. Organic soluble ApA receptors were synthesized and used for membrane transport studies of nucleotides.

Thesis Supervisor: Dr. Julius Rebek, Jr.
Title: Camille Dreyfus Professor of Chemistry

to

my parents

ACKNOWLEDGMENTS

I am sincerely grateful to Prof. Julius Rebek for giving me continuous encouragement, timely advice and freedom to develop my own working style. His fascinated expression when discussing chemistry helped me recover from low points in my research and taught me how research can be exciting and rewarding. I hope to build on what I have learned from this group and continue this group's legacy of creative research.

My former advisor, Prof. Jon Clardy, is responsible for giving me the initial opportunity to work in a chemistry research group. I greatly appreciate his generous and continued guidance via e-mail especially during my early years at MIT. I thank Prof. Bruce Ganem and his group for cultivating my interest in organic chemistry and equipping me with some basic laboratory skills to function comfortably in graduate school.

The work described in this thesis has been made possible with the direct and/or indirect help from many knowledgeable postdocs and graduate students in the Rebek group. In chronological order, my first mentor was Dr. Kobiro. Although we were baymates for only a few months, his valuable advice starting from basic lab techniques to the synthesis of intermediates leading to the cAMP receptor set me on the right track in a laboratory of overwhelmingly vast opportunities. Bettina patiently showed me how to perform NMR titrations for water-soluble molecules; a technique which I relied on for a significant portion of my work. Dr. Murray's efforts to extend the group's understanding of association constants and analysis of NMR titration data certainly influenced my analysis and determination of titration data. Morgan, my mentor and collaborator in the aqueous recognition projects always amazed me with his ability to critically and extensively analyze data, and taught me how to think about and present results. His discovery of water soluble mono(imide)carbazole molecule was critical for hydrogen bond analysis in water. Cecilia diligently performed all the nucleotide transport studies. The behavior of bis(imide)naphthalene with adenine in water was too complex; however, Belinda's attempt at analysis is greatly appreciated. Leticia, who has empowered our group with her expertise in crystallography, performed the single crystal X-ray diffraction analysis. Her fascination and enthusiasm towards chemistry has been refreshing and admirable.

I also enjoyed working with my baymates, René W., Jongmin, Rob M. and creative Ed who has, for the past two years, entertained me by harmonizing to the radio. I also thank all the past and present members of the Rebek group, especially Robert G., Blake, Ken, Jerry, Roland M., Dr. Oi, Dr. Azumaya, Mike, Carina, Chris, Kent and Brendan for encouragement, helpful discussions and even criticism on my projects. Outside the Rebek group, I thank my 'big sister' Laura, for always being a there to listen to me. I value the lively discussions over coffee with Larry, a wonderful friend and classmate. Dr. Tohma has helped me a lot in reestablishing my ties to Japan. I am grateful for our friendship and his continual encouragement.

My grandparents have supported me all along through thoughtful letters and beautiful poems. Last but not least, I thank my parents for investing a lot in my education (including those science, math and Japanese homework during summer vacation), being tremendously understanding, unconditionally supportive and giving me the freedom to pursue my own interests.

TABLE OF CONTENTS

SYNTHETIC SCHEMES

LIST OF FIGURES

LIST OF TABLES

A. EVALUATION OF WEAK INTERACTIONS IN WATER

1. INTRODUCTION

Complementarity of size, shape and chemical surface provide much of the driving force for molecular recognition phenomena, yet allocating the binding affinities to individual weak intermolecular interactions is difficult. For example, with biological molecules, site-directed mutagenesis has been used to obtain hydrogen bonding contributions in the context of enzyme-substrate and enzyme-transition state complementarity.[1-4] The peptide-binding vancomycins have likewise been used,[5,6] and have yielded new insights to the contributions of entropic effects.[7] Intramolecular hydrogen bond strengths between Gln and Asp side chains of peptide helices have been studied,[8] and newly developed unnatural amino acid replacement techniques have also been employed to evaluate the strengths of hydrogen bonds in peptides.[9,10]

With smaller synthetic receptors, rational design of hosts with directional interactions, such as complementary hydrogen-bonding arrays, have been studied extensively in aprotic organic solvents.[11-13] Adenine has been a particularly well-studied target for hydrogen bonding and aromatic stacking in such less competitive organic media.[13-22] On the other hand, recognition in aqueous media has utilized non-directional hydrophobic and ionic interactions coupled with specificity induced by shape and size.[12,23-36] Binding of adenine in water has not been studied as extensively as in organic solvents and introduces new challenges. In water, effects of hydrogen-bonding are considerably diminished, electrostatic interactions are dampened and hydrophobic interactions such as π-stacking are maximized.[34,37-39] Large rigid aromatic surfaces become good candidates for host molecules in aqueous media, however such molecules are quite insoluble and require attachment of solubilizing functionalities. Further consideration is that hydrophobic interactions do not have specificity and that the receptor must be carefully designed to position hydrogen bonding sites where they will be favored over non-specific hydrogen bonding to the solvent molecules. The solvent, water, itself also necessitates additional considerations such as pH and ionic strength.

The logical approach was to initially optimize the cleft geometry in organic solvents, then modify it to obtain an aqueous-soluble version. Efficient organic-soluble adenine derivative binding clefts had been designed and tested in this laboratory. This group has also developed a system for the recognition of adenine in aqueous media.[39] Drawing from these, water soluble adenine derivative receptors were synthesized and used to evaluate the energetic contribution of electrostatic interactions and hydrogen bonding in water.

2. EVALUATION OF A PHOSPHATE—GUANIDINIUM SALT BRIDGE IN WATER

The bulk of this section has previously appeared in print.[40]

Salt bridge is one of the important interactions observed between nucleic acids and proteins. Guanidiniums seem efficient at forming salt bridges to oxyanions[19,41-54] as evidenced by the phosphate backbone of the nucleic acids forming salt bridges to the guanidinium group of arginine, as well as to the primary ammonium group of lysine.[55] Accordingly, the energy contribution of such interaction is of great interest. The energetics of such charged hydrogen bonds have been previously investigated by mutagenesis studies with proteins. However, the environment of a protein interior is different from a much more solvent exposed aqueous solution and could be said to be more similar to the environment of an organic solvent. There has been studies by Schneider on energies of electrostatic interactions in water,[12,28-31,33] however, there are not too many studies on guanidinium salt bridges (involving hydrogens)[45,51-53] in aqueous solution.

The adenine and cAMP recognition systems previously developed in the group[15,47,56-58] were good candidates for investigating the phosphate-guanidinium salt bridge interaction in water if the receptors could be solubilized in water . The bicyclic guanidinium fragment used in the organic soluble cAMP receptor has been previously utilized by others[19,42-45,59] and has shown effective phosphate binding in water.[45] Thus, water soluble cAMP receptor **A1** and adenosine receptor **A2** were synthesized and used to evaluate the contribution of salt bridges to the binding of cyclic adenosine phosphates..

The adenine-binding module of receptors **A1** and **A2** combines the 3,6-diaminocarbazole spacer, previously described,[46,47,57] with the water-soluble version of the Kemp's triacid imide.[39] The concave surface of this module chelates the purine nucleus of adenine through simultaneous Watson-Crick and Hoogsteen hydrogen-bonding and aryl stacking.[57] Introducing a phenyl group on N-9 of the diaminocarbazole offers increased hydrophobic contacts, decreased conformational flexibility, and increased ester stability in hydroxylic media.

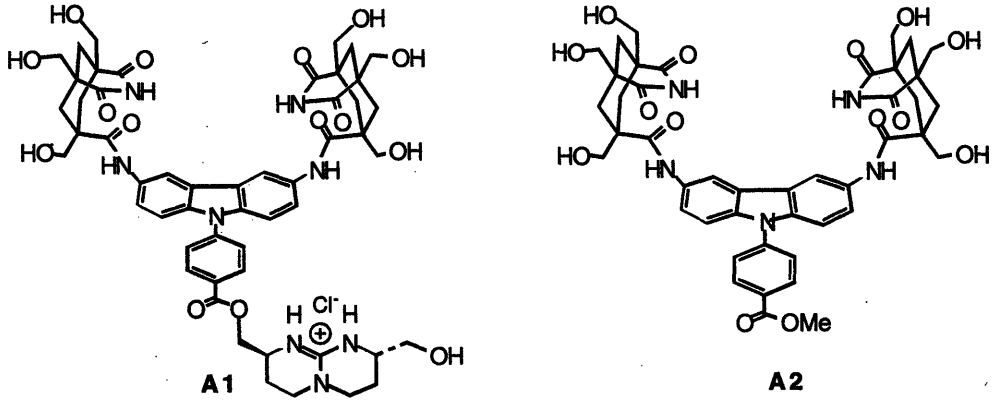

Figure A1. Water soluble cAMP and adenine receptors.

The receptors were assembled as outlined in Schemes A1 to A3. The water-soluble derivative of Kemp's triacid imide (**A5c**) was prepared as described previously (Scheme A1).[39] Monodeprotection of bicyclic guanidinium **A6**[59] proceeded quantitatively under mild conditions to give alcohol **A7** (Scheme 2). The scaffolding for receptors **A1** and **A2** was assembled by Ullmann-type coupling[60] of carbazole and methyl 4-iodobenzoate (**A8**).

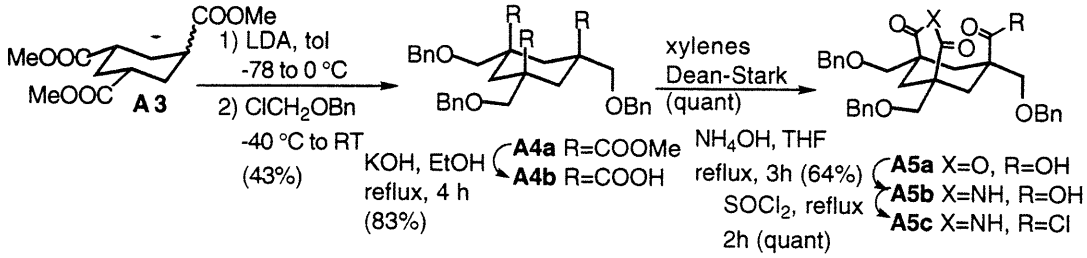

Scheme A1.

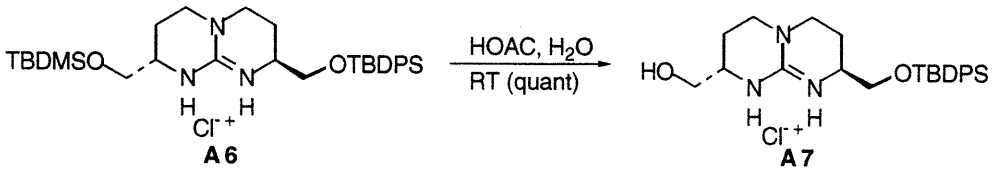

Scheme A2.

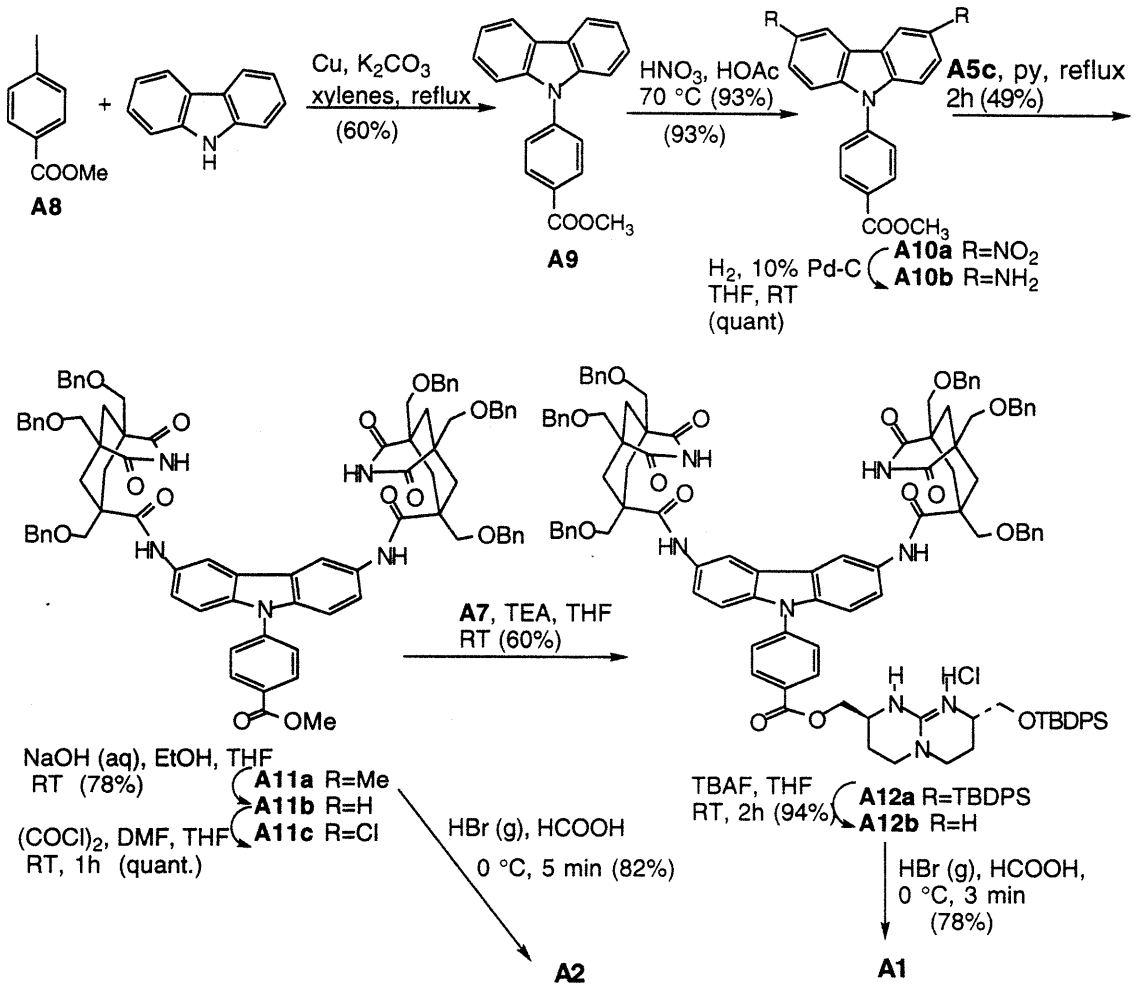

Scheme A3.

Nitration of **A9** with nitric acid proceeded easily in warm acetic acid to give dinitro **A10a**. Diamine **A10b**, generated by hydrogenation in THF, was air-sensitive and was immediately acylated with imide acyl chloride **A5c** to generate the benzyl-protected **A11a**. Deprotection of this with gaseous HBr in HCOOH gave cleft **A2**. Hydrolysis of **A11a**, followed by conversion to the acyl chloride (**A11b**) gave protected **A12a** after reaction with alcohol **A7**. This product contained some **A11b** as an inseparable impurity that could be removed only after deprotection of **A12a** to the free alcohol (**A12b**). Debenzylation with gaseous HBr yielded pure phosphate-binding cleft **A1** after ion-exchange chromatography.

The binding free energies were determined by ^{1}H NMR titration (Table A1). The downfield shift (from 10.4 to 12.5 ppm) of the exchangeable imide proton was monitored during constant-host titration of the receptors (0.3-0.5 mM) with the adenosine derivatives (30 mM or 150 mM for 9-ethyladenine) at ionic strength (I) of 51 and 501 mM (NaCl) under conditions previously described.[39] The interaction between the cacodylate buffer and **A1** was considered negligible since no proton shift of the dihydroxy-bicycloguanidinium was observed on the NMR upon varying cacodylate concentration. Haake *et al.* have also shown that free guanidinium ($CH_6N_3^+$) and free phosphate ($H_2PO_4^-$) have an association constant of only 1.37 M^{-1} in water.[61] Furthermore, titration of **A1** and 2',3'-cAMP using bis-tris buffer instead of cacodylate gave a binding constant only 1.5% higher than that using cacodylate buffer. This difference is clearly within experimental error (10%). Reduced pH and temperature served to sharpen the signal due to the imide protons by reducing the rate of chemical exchange with water. The water signal was suppressed using a $1\bar{3}3\bar{1}$ binomial pulse.[62,63] Association constants were obtained by non-linear leastsquares regression analysis and converted to free energies, ΔG^{283}. The binding constants were reproducible to within 10%. The statistical uncertainty in the curve fitting procedure varied from 2-17% at the 95% confidence level. When propagating error through the calculations though, the uncertainty was taken to be no less than 10%. For the charged guests with negligible dimerization constants (*i.e.* cAMP's), a simple 1:1 binding model was used.[64] For adenosine and 9-ethyladenine, guest dimerization was incorporated into the 1:1 binding model. Incorporation of this additional equilibrium into the 1:1 binding isotherm gives the following non-linear multivariable expression:

$$G_t = H_t\left(\frac{\delta-\delta_H}{\delta_{HG}-\delta_H}\right)^3+\left(\frac{2K_d}{Ka^2}-G_t-2H_t+\frac{1}{Ka}\right)\left(\frac{\delta-\delta_H}{\delta_{HG}-\delta_H}\right)^2 + \left(2G_t+H_t+\frac{1}{Ka}\right)\left(\frac{\delta-\delta_H}{\delta_{HG}-\delta_H}\right) \qquad \text{(A1)}$$

where G_t and H_t are the total concentration of guest and host at each titration point; K_d and K_a are the dimerization and 1:1 association constants, respectively; and δ, δ_H, and δ_{HG} are respectively, the observed, free host, and complex chemical shifts.

The dimerization constant of 9-ethyladenine was determined at both 51 mM (11 M^{-1}) and 501 mM (16 M^{-1}) ionic strength. The respective values were incorporated into the binding constant determinations with 9-ethyladenine at both ionic strengths. The dimerization constant of adenosine was determined only at 51 mM. Moderate to high binding constants show only small changes with small variations in dimerization (confirmed with 9-ethyladenine data) and significantly lower concentrations of adenosine were used in titrations. The 5.2 M^{-1} value was used in the determination of binding constants at both 51 mM and 501 mM.

Receptor **A2** shows nearly identical affinity to all four adenine derivatives with only slightly lower (0.03 - 0.08 kcal/mol) affinity at higher ionic strength. This reflects the sum of contributions from hydrogen-bonding and hydrophobic stacking with the purine nucleus, as well as the relative insensitivity of these forces to ionic strength. The similar affinity for 9-ethyladenine and adenosine shown by receptors **A1** and **A2** indicates that there is little or no interaction between the guanidinium and the hydroxyl groups of adenosine. With 2',3'- and 3',5'-cAMP, the phosphate-guanidinium interaction leads to significant (I = 51 mM) or moderate (I = 501 mM) increase in binding affinity (2',3'- and 3',5'-cAMP with **A1**, Table A1).

Table A1. Energy of binding between receptors and adenosine derivatives.

		K_a (M^{-1}) ± % uncertainty		ΔG^{283} (kcal/mol)	
receptor	guest	I = 51 mM	I = 501 mM	I = 51 mM	I = 501 mM
A1	9-ethyladenine	200 ± 6%[a]	180 ± 10%[b]	-2.98 ± 0.06[a]	-2.92 ± 0.06[b]
	adenosine	150 ± 5%[c]	130 ± 10%[c]	-2.82 ± 0.06[c]	-2.74 ± 0.06[c]
	2',3'-cAMP	660 ± 17%	330 ± 9%	-3.65 ± 0.10	-3.26 ± 0.06
	3',5'-cAMP	600 ± 6%	320 ± 3%	-3.60 ± 0.10	-3.24 ± 0.06
A2	9-ethyladenine	190 ± 4%[a]	180 ± 7%[b]	-2.95 ± 0.06[a]	-2.92 ± 0.06[c]
	adenosine	150 ± 13%[c]	140 ± 14%[c]	-2.82 ± 0.07[c]	-2.78 ± 0.08[c]
	2',3'-cAMP	190 ± 3%	180 ± 2%	-2.95 ± 0.06	-2.92 ± 0.06
	3',5'-cAMP	250 ± 6%	220 ± 9%	-3.11 ± 0.06	-3.03 ± 0.06

[a]A 9-ethyladenine dimerization constant of 11 M^{-1} was incorporated into the calculation. [b]A 9-ethyladenine dimerization constant of 16 M^{-1} was incorporated into the calculation. [c]An adenosine dimerization constant of 5.2 M^{-1} was incorporated into the calculation.

Molecular modeling studies performed by Dr. M. Morgan Conn indicated that the lowest energy conformation of the complex of **A1** and 2',3'-cAMP features a hydrogen bond between the hydroxyl proton (exocyclic to the guanidinium) and phosphate and a coplanar arrangement of the two delocalized charges at the phosphate and guanidinium. That is, hydrogen-bonding can occur between the guanidinium protons and phosphate oxygens in addition to an electrostatic interaction (Figure A2). Conversely, the corresponding complex of **A1** and 3',5'cAMP (Figure A3) suggests a perpendicular geometry between the two planes of delocalized charge, enabling electrostatic interactions but precluding a hydrogen-bonding interaction of a salt-bridge sort.[65]

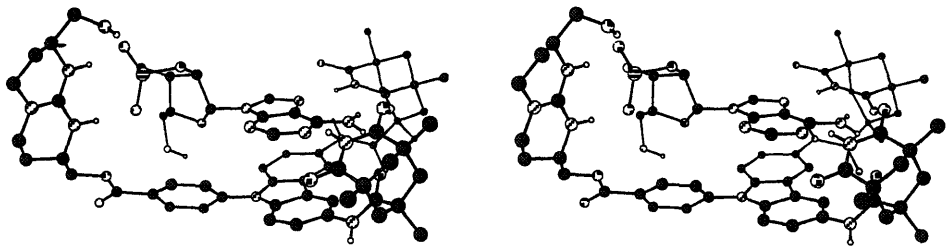

Figure A2. Predicted lowest energy conformation of the complex between **A1** without the hydroxyl groups and 2',3'-cAMP in cross-eyed stereoview. Hydrogens attached to carbon have been omitted for clarity.

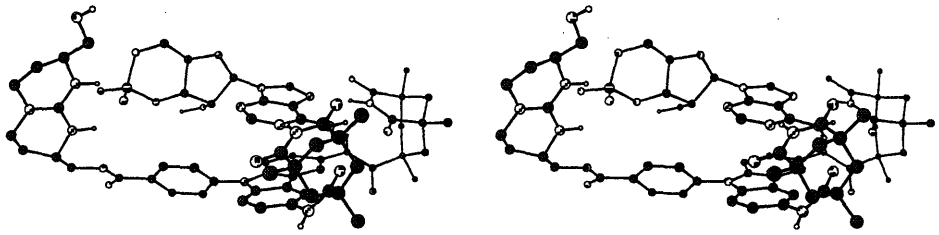

Figure A3. Predicted lowest energy conformation of the complex between **A1** without the hydroxyl groups and 3',5'-cAMP in cross-eyed stereoview. Hydrogens attached to carbon have been omitted for clarity.

The individual contribution of this electrostatic interaction can be approximated through the use of the following thermodynamic cycle:

$$\begin{array}{ccc} \textbf{A2} + \text{Adenosine} & \xrightarrow{\Delta(\Delta G)^{2}_{phos}} & \textbf{A2} + \text{cAMP} \\ \Big\downarrow \Delta(\Delta G)^{Ad}_{guan} & & \Big\downarrow \Delta(\Delta G)^{cAMP}_{guan} \\ \textbf{A1} + \text{Adenosine} & \xrightarrow{\Delta(\Delta G)^{1}_{phos}} & \textbf{A1} + \text{cAMP} \end{array} \qquad \text{(A2)}$$

where each $\Delta(\Delta G)$ is the free energy difference associated with an alteration in the host-guest composition. The free energy change associated with the guanidiniumphosphate interaction alone can be derived from this cycle according to eq A3.

$$\Delta(\Delta G)_{\text{phos-guan}} = \Delta(\Delta G)^{1}_{phos} - \Delta(\Delta G)^{2}_{phos} = \Delta(\Delta G)^{cAMP}_{guan} - \Delta(\Delta G)^{Ad}_{guan} \qquad \text{(A3)}$$

This gives energies for phosphate-guanidinium interactions alone in aqueous solution at pH 6.0 and 10 °C (Table A2) which show that the 2',3'-cAMP complex compared to 3',5'-cAMP complex has a 0.2 kcal/mol stronger interaction at either ionic strength. The molecular modeling studies indicated that there could be up to

three additional hydrogen bonds in the complex of **A1** with 2',3'-cAMP. This suggests that the strength of a charged hydrogen-bond exposed in water is lower than previously obtained in protein mutagenesis studies[1] (0.5-1.5 kcal/mol for neutral-neutral hydrogen bonds and 3-5 kcal/mol for neutral-charged hydrogen-bonds). It should be noted that these values are indeed generalized values for interactions in free solution, in contrast to protein mutagenesis studies where there are complications from altered backbone geometry, context-specific effects, and the non-aqueous environment of a protein interior. These values are also in good agreement with Schneider's values for exposed ionic interactions between ammonium ions and various oxyanions in water. When his values are converted to 51 mM, 283 K, each ionic interaction in Schneider's system contributes 0.8 kcal/mol toward binding.

Table A2. Free energy change for the phosphate-guanidinium interaction at different ionic strengths, accurate to ±0.1 kcal/mol

	$\Delta(\Delta G)$phos—guan	
guest	at I = 51 mM	at I = 501 mM
2',3'-cAMP	-0.7 kcal/mol	-0.4 kcal/mol
3',5'-cAMP	-0.5 kcal/mol	-0.2 kcal/mol

By considering the complex between **A1** and 3',5'-cAMP, an estimate of the energy of a phosphate-guanidinium electrostatic interaction alone can be derived. According to the analyses of Williams,[5,6,66-68] based on the pioneering work of Jencks and Page,[69,70] the phosphate-guanidinium interaction can be considered as a combination of energy factors arising from intermolecular translational and rotational entropy (T+R), restriction of rotors (r), hydrophobicity (h), polar interactions (p), conformational strain (conf) and van der Waals interactions (vdW). Thus,

$$\Delta(\Delta G)_{\text{phos-guan}} = \Delta\Delta G_{\text{T+R}} + \Delta\Delta G_{\text{r}} + \Delta\Delta G_{\text{h}} + \Delta\left(\sum \Delta G_{\text{p}}\right) + \Delta\Delta G_{\text{conf}} + \Delta\Delta G_{\text{vdW}} \qquad \text{(A4)}$$

By virtue of the similarity of the two substrates involved in the comparison, adenosine and cyclic adenosine monophosphate, the terms associated with bimolecular association, hydrophobicity, conformational strain, and van der Waals interactions can all be estimated to have a negligible contribution to the interaction (*i.e.* $\Delta\Delta G_{\text{T+R}}$, $\Delta\Delta G_{\text{h}}$, $\Delta\Delta G_{\text{conf}}$, $\Delta\Delta G_{\text{vdW}} \approx 0$). The factorization, then, is represented by equation A5.

$$\Delta(\Delta G)_{\text{phos-guan}} = \Delta\Delta G_{\text{r}} + \Delta\left(\sum \Delta G_{\text{p}}\right) \qquad \text{(A5)}$$

In the complex between **A1** and 3',5'-cAMP, there are two bond rotors (the guanidinium exocyclic C—C and C—O bonds) that are constrained relative to the complex with adenosine. The cost of restricting a single rotor through non-covalent interactions has been estimated as 0.9 ± 0.2 kcal/mol.[71] So, the phosphate-guanidinium interaction can be estimated to contribute up to a *maximum* of 2.4 ± 0.2 kcal/mol at 51 mM ionic strength (or 2.1 ± 0.2 kcal/mol at 501 mM ionic strength). If either of these rotors is restricted in the uncomplexed state or not confined in the complexed state, then this value will be accordingly lower.

In conclusion, a highly organized synthetic receptor binds cyclic adenosine monophosphates through a combination of hydrophobic, electrostatic, and hydrogen-bonding forces. Assuming these effects act independently, the phosphate-guanidinium interaction in this system is calculated to contribute, on average, 0.6 kcal/mol (I = 51 mM) and 0.3 kcal/mol (I = 501 mM) to binding. The enthalpy of such an electrostatic interaction in water alone is estimated to be no more than 2.4 kcal/mol.

3. EVALUATION OF A HYDROGEN BOND IN WATER

The bulk of this section has previously appeared in print.[72]

Hydrogen bonds have functional properties that are essential for life processes.[73] Naturally, a large number of studies have been conducted to further understand this interaction in that context. Enzyme studies have yielded stabilization energies of 0.5-1.8 kcal/mol for a neutral hydrogen bond.[3] Studies using vancomycins[67] gave values of 2.8-6.2 kcal/mol, a somewhat larger value; helical peptide studies[8] have given a smaller value of 0.4 kcal/mol; unnatural amino acid replacement studies[9,10] indicated 1.5-2.0 kcal/mol per hydrogen bond. The common feature among these examples is that the hydrogen bond is not completely solvent exposed.

Hydrogen bonds in water exposed environments are also important, and several synthetic receptors have been developed to address such issues. Water-soluble receptors for nucleic acid components have given a measure of ionic interactions and salt bridges[29,33,34,40] (i.e., charged hydrogen bonds) and permits now a direct assessment of uncharged hydrogen-bonding in water.

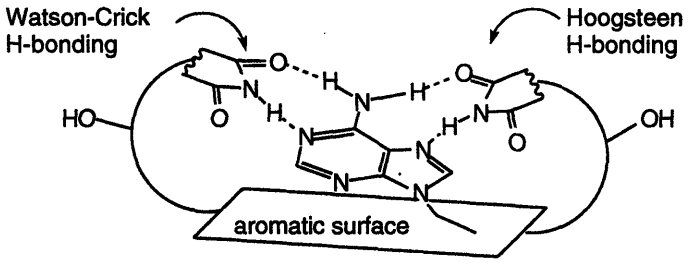

Figure A4. Basic design for a water-soluble adenine receptor.

The structures involve Kemp's triacid derivatives, outfitted with imides and stacking surfaces for complementarity to the purine nucleus of adenines (Figure A4). Peripheral hydroxyl groups impart water solubility. Dr. Brian A. Murray had previously synthesized and attempted to investigate the behavior of carbazole *mono*(imide) and *bis*(imide) derivatives shown in Scheme A4. Unfortunately, the *mono*(imide) derivative was unreasonably insoluble in water for any NMR study and prohibited further investigation of these systems.

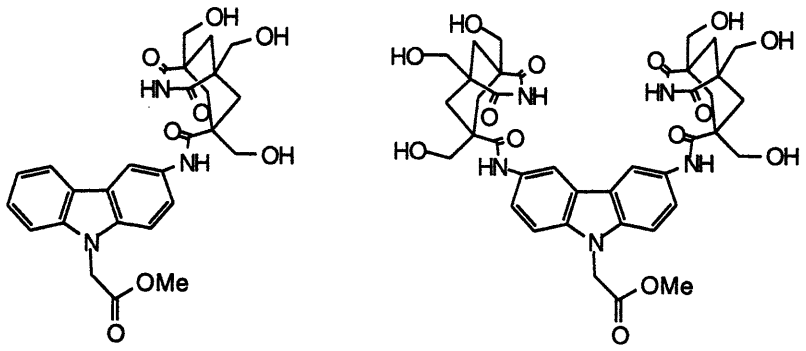

Scheme A4.

Dr. M. M. Conn found that replacement of the methyl ester to a propyl amide greatly enhances the water-solubility of the carbazole receptors. We have now prepared a soluble carbazole *mono*(imide) derivative **A13** and *bis*(imide) **A14** for comparison with the naphthyl *mono*(imide) **A15** and *bis*(imide) **A16** (Scheme 5), following well-trodden paths[39,40] (Scheme A6-A8). Receptor **A13** binds adenines similarly to **A15**, but provides a different hydrophobic platform. The arrangement of imides in receptor **A14** is known to chelate adenines in organic solvents through simultaneous Watson-Crick and Hoogsteen base-pairing modes with high binding affinities ($K_a > 10^5\ M^{-1}$), dominated by hydrogen bonding.[57] In contrast, hydrophobic effects contribute most of the affinity of related imide-receptors for adenine in water,[39,40] and overwhelm the hydrogen bonding component.

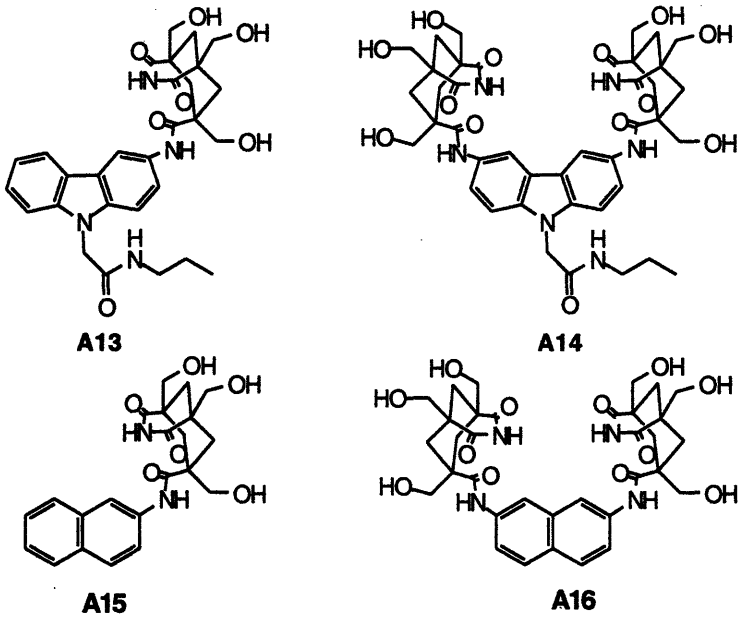

Scheme A5.

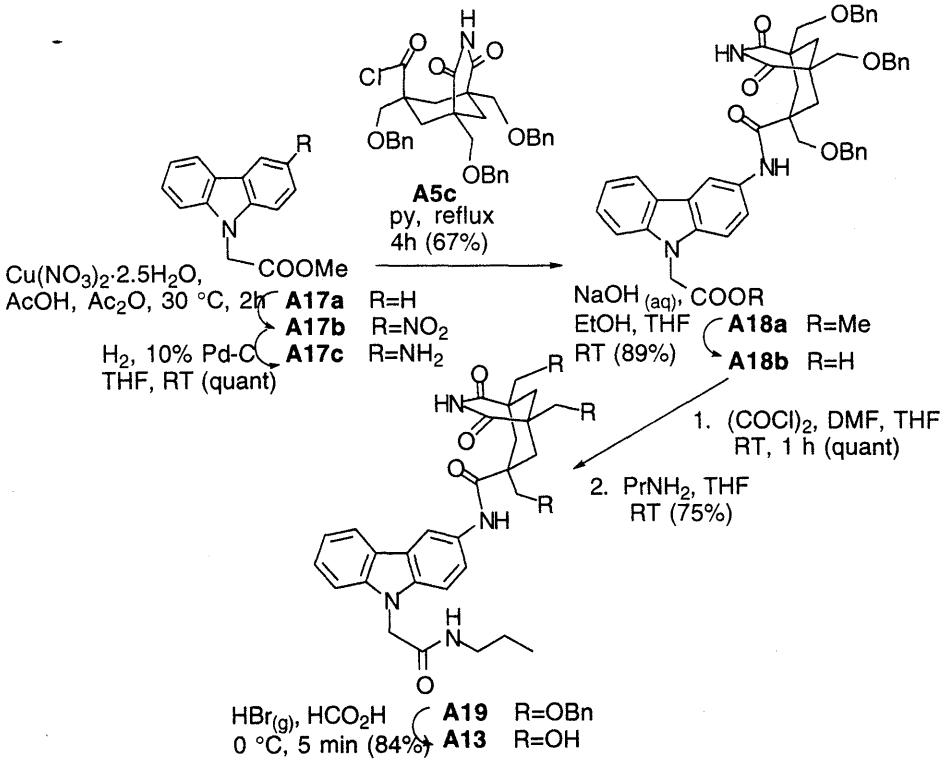

Scheme A6.

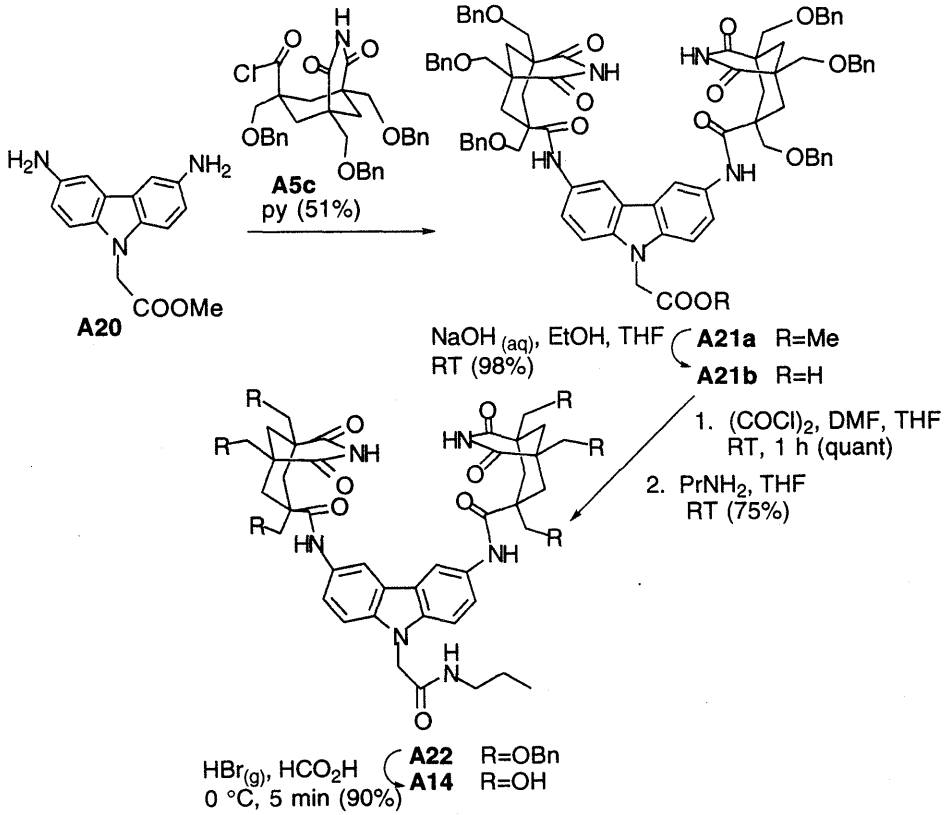

Scheme A7.

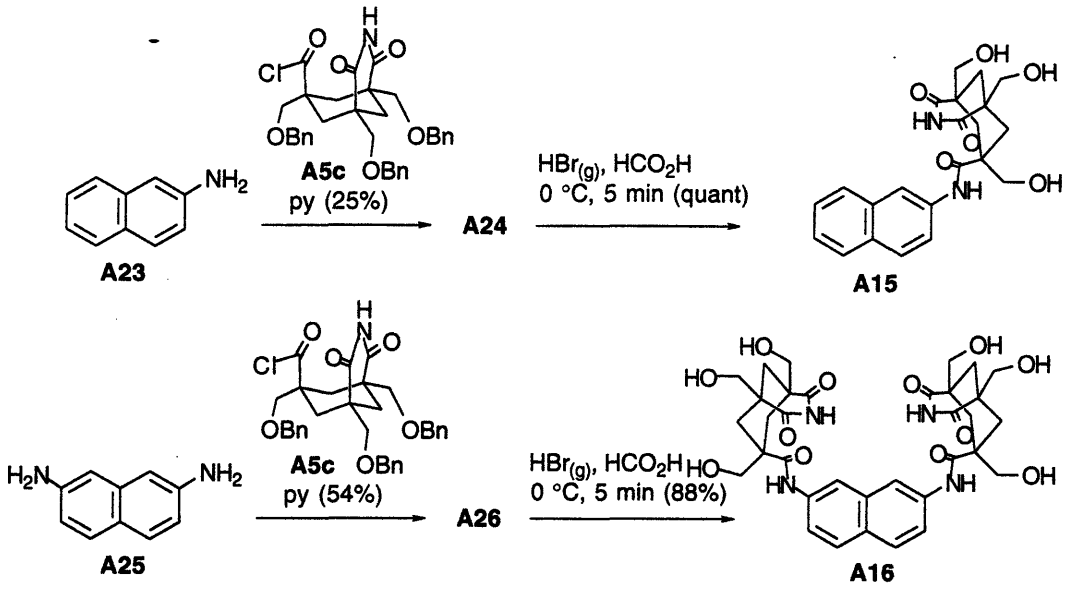

Scheme A8.

Titrations of 9-ethyladenine with the receptors were performed at five different temperatures from 3-27 °C at pH 6 (cacodylate buffer) and ionic strength of 51mM (NaCl), monitoring the imide proton shift as described previously.[40] Van't Hoff (1/T vs. lnK) analysis was used to determine enthalpic and entropic contributions to binding. Comparing these thermodynamic parameters, interactions involved in binding 9-ethyladenine, particularly hydrogen bonding, in a solvent exposed environment were studied.

Results and Discussion

The stoichiometry of the complex between **A14** and 9-ethyladenine was determined to be 1:1. The naphthalene based *bis*(imide) **A16** showed a non-chelating 2:1 binding mode in addition to 1:1 binding. Accordingly, this system was not further characterized. The titration results are summarized in Table A3.

Table A3. Association constants of the receptors with 9-ethyladenine and enthalpy and entropy of binding determined from Van't Hoff plots.

	Ka (M^{-1}) with 9-ethyladenine*						ΔH	ΔS	ΔG^{298}
	3 °C	9 °C	10 °C	15 °C	21 °C	27 °C	(kcal/mol)	(cal/mol·K)	(kcal/mol)
A13	49±6	—	36±4	30±4	25±4	21±2	-5.8	-13	-1.9
A14	79±6	—	62±3	45±4	35±2	28±2	-7.4	-18	-2.0
A15	44±4	26±2	—	18±1	14±1	10±1	-9.2	-26	-1.5

*9-ethyladenine dimerization constants of 13.9, 9.51, 8.8, 6.47, 4.60, 3.05 M^{-1} at 3, 9, 10, 15, 21, 27 °C respectively were incorporated into the calculation. The uncertainties are at the 95% confidence level.

The values of association constants at 10 °C when compared with other water soluble adenine receptors[39,40] show that the recognition elements within these receptors are focused on the purine nucleus and involve a combination of hydrogen bonding and aryl stacking forces. Comparison of the results for the naphthyl, fluorenyl,[39] and carbazolyl surfaces indicates that the amide side chain of the latter is not involved in a direct contact with adenines.

The $\Delta\Delta H$ provided by the *bis*(imide) system is -1.6 kcal/mol. This is the net difference between the strength of the newly formed hydrogen bonds in the complex and in the bulk solvent, and the lost hydrogen bonds of the free receptor and purine with the solvent (no net change in the number of hydrogen bonds occurs). Since receptors **A13** and **A14** are expected to have identical hydrophobic overlap with the bound adenine, the enhanced binding is primarily due to the two additional hydrogen bonds present in the complex between 9-ethyladenine and **A14**. Thus, the enthalpy per hydrogen bond in water can be estimated to be 0.8 kcal/mol per hydrogen bond in the adenine receptor complex.

The entropy difference seen in the *bis*(imide) system is -5 cal mol^{-1} K^{-1}. The favorable liberation of bound water is opposed by the loss of entropy in fixing the amide rotors in one of two equally probable positions[56] (convergent vs. divergent imides)[14] and fixing the purine nucleus into a more confined cleft. Statistically, restricting the amide rotor into one of the two equally probable conformations is expected to contribute $-R\ln(1/2) = 1.3$ cal mol^{-1} K^{-1} to entropy of binding.[74] When two imides chelate the adenine, hydrogen bonds and stacking are probably more effective in reducing the low frequency vibrations of 9-ethyladenine relative to the receptor within the complex. The remaining -3.7 cal mol^{-1} K^{-1} is expected to come from a tighter fit resulting in **A14** than in the *mono*(imide) **A13**. Thus, ΔH just compensates for the unfavorable ΔS and gives a small ΔG^{298} of 0.2 kcal/mol for a single hydrogen bond in this solvent-exposed system.

$$\Delta G^{298} = [-1.6 - (298)(-3.7)] / 2 = 0.2 \text{ kcal/mol}$$

To our knowledge other experimental values of hydrogen bond strengths in water are free energy values.[1-4,75] In contrast, the estimated ΔG here is lower than the free energy values derived by Fersht[1,4] from site-directed mutagenesis studies. The lower value is attributed to the relatively exposed aqueous environment in which the present receptors operate versus the more buried, less aqueous environment ones at the active sites of the enzymes. Electrostatic effects such as hydrogen bonds are expected to be magnified in the lower dielectric of the enzyme interiors. In addition, the alternating hydrogen bond donor-acceptor arrangement of the two new hydrogen bonds formed in this system results in some unfavorable secondary interactions.[76]

The difference between receptors **A13** and **A15** lies solely in the aromatic surfaces; the hydrogen bond component of the complexation is expected to be identical. The enthalpy difference of -3.4 kcal/mol suggests that hydrophobic interaction is stronger with naphthalene than carbazole. This may also be the reason for the

preference for 2:1 binding mode seen with receptor **A16**. As in the complexation studies with cyclophanes in various solvents by Diederich et al.,[38] the enthalpic component of hydrophobic binding in water seems to be driven by the formation of stronger van der Waals interactions between the polarizable aromatic surfaces, the loss of less favorable ones with water (water has low molecular polarizability), and the release of water from the reduced hydrogen bonding environment to the strongly hydrogen bonding environment in the bulk solvent.

An alternate explanation is that there is an intrinsic attraction between naphthyl and adenine surfaces, much like the self-association of purine and pyrimidine derivatives in aqueous solution.[77] Gellman has shown that there is little or no "hydrophobic collapse" or association of the two aromatic groups in dinaphthalenes of type **A** (Scheme A9) in water, whereas diadenine **B** and naphthalene-adenine **C** both show considerable stacking.[78,79] The aromatic surface areas being similar, polar interactions rather than hydrophobic interactions may be operating in these adenine-naphthyl systems. Perhaps the more polarizable character of the naphthyl compared to the inherently polarized carbazolyl surface allows it to match its polarization with adenine and yield a more favorable ΔH for **A15**.

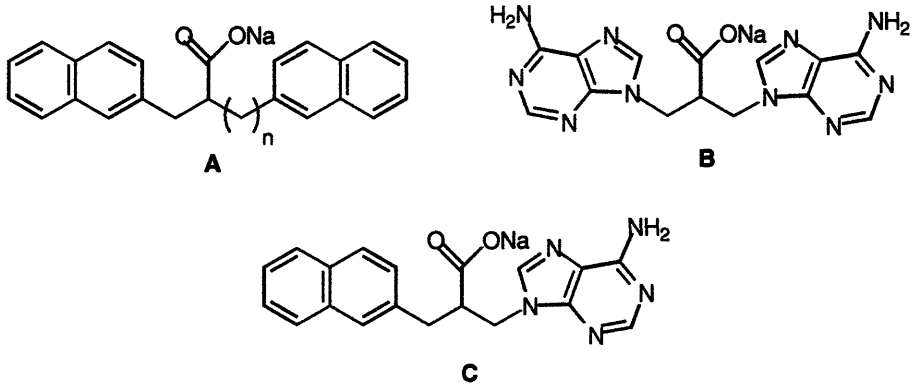

Scheme A9.

The entropic difference between the complex of **A13** and the complex of **A15** seems relatively large, -13 cal mol^{-1} K^{-1}. Since the **A15** complex showed stronger hydrophobic interactions it appears that these favorable interactions result in a much more tightly bound rigid complex than the corresponding carbazole complex. Similar phenomena of more negative ΔH correlating to more negative ΔS has been seen with hydrophobic effects in protein folding.[80,81] Our observation of enthalpy-entropy compensation effect suggests that even with small molecules, associations governed mostly by hydrophobic effect in water will show this phenomena.

In summary, four water-soluble adenine receptors, *mono*(imide) receptors **A13** and **A15**, and *bis*(imide) **A14** and **A16** were synthesized. Association constants obtained at different temperatures with 9-ethyladenine allowed determination of enthalpy and entropy of complexation. Comparison of the two carbazole receptors **A13** and **A14** showed that the enthalpy of a single hydrogen bond in aqueous solution can be estimated to be 0.8 kcal/mol. Comparison of the two *mono*(imide) receptors **A13** and **A15** showed that naphthalene has

stronger hydrophobic interactions with 9-ethyladenine than carbazole. The entropy of binding is accordingly less favorable for **A15**, giving rise to overall similar free energies of binding for **A13** and **A15** in the temperature range studied.

4. EXPERIMENTAL

4.1 General.

Air/water-sensitive reactions were performed in flame-dried glassware under argon. Tetrahydrofuran was distilled from Na/benzophenone ketyl. Toluene was distilled from calcium hydride. Unless otherwise stated, all other commercially available reagents were used without further purification.

^{1}H NMR spectra were obtained on Bruker AC-250, Varian XL-300, Varian UN-300, and Varian VXR-500 spectrometers. All chemical shift values are reported in ppm downfield from TMS for organic solvents, or DSS for H_2O/D_2O. Spectra taken in $CDCl_3$ were referenced to either TMS (0.00, for compounds with overlapping aromatic protons) or residual $CHCl_3$ (7.26). Spectra taken in DMSO-d_6 were referenced to residual solvent (2.50). Fourier transform infrared spectra were taken on a Perkin Elmer infrared spectrometer. Flash chromatography[82] was performed using Silica Gel 60 (EM Science, 230400 mesh).

4.2 Synthesis.

Methyl Cyclohexane-1,3,5-tricarboxlyate (A3)was prepared according to Askew *et al.*[83]

Tribenzyloxy Triester A4a. Trimethyl ester (5.003 gm, 19.5 mmol) in toluene (100 mL) was added dropwise over a 30-min period to a -78 °C solution of LDA (1.5 M in cyclohexane, 45 mL, 67.5 mmol) in toluene (100 mL). Once the addition was complete, the solution was stirred at -78 °C for an additional 30 min. It was then brought to 0 °C in an ice bath and stirred for 30 min, during which time the solution became noticeably more viscous. The solution was cooled to -40 °C for 15 min. Benzylchloromethyl ether (8.5 mL, 62 mmol) was then added to the solution, which gradually cleared. The solution was stirred for another 45 min at -40 °C, 45 min at -20 °C, 45 min at 0 °C, and then for an additional 3 hours at 25 °C. It was then quenched with saturated NH_4Cl (200 mL). The resulting solution was extracted with ether (300 mL). The ether layer was washed with HCl (2 x 150 mL, 1.2 M), NaOH (2 x 150 mL, 1 M), then washed with brine (100 mL). The solution was dried (Na_2SO_4), then evaporated *in vacuo* to give 12.266 g of brown, viscous oil which was recrystallized from MeOH (100 mL) to yield 4.143 g of colorless crystals. A second crop of 1.022 g was obtained from the mother liquor. The overall yield was 5.165 g (43%): mp 110-112 °C; IR (KBr) 3050, 2950, 1740, 1730 cm^{-1}; ^{1}H NMR (250 MHz, $CDCl_3$) δ 7.4-7.1 (m, 15 H), 4.45 (s, 6 H), 3.70 (s, 6 H), 3.35 (s, 9 H), 2.70 (d, 3 H. J = 13 Hz), 1.19 (d, 3 H. J = 13 Hz); HRMS (EI) calcd for $C_{36}H_{42}O_9$, 618.2829; found, 618.2840.

Tribenzyloxy Triacid A4b. Triester **A4a** (1.635 g, 2.65 mmol) and KOH (4.568 g, 81 mmol) was heated in refluxing EtOH (50 mL) for 4 h. Solvent was then removed *in vacuo*, and the resulting slurry was poured into

water (100 mL). The aqueous layer was washed with ether (2 x 50 mL), acidified (concentrated HCl), then extracted with ether (2 x 100 mL). Drying (Na_2SO_4) and evaporation of the organic layer gave 1.253 g (83%) of the tracid as a pale yellow solid which was used without further purification: ^{1}H NMR (250 MHz, DMSO-d_6) δ 12.15 (br s, 3 H), 7.4-7.1 (m, 15 H), 4.40 (s, 6 H), 3.42 (s, 6 H), 2.40 (d, 3 H. J = 13 Hz), 1.40 (d, 3 H. J = 13 Hz).

Anhydride acid A5a. A solution of triacid (471 mg, 0.818 mmol) in xylenes (50 mL) was heated with azeotropic removal of water (80 mL of water was removed over a 1.5 h period). Removal of the remaining xylenes gave 455 mg (quant) of the anhydride acid as a pale yellow foam, which was used without further purification; ^{1}H NMR (250 MHz, DMSO-d_6) δ 11.20 (br s, 1 H), 7.4-7.1 (m, 15 H), 4.6-4.40 (m, 6 H), 3.82-3.75 (m, 2 H), 3.55-3.20 (m, 4 H), 2.6-2.4 (m, 3 H), 1.8-1.40 (m, 3 H).

Imide acid A5b. A solution of 6.357 g (11.4 mmol) of anhydride **A5a** and NH_4OH (5 mL) in THF (100 mL) was heated to reflux for 2 h. Solvent was removed *in vacuo*, and the resulting solid dissolved in CH_2Cl_2 (150 mL). The organic layer was washed with 1 N HCl (100 mL), then dried over Na_2SO_4. Removal of solvent provided 4.095 g (64%) of imide **A5b** as an off-white solid: mp 138-140 °C; IR (KBr) 3166, 2860, 1713 cm^{-1}; ^{1}H NMR (300 MHz, DMSO-d_6) δ 12.48 (s, 1 H), 10.58 (s, 1 H), 7.34-7.24 (m, 15 H), 4.45 (d, 6 H. J = 19 Hz), 3.72 (d, 2 H. J = 8.4 Hz), 3.34-3.30 (m, 4 H), 2.33 (d, 1 H. J = 13 Hz), 2.20 (d, 2 H. J = 13 Hz), 1.51 (t, 3 H. J = 13 Hz); HRMS (EI) calcd for $C_{33}H_{35}NO_7$, 557.2414; found, 557.2416.

Imide acid chloride A5c. A solution of the imide acid **A5b** (300 mg, 0.54 mmol) in thionyl chloride (15 mL) was heated to reflux for 2 h. The thionyl chloride was removed under reduced pressure to yield 312 mg of the imide acid chloride **A5c** (quant), which was used without further purification.

(2S,8S)-2-(Hydroxymethyl)-8-[[(*tert*-butyldiphenylsilyl)oxy]methyl]3,4,6,7,8,9-hexahydro-2*H*-pyrimido[1,2-a]pyrimidine Hydrochloride (A7). Acetic acid (15 mL) was added to a solution of bicyclic guanidinium **A6**[59] (252 mg, 0.428 mmol) in THF (5 mL) with stirring at room temperature for 24 h. The reaction mixture was concentrated *in vacuo*. Hexanes and diethyl ether were added and the white precipitate was triturated. The solids were recrystallized from CH_2Cl_2 and hexanes to give 200 mg (quant) of clean **A7**: mp 112-117 °C; $[\alpha]^{20}_D$ +44° (c = 0.0044, $CHCl_3$); IR (KBr) 3278, 2931, 1624, 1112, 703 cm^{-1}; ^{1}H NMR (300 MHz, $CDCl_3$) δ 9.29 (s, 1 H), 7.77.6 (m, 5 H), 7.45-7.35 (m, 6 H), 4.12 (br s, 1 H), 3.80 (m, 1 H), 3.75 (m, 1 H), 3.57 (m, 4 H), 3.25 (m, 4 H), 2.07 (m, 1 H), 1.90 (m, 3 H), 1.66 (s, 9 H); HRMS (EI) calcd for $C_{25}H_{36}N_3O_2Si$ (M - Cl), 438.2577; found, 438.2580.

4-Iodobenzoic acid methyl ester (A8). Thionyl chloride (10 mL) was added dropwise (1.5 h) to a cooled (0 °C) heterogeneous solution of 4-iodobenzoic acid (10.0 g, 40.0 mmol) in MeOH (100 mL). Upon complete addition, the solution was warmed to room temperature to yield white solids **A8** (8.67 g). A second crop was

obtained from the remaining reaction mixture to give another 947 mg of **A8**. The overall yield of **A8** was 9.62 g (92%): mp 115.4-115.7 °C; ^{1}H NMR (300 MHz, $CDCl_3$) δ 7.81 (d, 2 H. J = 8.7 Hz), 7.74 (d, 2 H. J = 8.7 Hz), 3.91 (s, 3 H); HRMS (EI) calcd for $C_8H_7O_2I$, 261.9491; found, 261.9493.

***N*-(4-(Methoxycarbonyl)phenyl)carbazole (A9).** A paste consisting of carbazole (6.14 g, 36.7 mmol), **A8** (9.92 g, 36.7 mmol), K_2CO_3 (5.07 g), copper powder (190 mg) and xylene (10 mL) was stirred with a mechanical stirrer at 200 °C for 1 h. Benzene (100 mL) was added and the whole was heated to reflux for 2 h. Upon cooling the reaction mixture to room temperature, solids were removed and the brown filtrate was concentrated. Recrystallization from MeOH yielded 6.67 g (60%) of clean aromatic **A9**: mp 120.7-121.5 °C; IR (KBr) 3050, 2946, 1721, 1602, 1513, 1452, 1432, 1290, 1280, 1225, 1168, 1115, 1102 cm^{-1}; ^{1}H NMR (500 MHz, $CDCl_3$) δ 8.29 (d, 2 H. J = 8.5 Hz), 8.15 (dd, 2 H, J = 7.5, 0.5 Hz), 7.69 (d, 2 H, J = 8.0 Hz), 7.48 (dd, 2 H, J = 8.2, 0.7 Hz), 7.43 (dt, 2 H, J = 7.6, 1.0 Hz), 7.32 (dt, 2 H, J = 7.2, 0.8 Hz), 4.00 (s, 3 H); HRMS (EI) calcd for $C_{20}H_{15}NO_2$, 301.1103; found, 301.1100.

***N*-(4-(Methoxycarbonyl)phenyl)-3,6-dinitrocarbazole (A10a).** To a stirred mixture of **A9** (2.94 g, 9.75 mmol) and 48 mL of acetic acid was added nitric acid (70.4%, 29 mL) over 12 min. The mixture was stirred at 70 °C for 4.5 h and cooled to room temperature. Addition of water yielded precipitates which were filtered, washed with water and dried *in vacuo* to yield 3.55 g (93%) of crude **A10a** which was used without further purification: ^{1}H NMR (300 MHz, DMSO-d_6) δ 9.66 (d, 2 H, J = 2.4 Hz), 8.42 (dd, 2 H, J = 9.2, 2.3 Hz), 8.30 (d, 2 H, J = 8.7 Hz), 7.91 (d, 2 H, J = 8.4 Hz), 7.62 (d, 2H, J =9.3Hz), 3.94 (s, 3 H).

***N*-(4-(Methoxycarbonyl)phenyl)-3,6-diaminocarbazole (A10b).** A heterogeneous solution of **A10a** (486 mg, 1.24 mmol) and 10% Pd-C (55.1 mg) in THF (50 mL), was stirred under H_2 atmosphere at room temperature for 24 h. The reaction mixture was filtered through Celite then concentrated in vacuo to give 510.3 mg (quant) of crude **A10b** as a brown film which was used without further purification: ^{1}H NMR (300 MHz, DMSO-d_6) δ 8.14 (d, 2 H, J = 9.0 Hz), 7.69 (d, 2 H, J = 8.5 Hz), 7.25 (d, 2 H, J = 8.5 Hz), 7.13 (d, 2 H, J = 2.0 Hz), 6.71 (dd, 2 H, J = 8.4, 2.0 Hz), 4.93 (brs, 4 H), 3.31 (s,3 H).

***N*-(4-(Methoxycarbonyl)phenyl)-3,6-bis[((*cis*,*cis*-2,4-dioxo-1,5,7tris((benzyloxy) methyl)-3-azabicyclo[3.3.1]non-7-yl)carbonyl)amino]carbazole (A11a).** A solution of diaminocarbazole **A10b** (1.23 g, 3.73 mmol) and acid chloride **A5c** (5.37 g, 9.33 mmol) in pyridine (180 ml) was stirred at room temperature under argon for 2 h. The whole was concentrated in vacuo and the dark residue was taken up in CH_2Cl_2. The organic phase was washed with 1.2 N HCl (300 mL) then dried over $MgSO_4$, filtered and concentrated *in vacuo*. The resulting residue was flash-chromatographed through a silica gel column (20% EtOAc/CH_2Cl_2) to give 2.55 g (49%) of **A11a**: mp 125-145 °C (dec); IR (KBr) 3384, 2861, 1702, 1604, 1466, 1281, 1195, 1101, 738, 698 cm^{-1}; ^{1}H NMR (300 MHz, DMSO-d_6) δ 10.63 (s, 2 H), 9.42 (s, 2 H), 8.31 (s, 2 H), 8.23 (d, 2 H. J = 8.5 Hz), 7.79 (d, 2 H, J = 8.5 Hz), 7.49 (d, 2 H, J = 9.5 Hz), 7.42 (d, 2 H, J = 8.8 Hz), 7.28-7.00

(m, 30 H), 4.51 (s, 8 H), 4.46 (s, 4 H), 3.41 (d, 4 H, J = 9.1 Hz), 2.58 (d, 4 H, J = 13.5 Hz), 2.34 (d, 2 H, J = 11.9 Hz), 1.61 (d, 4 H, J = 14.3 Hz), 1.60 (d, 2 H, J = 9.9 Hz); HRMS (FAB in 3-nitrobenzyl alcohol) calcd for $C_{86}H_{84}N_5O_{14}$ (M + H),1410.6015; found, 1410.6007.

***N*-(4-(Methoxycarbonyl)phenyl)-3,6-bis[((*cis*,*cis*-2,4-dioxo-1,5,7-tris-(hydroxymethyl)-3-azabicyclo[3.3.1]non-7-yl)carbonyl)amino]carbazole (A2).** HBr(g) was bubbled for 5 min through a solution of the benzylated cleft **A11a** (8.9 mg, 0.00631 mmol) in formic acid (1mL) at 0 °C, followed by argon for 5 min. The whole was concentrated *in vacuo* to give brown solid which upon washing with minimum amount of MeOH (2 mL) yielded 4.5 mg (82%) of white solid **A2**: mp 260-270 °C (dec); IR (KBr) 3421, 3209, 1700, 1466, 1400, 1290, 1200, 1057 cm^{-1}; ^1H NMR (300MHz, DMSO-d_6) δ 10.41 (s, 2 H), 9.26 (s, 2 H), 8.38 (d, 2 H, J = 2.1 Hz), 8.24 (d, 2 H, J = 8.4 Hz), 7.80 (d, 2 H, J = 8.4 Hz), 7.52 (dd, 2 H, J =2.2, 8.8 Hz), 7.43 (d, 2 H, J = 9.2 Hz), 5.12 (br, 2 H), 4.77 (br, 4 H), 3.92 (s, 3 H), 3.79 (d, 4 H, J = 10.6 Hz), 2.42 (d, 4 H, J = 14.1 Hz), 2.21 (d, 2 H. J = 11.9 Hz), 1.51 (d, 4 H, J = 14.3 Hz), 1.35 (d, 2 H. J = 13.1 Hz); HRMS (FAB in glycerol) calcd for $C_{44}H_{48}N_5O_4$ (M + H), 870.3198; found, 870.3201.

***N*-(4-Carboxyphenyl)-3,6-bis[((*cis*,*cis*-2,4-dioxo-1,5,7-tris-((benzyloxy)methyl)-3-azabicyclo[3.3.1]non-7-yl)carbonyl)amino]carbazole (A11b).** To a solution containing **A11a** (361 mg, 0.256 mmol) in ethanol (10 mL) and THF (10 mL), 1N NaOH (1.55 mL, 6 equiv) was added. The solution was stirred at room temperature for 20 h. The basic solution was acidified to approximately pH 2 with 5% HCl to precipitate the product. The whole was concentrated *in vacuo* and the solid were taken up in CH_2Cl_2 (50 mL) and brine (50 mL). The organic layer was separated, dried over $MgSO_4$, filtered and concentrated to give crude acid **A11b** (304 mg) which was flash-chromatographed through a silica gel column (5-7% MeOH/CH_2Cl_2) to give 277 mg (78%) of clean **A11b**: mp 141.5-143.0 °C; IR (KBr) 3134, 1700,1603, 1100 cm^{-1}; ^1H NMR (300MHz, $CDCl_3$) δ 9.19 (s, 2 H), 8.03 (s, 2 H), 7.94 (s, 2 H), 7.75 (d, 2 H. J = 8.2 Hz), 7.40-7.23 (m, 34 H), 7.18 (d, 2 H, J = 8.4 Hz), 7.08 (d, 2 H, J = 8.8 Hz), 4.62-4.52 (m, 12 H), 3.85 (d, 4 H, J = 9.1 Hz), 3.57 (d, 4 H, J = 9.1 Hz), 3.48 (s, 4 H), 2.60 (d, 4 H, J = 14.2 Hz), 2.50 (d, 2 H, J = 13.3 Hz), 1.79 (d, 2 H, J = 13.0 Hz), 1.67 (d, 4 H, J = 14.2 Hz); HRMS (FAB in 3nitrobenzyl alcohol) calcd for $C_{85}H_{82}N_5O_{14}$ (M + H), 1396.5858; found, 1396.5857.

***N*-(4-(Chlorocarbonyl)phenyl)-3,6-bis[((*cis*,*cis*-2,4-dioxo-1,5,7-tris-((benzyloxy)methyl)-3-azabicyclo[3.3.1]non-7-yl)carbonyl)amino]carbazole (A11c).** To a solution of **A11b** (410 mg, 0.293 mmol) and DMF (6 μL) in THF (9 mL) was added dropwise oxalyl chloride (400 μL). The yellow solution was stirred for 1 h and concentrated *in vacuo* to give 414 mg (quant) of yellow solid **A11c**, which was used without further purification.

Hexakis(bezyloxymethyl)carbazolediimide tBDPS Bicyclic Guanidinium Ester Hydrochloride (A12a). Monohydroxy guanidinium **A7** (154 mg, 0.322 mmol), acid chloride **A11c** (414 mg, 0.293 mmol),

TEA (400 RL) and THF (17 mL) were stirred at room temperature for 20 h. The reaction mixture was concentrated then taken up in $CHC1_3$ (70 mL) and 1.2 N HCl (50 mL). The organic layer was dried over $MgSO_4$, filtered, and concentrated *in vacuo* to give crude material which was flash-chromatographed once through a silica gel column (10% MeOH/$CHCl_3$) to give a mixture of **A11b** and **A12a** (1:12, 310 mg) which was used without further purification: ^{1}H NMR (300 MHz, DMSO-d_6, **A13a** only) δ 10.60 (s, 2 H), 9.42 (s, 2 H), 8.29 (m, 4 H), 7.84 (d, 2 H. J = 8.4 Hz), 7.62 (m, 3 H), 7.53-7.26 (m, 43 H), 4.53-4.48 (m, 12 H), 3.98 (dd, 1 H. J = 6.9, 1.5 Hz), 3.86 (m, 1 H), 3.79 (d, 4 H. J = 9.0 Hz), 3.68-3.55 (m, 2 H), 3.46 (d, 4 H. J = 10 Hz), 3.41 (s, 4 H), 2.59 (d, 4 H. J = 13 Hz), 2.36 (d, 2 H. J = 13 Hz), 1.99 (m, 4 H),1.62 (m, 6 H),1.02 (s, 9 H).

Hexakis(bezyloxymethyl)carbazolediimide Hydroxy Bicyclic Guanidinium Ester Hydrochloride (A12b). A solution of the above mixture (310 mg, 0.167 mmol), THF (800 μL) and TBAF (600 μL) was stirred at room temperature for 2 h, concentrated, and taken up in $CHCl_3$ (40 mL) and water (30mL). The organic layer was dried over $MgSO_4$, filtered and evaporated to give a yellow residue. Diethyl ether (5 mL) was added to dissolve *t*BDPSF and precipitate the desired product. The solids were collected by centrifugation and then flash-chromatographed through a silica gel column (15-20% MeOH/$CHCl_3$) to yield 254 mg (56% yield from **A11c**) of **A12b**: IR (KBr) 3262, 2923, 2854, 1702, 1624, 1100, 739, 698 cm^{-1}; ^{1}H NMR (500 MHz, DMSO-d_6) δ 10.59 (s, 2 H), 9.42 (s, 2 H), 8.32-8.28 (m, 4 H), 7.84 (d, 2 H, J = 8.5 Hz), 7.62 (s, 1 H), 7.51 (d, 2 H. J = 9.5 Hz), 7.49 (s, 1 H), 7.41 (d, 2 H, J = 8.5 Hz), 7.35-7.20 (m, 30 H), 5.74 (m, 1 H), 4.54-4.44 (m, 12 H), 4.30 (dd, 1 H. J = 8.0, 9.7 Hz), 3.86 (m, 1 H), 3.78 (d, 4 H. J = 8.5 Hz), 3.54 (m, 1 H), 3.46 (s, 4 H), 3.15 (m, 1 H), 2.58 (d, 4 H, J = 14 Hz), 2.35 (d, 2 H, J = 13 Hz), 2.12 (m, 1 H), 1.92 (m, 2 H), 1.63-1.59 (m, 7 H); HRMS (FAB in glycerol) calcd for $C_{84}H_{87}O_{15}N_8$ (M-Cl), 1577.7073; found, 1577.7066.

Hexahydroxy-Kemp-imide *p*-Carbazole Phenyl Hydroxybicyclic Guanidinium Ester Hydrochloride (A1). HBr(g) was bubbled for 3 min through the benzylated cleft **A12b** (253 mg, 0.157 mmol) in formic acid (12 mL) at 0 °C, followed by Ar for 5 min. The solution was concentrated *in vacuo* to give orange solids which upon trituration in $CHCl_3$ and THF gave a pale orange solid, which was further purified by passing through an anion exchange resin (Dowex 1x8-200, prepared by flushing satd NH_4Cl(aq), eluted with water) to give 131 mg (78%) of receptor **A1**: mp 240-280 °C (dec); $[\alpha]^{20}_D$ +66° (c = 0.0028, H_2O); IR (KBr) 3207, 1696, 1618, 1513, 1464, 1400, 1274, 1196, 1052 cm^{-1}; ^{1}H NMR (300 MHz, DMSO-d_6) δ 10.38 (s, 2 H), 9.26 (s, 2 H), 8.36 (s, 2 H), 8.30 (d, 2 H, J = 8.4 Hz), 7.84 (d, 2 H, J = 8.7 Hz), 5.17 (t, 1 H, J = 4.8 Hz), 5.11 (t, 1 H, J = 4.8 Hz), 4.77 (t, 4 H, J = 5.4 Hz), 4.48 (dd, 1 H, J = 3.7, 10 Hz), 4.31 (t, 1 H, J = 9.7 Hz), 3.89-3.75 (m, 5 H), 3.59-3.46 (m, 1 H), 3.07-3.03 (m, 2 H), 2.42 (d, 4 H, J = 15 Hz), 2.21 (d, 2 H, J = 13 Hz), 1.92 (m, 2 H), 1.65 (m, 1 H), 1.49 (d, 4 H, J = 13 Hz), 1.35 (d, 2 H, J = 13 Hz); HRMS (FAB in glycerol) calcd $C_{52}H_{61}O_{15}N_8$ (M-Cl), 1037.4256; found, 1037.4248.

***N*-((Methoxycarbonyl)methyl)-3-nitrocarbazole (A17b).** Alkyl carbazole **A17a**[57] (2.20g, 9.194 mmol) was added at once to a solution of $Cu(NO_3)_2 \cdot 2.5H_2O$ (4.6 mmol, 1 equiv) in Ac_2O (10 mL) and AcOH

(15 mL) at 32 °C under a drying tube. Additional AcOH (5 mL) was added and the reaction was stirred for 5 h before being poured into water (300 mL). Filtration and drying gave 2.485 g (95%) of the mononitro product as yellow solid which was used without further purification: ^{1}H NMR (300 MHz, acetone-d_6) δ 9.114 (d, 1H, J=2.4 Hz), 8.401 (dd, 1H, J=8.4, 0.6 Hz), 8.366 (dd, 1H, J=9.0, 2.4 Hz), 7.738 (d, 1H, J=9.0 Hz), 7.660 (d, 1H, J=8.1 Hz), 7.589 (dd, 1H, J=7.6, 1.1Hz), 7.385 (dd, 1H, 7.3, 1.5 Hz), 5.431 (s, 2H), 3.727 (s, 3H).

***N*-((Methoxycarbonyl)methyl)-3-aminocarbazole (A17c).** Nitrocarbazole **A17b** (478 mg, 1.681 mmol) was dissolved in THF (50 mL) and hydrogenated at balloon pressure for 1.6 h with 10% Pd-C (218 mg, 46 wt%). The suspension was filtered through Celite and concentrated *in vacuo*. The unstable solid was used immediately without further purification.

***N*-((Methoxycarbonyl)methyl)-3-[((cis, cis-2,4-dioxo-1,5,7-tris((benzyloxy)methyl)-3-azabicyclo[3.3.1]non-7-yl)carbonyl)amino] carbazole (A18a).** Acid chloride **A5c**[40] (1.036 g, 1.799 mmol) and aminocarbazole **A17c** (1.5 equiv) were heated in refluxing pyridine to yield 953 mg (67%) of the monoimide **A18a** after gravity chromatography (10-15% EtOAc/$CHCl_3$), which was used without further purification: ^{1}H NMR (500 MHz, d_6-DMSO) δ 10.670 (s, 1 H), 9.357 (s, 1 H), 8.067 (d, 1 H, J=7.1 Hz), 7.5-7.2 (m, 21 H), 5.331 (s, 2 H), 4.511 (s, 2H), 4.506 (s, 2H), 4.476 (s, 2 H), 3.772 (d, 2 H, J=9.0 Hz), 3.650 (s, 3H), 3.458 (s, 2H), 3.404 (d, 2H, J=9.0 Hz), 2.545 (d, 2 H, J=14.4 Hz), 2.338 (d, 1H, J=12.5 Hz), 1.608 (d, 2 H, J=13.7 Hz), 1.596 (d, 1 H, J=12.9 Hz).

N-(Carboxymetnyl)-3-[((cis, cis-2,4-dioxo-1,5,7-tris((benzyloxy)methyl)-3-azabicyclo[3.3.1]non-7-yl)carbonyl)amino]carbazole (A18b). Imide **A18a** (953 mg, 1.20 mmol) was hydrolyzed with 1 N NaOH (2 equiv) in THF (3.6 mL) and EtOH (2 mL) and stirring at room temperature for 6.5 h. Organic solvents were evaporated and the residue suspended in water (10 mL). After acidification with 10% HCl, the solid was isolated by filtration and dried under vacuum to give 831 mg (89%) of white powder which was used without further purification: HRMS (EI) calcd for $C_{47}H_{45}N_3O_8$, 779.3207; found, 779.3210.

***N*-(((Propylamino)carbonyl)methyl)-3-[((cis, cis-2,4-dioxo-1,5,7-tris(benzyloxy)methyl)-3-azabicyclo[3.3.1]non-7-yl)carbonyl) amino]carbazole (A19).** Acid **A18b** (102 mg, 0.131 mmol) was dissolved in anhydrous THF (4 mL) under argon. Catalytic DMF (<1 μL) was added, followed by oxalyl chloride (80 μL, 7.0 equiv). The reaction was stirred at room temperature for 45 min, and solvent was removed *in vacuo*. The residue was re-dissolved in anhydrous THF on ice under argon. Propylamine (150 μL, 13.9 equiv) was added. The reaction was warmed to room temperature and stirred for a total of 53h. Solvent was evaporated. The residue was taken up in chloroform (50 mL), washed with 1 N HCl (50 mL), and brine (25 mL), and dried over Na_2SO_4. Evaporation of solvent followed by chromatography (30-50% EtOAc/CH_2Cl_2) yielded **A19** (80 mg, 75%) as a white powder: IR (KBr) 3356, 1701, 1533, 1493, 1465, 1363, 1323, 1201, 1099, 746, 698 cm^{-1}; ^{1}H NMR (500 MHz, DMSO-d_6) δ 10.660 (s, 1 H), 9.348 (s, 1 H), 8.233 (br t, 1 H), 8.063

(s, 4 H), 7.487 (d, 2 H, J = 8.5 Hz), 7.41-7.25 (m, 18 H), 7.185 (t, 1 H, J = 7.3 Hz), 4.969 (s, 2 H), 4.511 (s, 4 H), 4.505 (s, 2 H), 4.476 (s, 2 H), 3.772 (d, 2 H, J = 9.0 Hz), 3.461 (s, 2 H), 3.403 (d, 2 H, J = 8.8 Hz), 3.042 (q, 2 H, J = 6.1 Hz), 2.545 (d, 2 H, J = 13.9 Hz), 2.346 (d, 1 H, J = 12.5 Hz), 1.606 (d, 3H, J = 13.7 Hz), 1.426 (q, 2 H, J = 7.3 Hz), 0.840 (t, 3 H, J = 7.3 Hz); HRMS (FAB in 3-nitrobenzyl alcohol) calcd for $C_{50}H_{53}N_4O_7$ (M+H), 821.3914; found, 821.3914.

***N*-(((Propylamino)carbonyl)methyl)-3-[((cis, cis-2,4-dioxo-1,5,7-tris(hydroxymethyl)-3-azabicyclo[3.3.1]non-7-yl)carbonyl)amino]carbazole (A13).** Benzyl-protected imide **A19** (72 mg, 87.7 μmol) was dissolved in HCOOH (4.6 mL) and stirred on ice for 40 min. $HBr_{(g)}$ was bubbled through the solution for 9 min, followed by Ar (g) for 2h. Solvent was removed *invacuo*. The waxy solid was dissolved in MeOH (1 mL) and precipitated by addition of ether (5 mL). The product was filtered and dried under vacuum to give **A13** (40.5 mg, 84%) as a white solid: IR (KBr) 3326 (br), 1693, 1540, 1492, 1466, 1432, 1325, 1204, 1056, 804, 749 cm^{-1}; ^1H NMR (300 MHz, DMSO-d_6) δ 10.445 (s, 1 H), 9.200 (s, 1 H), 8.245 (br t, 1 H), 8.115 (s, 1 H), 8.075 (d, 1 H, J = 8.1 Hz), 7.486 (d, 1 H, J = 8.1 Hz), 7.398 (m, 3 H), 7.177 (t, 1H, J = 7.5 Hz), 4.969 (s, 2 H), 3.770 (d, 2 H, J = 10.5 Hz), 3.389 (s, 2 H), 3.318 (d, 2 H, J = 10.2 Hz), 3.040 (q, 2 H, J = 6.5 Hz), 2.375 (d, 2 H, J = 14.1 Hz), 2.205 (d, 1 H, J = 12.6 Hz), 1.487 (d, 2 H, J = 14.7 Hz), 1.425 (q, 2 H, J = 6.9 Hz), 1.328 (d, 1H, J = 12.9 Hz), 0.839 (t, 3 H, J = 7.5 Hz); HRMS (FAB in 3-nitrobenzyl alcohol) calcd for $C_{29}H_{35}N_4O_7$ (M+H), 551.2506; found, 551.2510.

***N*-((methoxycarbonyl)methyl)-3,6-bis[((cis, cis-2,4-dioxo-1,5,7-tris(benzyloxy) methyl)-3-azabicyclo[3.3.1]non-7-yl)carbonyl)amino]carbazole (A21a).** Diamine **A20**[57] (264 mg, 0.981 mmol) and acid chloride **A5c**[40] (1.354 g, 2.35 mmol) were dissolved in pyridine (60 mL) and stirred over night under argon at room temperature. The deep red solution was concentrated and the solids were taken up in CH_2Cl_2 (150 mL) and 1 N HCl (200 mL). The aqueous layer was extracted with CH_2Cl_2 (2 x 100 mL). Combined organics were washed with brine (100 mL), and the aqueous layer was extracted with CH_2Cl_2 (2 x 70 mL). Combined organics were dried over Na_2SO_4, filtered and concentrated to give a red solid which was flash chromatographed through a silica gel column (35, 40% ethylacetate/$CHCl_3$) to give 402 mg of **A10a** (30%) as a pale yellow solid. This was used without further purification: IR (KBr) 3431, 3212, 2923, 2860, 1703, 1699, 1467, 1453, 1281, 1196, 1101, 738, 698 cm^{-1}; ^1H NMR (300 MHz, DMSO-d_6) δ 10.641 (s, 2 H), 9.322 (s, 2 H), 8.120 (s, 2 H), 7.44-7.24 (m, 34 H), 5.312 (s, 2 H), 4.518 (s, 8 H), 4.480 (s, 4 H), 3.789 (d, 4 H, J = 8.64 Hz), 3.745 (s, 3 H), 3.46-3.38 (m, 8 H), 2.574 (d, 4 H, J = 14.2 Hz), 2.348 (d, 2 H, J = 12.9 Hz), 1.64-1.58 (m, 6 H).

***N*-(carboxymethyl)-3,6-bis[(((cis, cis-2,4-dioxo-1,5,7-tris(benzyloxy) methyl)-3-azabicyclo[3.3.1]non-7-yl)carbonyl)amino]carbazole (A21b).** Methylester **A21a** (671 mg, 0.498 mmol) was hydrolyzed in 1 N NaOH (4 mL), THF (16 mL) and EtOH (25 mL) with stirring at room temperature in 30 min. The reaction mixture was cooled to 0 °C and 10% HCl was added until pH3. Organic

solvents were removed in vacuo and the resulting aqueous suspension was extracted by CH_2Cl_2, dried over $MgSO_4$, filtered, and concentrated to yield crude **A21b** (quant) which was used without further purification: ^1H NMR (300 MHz, DMSO-d_6) δ 10.64 (s, 2 H), 9.32 (s, 2 H), 8.07 (s, 2 H), 7.42-7.26 (m, 34 H), 4.72 (br s, 2 H), 4.52 (s, 8 H), 4.48 (s, 4 H), 3.79 (d, 4 H, J = 8.9 Hz), 3.46 (s, 4 H), 3.42 (d, 4 H, J = 9.4 Hz), 2.57 (d, 4 H, J = 13.8 Hz), 2.35 (d, 2 H, J = 12.9 Hz), 1.62 (d, 4 H, J = 14.2 Hz), 1.59 (d, 2 H, J = 12.9 Hz).

***N*-(((Propylamino)carbonyl)methyl)-3,6-bis[((cis, cis-2,4-dioxo-1,5,7-tris(benzyloxy) methyl)-3-azabicyclo[3.3.1]non-7-yl)carbonyl) amino]carbazole (A22).** Acid **A21b** (388 mg, 0.291 mmol) was dissolved in THF (8.8 mL). Catalytic amount (1 drop) of DMF then oxalylchloride (177 μL, 7 equiv) were added and the reaction mixture was stirred at room temperature for 1h. This was concentrated in vacuo, filled with Ar and cooled in an ice bath. THF (8.8 mL) was placed to dissolve the solids, propylamine (335 μL, 14 equiv) was added and was stirred for 24h. Solvent was evaporated and the residue was taken up in $CHCl_3$ (80 mL) and 1N HCl (100 mL). The aqueous layer was washed with $CHCl_3$ (2 x 50 mL), combined organics were washed with brine (80 mL), then dried over Na_2SO_4, filtered and concentrated. The resulting residue was flash chromatographed through a silica gel column (2, 5% MeOH/$CHCl_3$) to yield the desired product (307 mg, 76%): IR (KBr) 3328, 2923, 2853, 1701, 1534, 1493, 1453, 1200, 1099, 737, 697 cm^{-1}; ^1H NMR (300 MHz, DMSO-d_6) δ 10.645 (s, 2 H), 9.324 (s, 2 H), 8.222 (t, 1 H, J = 5.68 Hz), 8.107 (s, 2 H), 7.46-7.21 (m, 34 H), 4.950 (s, 2 H), 4.56-4.45 (m, 12 H), 3.786 (d, 4 H, J = 8.96 Hz), 3.462 (s, 4 H), 3.416 (d, 4 H, J = 9.12 Hz), 3.044 (dt, 2 H, J = 5.87, 6.28 Hz), 2.573 (d, 4 H, J = 13.85), 2.346 (d, 2 H, J = 12.04), 1.64-1.58 (m, 6 H), 1.432 (q, 2 H, J = 7.10 Hz), 0.850 (t, 3 H, J = 7.42 Hz); HRMS (FAB in glycerol)calcd $C_{83}H_{87}N_6O_{13}$ (M + H), 1375.6331; found, 1375.6326.

***N*-(((Propylamino)carbonyl)methyl)-3,6-bis[((cis, cis-2,4-dioxo-1,5,7-tris(hydroxymethyl)-3-azabicyclo[3.3.1]non-7-yl)carbonyl)amino] carbazole (A14).** The benzyl protected cleft **A22** (158 mg, 0.115 mmol), was dissolved in formic acid (10 mL) and placed in an ice bath , $HBr_{(g)}$ was bubbled for 3 min. The yellow solution was concentrated in vacuo to give orange solids which was triturated in 5:1 MeOH/Et_2O (6 mL) mixture overnight. The solids were separated, and washed with ether to give receptor **A14** as off-white solids (100 mg, quant): IR (KBr) 3381, 2933, 2873, 1692, 1544, 1492, 1544, 1492, 1472, 1201, 1058 cm^{-1}; ^1H NMR (300 MHz, DMSO-d_6) δ 10.414 (s,2H), 9.156 (s, 2H), 8.231 (t, 1H, J = 5.54 Hz), 8.176 (s, 2H), 7.454 (d, 2H, J = 8.8 Hz), 7.371 (d, 2H, J = 8.8 Hz), 4.940 (s, 2H), 4.10-3.30 (m, 18H), 3.045 (td, 2H, J = 6.88, 6.03 Hz), 0.852 (t, 3H, J = 7.33 Hz); HRMS (FAB in glycerol) calcd $C_{41}H_{51}N_6O_{13}$ (M+H), 835.3514; found, 835.3520.

2-[((cis, cis-2,4-dioxo-1,5,7-tris(benzyloxy)methyl)-3-azabicyclo[3.3.1] non-7-yl)carbonyl) amino]naphthalene (A24). Acid chloride **A5c**[40] (181 mg, 0.31 mmol) was reacted with β-naphthalene (68 mg, 0.48 mmol) in pyridine (5 mL) with catalytic dimethylaminopyridine. The dark red solution was stirred overnight, and the solvent was removed *in vacuo*. The resulting oil was dissolved in CH_2Cl_2 (15 mL) and washed with 2 N HCl (2 mL). The product was flash chromatographed through a silica gel column (5:2

hexanes/ethyl acetate) to give 53 mg (25%) of product, as a pale pink solid: mp 75-82 °C; IR (KBr) 3100, 2800, 1690, 1680 cm^{-1}; ^1H NMR (250 MHz, $CDCl_3$) δ 8.02 (d, J = 1.8 Hz, 1 H), 7.93 (br s, 1 H), 7.77-7.71 (m, 2 H), 7.62 (br s, 1 H), 7.47-7.15 (m, 19 H), 4.59 (d, J = 12.1 Hz, 2 H), 4.53 (d, J = 12.1 Hz, 2 H), 4.49 (s, 2 H), 3.80 (d, J = 9.2 Hz, 2 H), 3.55 (d, J = 9.2 Hz, 2 H), 3.46 (s, 2 H); 2.55 (d, J = 14.1 Hz, 2 H); 2.45 (d, J = 13.9 Hz, 1 H), 1.78 (d, 13.4 Hz, 1 H), 1.64 (d, J = 14.2 Hz, 2 H); HRMS (EI) calcd for $C_{43}H_{42}N_2O_6$, 682.3042 found, 682.3040.

2-[((cis, cis-2,4-dioxo-1,5,7-tris(hydroxymethyl)-3-azabicyclo[3.3.1]non-7-yl)carbonyl) amino]naphthalene (A15). The benzyl protected host **A24** (53 mg, 0.08 mmol) was dissolved in formic acid (10 mL) at 0 °C. $HBr_{(g)}$ was bubbled through the solution with stirring for 10 min. The solvent was removed under reduced pressure to yield host **A15** as a very pale pink solid (32 mg, quant.) which was precipitated using methanol and CH_2Cl_2: mp 289-290 °C; IR (KBr) 3600-3100, 2800, 1690, 1680 cm^{-1}; ^1H NMR (500 MHz, DMSO-d_6) δ 10.36 (br s, 1 H), 9.32 (br s, 1 H), 8.06 (s, 1 H), 7.82-7.76 (m, 3 H), 7.57 (dd, J = 1.9, 8.7 Hz, 1 H), 7.45-7.38 (m, 2 H), 3.73 (d, J = 7.0 Hz, 2 H), 3.38 (s, 2 H), 3.31 (d, J = 7.0 Hz, 2 H), 2.37 (d, J = 13.8 Hz, 2 H), 2.18 (d, J = 13.0 Hz, 1 H), 1.46 (d, J = 14.1 Hz, 2 H), 1.32 (d, J = 13.0 Hz, 1 H); HRMS (EI) calcd for $C_{22}H_{24}N_2O_6$, 412.1634 found, 412.1632.

2,7-bis[((cis, cis-2,4-dioxo-1,5,7-tris(benzyloxy)methyl)-3-azabicyclo[3.3.1]non-7-yl)carbonyl) amino]naphthalene (A26). Acid chloride **A5c**[40] (496 mg, 0.862 mmol) and 2,7-diaminonaphthalene (5.8 mg, 0.372 mmol) were heated for 2h in 15 mL of refluxing pyridine. The solvent was removed *in vacuo*. The resulting black residue was dissolved in CH_2Cl_2 (50 mL) washed with 1 N HCl (75 mL) and brine (50 mL). The organics were dried over $MgSO_4$, filtered and dried to give reddish brown residue which was flash chromatographed through a silica gel column (20% EtOAc/CH_2Cl_2) to give 249.6 mg (54%) of orange solids: mp 86-90 °C; IR (KBr) 3200, 3000, 1690, 1680 cm^{-1}; ^1H NMR (250 MHz, acetone-d_6) d 9.56 (s, 2 H), 8.76 (s, 2 H), 8.00 (d 2 H, J = 1.5 Hz), 7.67 (d, 2H, J = 8.8 Hz), 7.40 (dd, 2H, J = 2.0, 9.0 Hz), 7.39-7.25 (m, 30 H), 4.60-4.54 (m, 6 H), 3.88 (d, J = 9.0 Hz, 4 H), 3.54 (s, 4 H), 3.52 (d, 4 H, J = 7.2 Hz), 2.69 (d, 4 H, J = 13.8 Hz), 2.53 (d, 2H, J = 13.0 Hz), 1.77 (d, 6 H, J = 13.5 Hz).

2,7-bis[((cis, cis-2,4-dioxo-1,5,7-tris(hydroxymethyl)-3-azabicyclo[3.3.1]non-7-yl)carbonyl) amino]naphthalene (A16). The benzyl protected host **A26** (240.6 mg, 0.1945 mmol) was dissolved in formic acid (12 mL, 98%), cooled to 0 °C, and $HBr_{(g)}$ was bubbled for 15 min followed by argon for 10min. Formic acid was removed under reduced pressure. The resulting brown residue was triturated in diethylether overnight. The solids were triturated in ether then dried to yield 119.8 mg (88%) of pale purple powder. ^1H NMR (300 MHz, DMSO-d_6) δ 10.42 (s, 2 H), 9.28 (s, 2 H), 7.96 (s, 2 H) 7.71 (d, J = 9.0 Hz, 2 H), 7.45 (d, J = 8.7 Hz, 2 H), 4.40-3.90 (br s, 6 H), 3.77 (d, J = 10.5 Hz, 4 H), 3.41 (s, 4 H), 3.33 (d, J = 10.8 Hz, 4 H), 2.39 (d, J = 13.8 Hz, 4 H), 2.20 (d, J = 13.8 Hz, 2 H), 1.48 (d, J = 13.2 Hz, 4 H), 1.34 (d, J = 13.2 Hz, 2 H); HRMS (FAB in glycerol and methanol) calcd for $C_{34}H_{41}N_4O_{12}$ (M + H), 697.2721 found, 697.2716.

4.3 Titrations

Titrations for section 1. Titrations were performed at 283 K on a Varian VXR-500 instrument, in a 9:1 mixture of H_2O/D_2O with 1.0 mM DSS buffered with 10 mM cacodylate buffer to pH = 6.0. Ionic strength of the solution was adjusted with NaCl to 51 or 501 mM. All titrations were done at constant host concentration: aliquots of a solution of 0.35 mM (or 0.50 mM) host and 200 mM (or 30 mM) guest were added to a 0.35 mM (or 0.50 mM) host solution. The resulting curves obtained by following the chemical shift of the imide proton were fitted to the 1:1 binding isotherm[64] with (for 9-ethyladenine and adenosine) or without (for 2',3'-cAMP and 3',5'-cAMP) incorporating guest dimerization. Non-linear least squares regression was used to curve-fit the expeimental data with the Simplex algorithm as implemented in Systat 5.2.[84]

Titrations for section 2. Each of the receptors were titrated with 9-ethyladenine at 3, 9, 15, 21, 27 ± 0.3 °C following the procedure described above and in a previous publication.[40]

4.4 Dimerization Determination

Guest Dimerization Determination for Section 1. The change in chemical shifts of C^2H and C^8H purine protons was monitered at 500 MHz as the concentration of 9-ethyladenine (up to 250 mM) or adenosine (up to 30 mM) was increased in D_2O (or 9:1 mixture of H_2O/D_2O for 9-ethyladenine at 501 mM ionic strength) with 1.0 mM DSS buffered with 10 mM cacodylate buffer to pD (or pH) = 6.0. Ionic strength of the solution was adjusted with NaCl to 51 or 501 mM. For 9-ethyladenine at 51 mM ionic strength, the dimerization constant (Kdim) at 283 K was extrapolated from K_{dim} measurements made at 3, 9, 15, 21 and 27 °C. For 9-ethyladenine at 501 mM ionic strength and adenosine at 51 mM ionic strength, the change in chemical shift was observed at 283 K. The resulting curves were fitted to a dimerization curve using the Simplex algorithm as implemented. The resulting dimerization constants from the two protons (C^2H and C^8H) were averaged.

Guest Dimerization Determination for Section 2.

Dimerization constants for 9-ethyladenine were obtained at 3, 9, 15, 21, 27 ± 0.5 °C from three protons (C^2H, C^8H and ethyl CH_2). These constants were averaged and incorporated into the calculation to determine binding constants. The dimerization at 10 °C was obtained through extrapolation of the five experimentally determined values.

4.5 Stoichiometry Determination

Stoichiometry of complexation for receptors **A14** and **A16** with 9-ethyladenine were determined using the method of Job.[64] Eleven samples containing varying ratios of receptor and 9-ethyladenine in increments of 10% with a combined concentration of 1 mM were prepared using the same buffered solution as in the titrations. NMR of these samples were taken at 10 °C using the same procedure as in the titrations. The change in imide chemical shift was converted to concentration of complex in each sample. Once the concentration of the

complex was determined, this was plotted against the ratio of total receptor to total 9-ethyladenine concentrations.

4.6 Molecular Modelling

All molecular modelling was performed by Dr. M. Morgan Conn on a Silicon Graphics 4D30G+ with MacroModel 3.5X.[85] The conformations of the complexes between **A13** and the cylic adenosine monophosphates were derived by minimization (using the MULT routine and the TNCG algorithm[86]) of 300 structures sampled during a 60-ps stochastic dynamics simulation (300 K, 1.5-fs timestep, all-atom AMBER* force field modified with 6,12-Lennard Jones hydrogen bonding potential and McDonald—Still amide parameters,[87] and GB/SA continuum water solvation[88]) following a 5-ps equilibration period. For simplicity, the hydroxymethyl groups on the Kemp's imide moieties were approximated as methyl groups.

B. EVALUATION OF A LOW BARRIER HYDROGEN BOND ENERGY

1. INTRODUCTION

Unusually strong hydrogen bonds, known as low barrier hydrogen bonds (LBHB), have emerged as a new rationale for the exceptional catalytic abilities of some enzymes.[89-92] The existence of strong hydrogen bonds in solution and especially in the gas phase and the solid state has been established for some time,[93-98] and the criteria for their detection are agreed upon; the energetics involved are harder to assess. Recently, there has been some debate on the magnitude of stabilization of the LBHB, partly due to the lack of extensive solution data on its energetics.[99-103]

Comparison of energies of "normal" hydrogen bonds vs. strong hydrogen bonds in the gas phase have often involved somewhat dissimilar situations[97] such as charged vs. uncharged or conjugated vs. highly conjugated systems (Scheme B1). These problems obscure whether the enhanced strength comes from the short distance and matched pKa[103-106] between the hydrogen bond donor and acceptor or some other factors. For condensed phases, some estimates for the additional stabilization from a LBHB exceed 10 kcal/mol.[91,92,100] This large value has been explained from a rough comparison between the unusually basic proton sponges **B** and **C** with normally basic 1,8-diamino naphthalene **A** and simple allyl dimethylammonium ion **D**.[100]

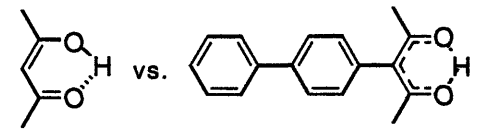

32.8 kJ/mol 117 kJ/mol

$(MeOH)_2$ vs. $[(MeOH)_2H^+]$

32 kJ/mol 131 kJ/mol

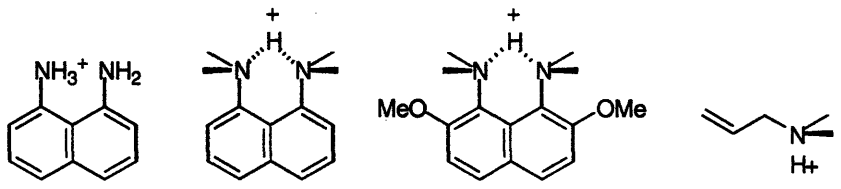

A **B** **C** **D**

$pK_a = 4.6$ $pK_a = 12.3$ $pK_a = 16.1$ $pK_a = 8.8$

Scheme B1

Their explanation is that the extremely strong LBHB formed in the protonated **B** and **C** account for the large increase in pKa's observed in those compounds relative to the similar aromatic diamine **A**. Why **A** does not form such a favorable hydrogen bond is not obvious. However, these two systems are not comparable since **B** and **C** have a very destabilized high-energy unprotonated state compared to the unstrained **A** and **D** (Scheme B1). One of the ways in which a reaction could be made extremely favorable (i.e., energetically downhill) is to raise the ground state energy of the reactant. This concept has been utilized by Staab[107] to design various "proton sponge" -type aromatic diamines which have high pKa's and a ^1H NMR signal in the range of a LBHB shift. In

both **B** and **C**, the size of the methyl groups on the amines does not allow them to be in the same plane as the aromatic. To relieve this unfavorable steric problem, the nitrogens can become sp^3 hybridized with the lone pairs pointing toward each other, but once again the lone pairs create a repulsive destabilizing effect on these free bases. Placing a proton between these two lone pairs relieves the strain in the molecule, leading to an energetically-favorable reaction. The resulting high pKa is due to the largely exothermic nature of the reaction, not the formation of an inherently super-exothermic interaction. The destabilized neutral state is evident from the crystal structure of neutral **B**[108] where the naphthalene is distorted from planarity and the nitrogens are 2.79Å apart (a much larger distance than if the naphthalene were planar and the C_{naphth}—N bonds were parallel, 2.45Å). The crystal structure of **B** showed that the naphthalene is close to planar, and that the nitrogens are 2.60Å apart.[109]

In contrast to the proton sponges where monoprotonation leads to the formation of a LBHB, diacids form such hydrogen bonds when monodeprotonated to the acid-carboxylate.[97] Few examples of those that do and do not form LBHB's are shown below(Table B1). Considering the neutral proton sponge as analogous to a dicarboxylate and the diacid analogous to a diprotonated proton sponge, the difference in these systems is that in diacids, the first pKa is readily observable and in proton sponges the second pKa is readily observable. In both cases, the second pKa involves a conjugate base which is highly destabilized by unfavorable lone pair (and steric for proton sponges) interactions which is releived in the conjugate acid by placing a proton between the lone pairs.

The presence of LBHB's only in conformationally restricted molecules, the absence of intermolecular LBHB in hydrogen malonate, *trans*-1,2-dicarboxy cyclohexane and those which cannot intramolecularly LBHB, all point to a moderately exothermic LBHB. The observation that hydrogen-malonate does not form a LBHB is somewhat puzzling. Perhaps the enolic tautomer allowing conjugation between the two acids is more favorable. There, LBHB does not form because the two oxygens involved in hydrogen bonding no longer have matched pKa's. In *trans*-1,2-dicarboxy cyclohexane, stereoelectronics should favor the axial conformation which does not allow intramolecular LBHB formation. The equatorial conformer appears to be able to form a LBHB, however this is not observed. The absence of intermolecular LBHB in these examples does not mean that it is unheard of in solution. LBHB's have been reported in the solution phase between imidazole—carboxylic acid pairs.[105]

Table B1. Some compounds which form LBHB's and analogues which do not form LBHB's.

Yes LBHB	No LBHB
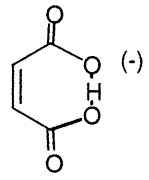 hydrogen-maleate	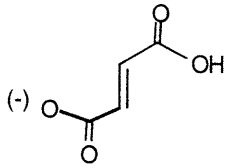 hydrogen-fumarate
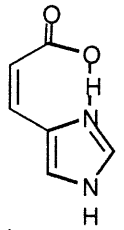 *cis*-urocanate	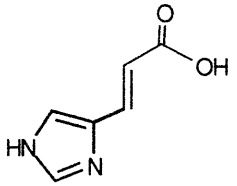 *trans*-urocanate
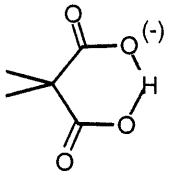 hydrogen-2,2-dimethyl malonate	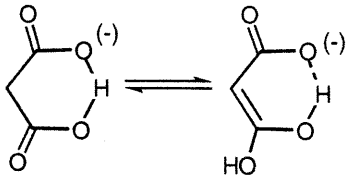 hydrogen-malonate
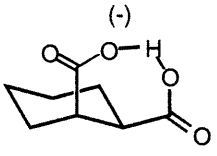 hydrogen-*cis*-1,2-dicarboxy cyclohexane	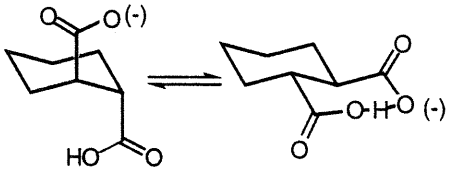 hydrogen-*trans*-1,2-dicarboxy cyclohexane

In contrast to the earlier large energy estimate for the extra stabilization energy from a LBHB, a study that compares enzyme-inhibitor complexes indicates a much more modest value of ~2 kcal/mol.[110] The latter value is in the range for a conventional hydrogen bond determined in enzymes by site directed mutagenesis[3] or in unnatural amino acid replacement experiments.[10] A recent solution study examining diacids in DMSO[111] indicates a slightly higher value of 4.4 kcal/mol . To complement these former findings and estimates, these issues were examined using small molecules in non-polar solutions.

2. XDK DERIVATIVE AS A MODEL COMPOUND

The bulk of this section has been submitted for publication.

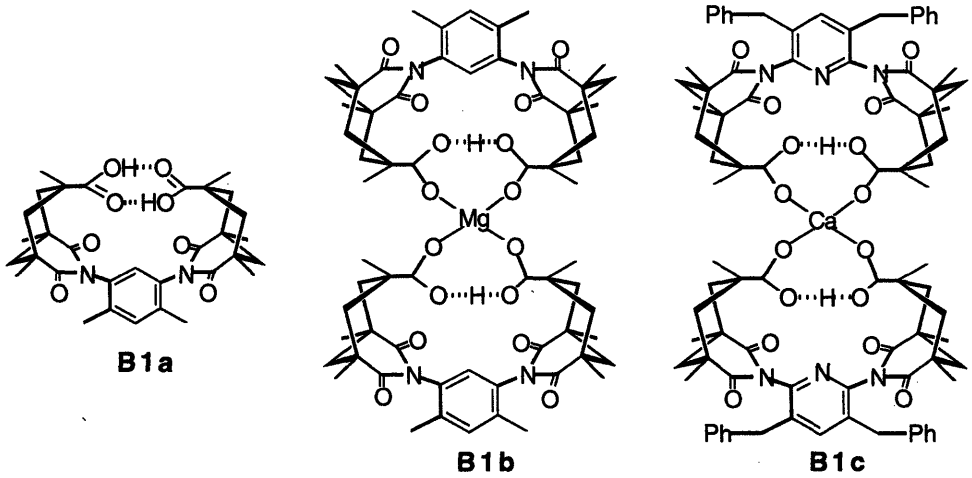

Scheme B2.

The system involving *m*-xylidenediamine-bis(Kemp's triacid)imide (XDK) **B1a** (Scheme B2), a structure of some utility as a model in bioinorganic chemistry[112] was examined first. The diacid **B1a** and salt derivatives **B1b** and **B1c** shown in Scheme B2 have also been studied in the solid state.[113,114] The XDK structure features two carboxylic acids, rigidly locked into a conformation with both acids directed at each other in the sense of a hydrogen-bonded carboxylic acid dimer (Scheme B3).[115] This permits —even enforces— the formation of two intramolecular hydrogen bonds in XDK and provides an unstrained stable diacid. Of the four types of hydrogen bonds that could be formed between two acids (Scheme B3), XDK only allows the syn-syn pattern. Upon deprotonation of XDK, a symmetrical monoanion is obtained (e.g. **B1b** or **B1c**) in which the acid and base components of the intramolecular hydrogen bond are related (i.e., $\Delta pKa = 0$). This balance of pKa's is believed to be an essential feature of the LBHB.

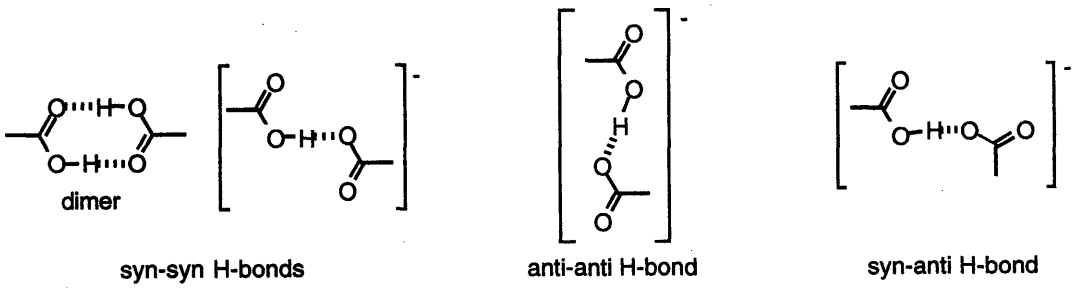

Scheme B3.

The magnesium complex **B1b** in DMSO does indeed show a downfield ^1H NMR signal at 19 ppm, a clear indication of a strongly hydrogen bonded-proton. We had also observed a short hydrogen bond in the crystal structure of calcium complex **B1c**. The relevant O—O distance was 2.43 Å in **B1c**, while in **B1a** the O—O

distance of the two conventional hydrogen bonds were 2.68 Å and 2.69 Å. Diacid **B1a** had also shown peculiar pKa's in aqueous ethanol. The first pKa (4.8) was only slightly lower than that of other analogous diacids under comparable conditions, but the second pKa of 11.1 was remarkably high.[115] We had attributed the large ΔpKa to the packaging of two negative charges in a small volume of space, especially when the more basic syn lone pairs were directed at one another. Large ΔpKa's have also been observed in hydrogen maleate and hydrogen phthalate which form short and strong hydrogen bonds. An unusually strong LBHB in the XDK monoanion might also explain the large ΔpKa in **B1a**, although it is generally believed that such hydrogen bonds cannot persist in polar, protic media, especially in water. In this solvent differential solvation of the carboxylates can create an asymmetric environment that induces polarity to the hydrogen bond.[116,117] Many strong hydrogen bonds however, do show NMR signals consistent with a LBHB in DMSO.[97,111,116,117]

Synthesis

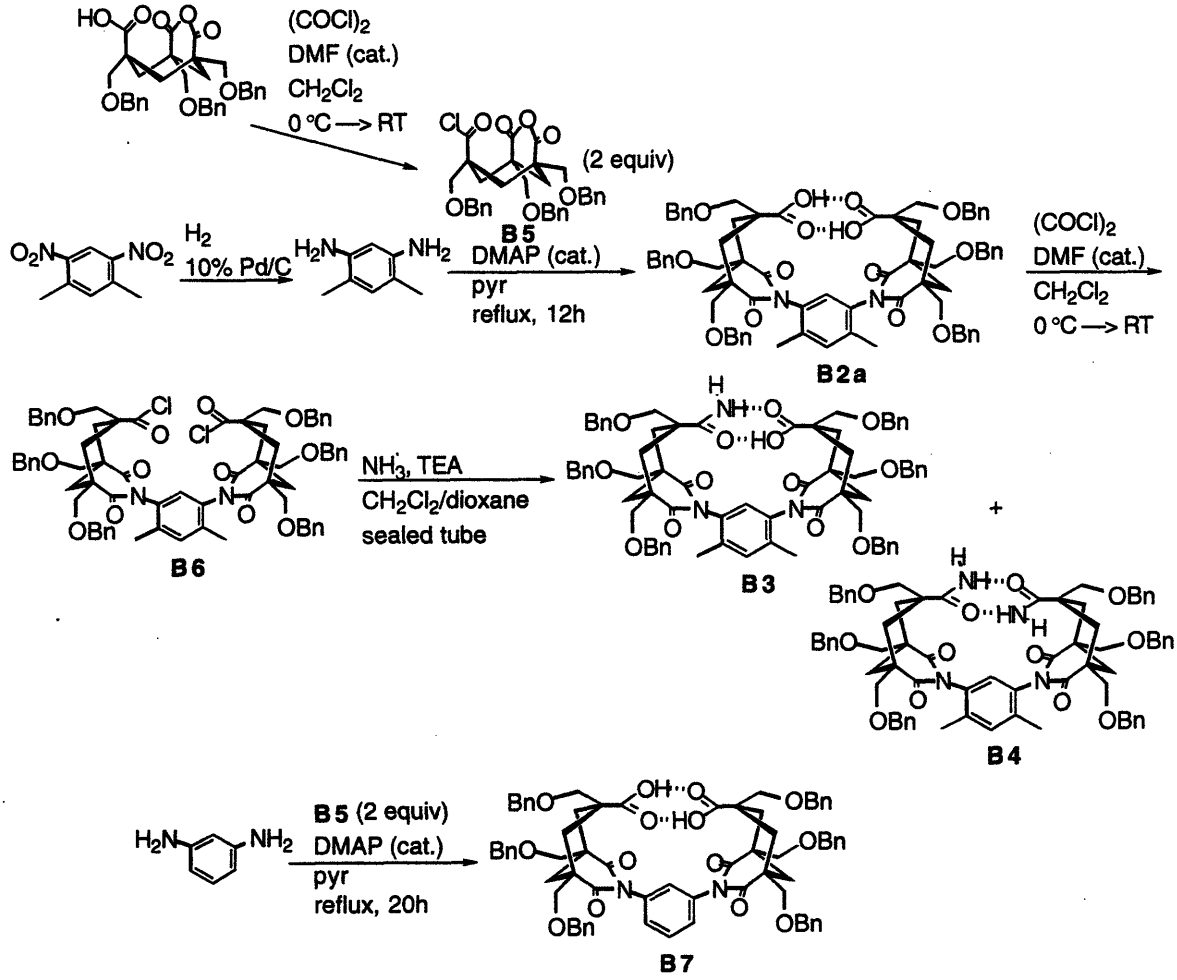

Scheme B4.

In order to evaluate the properties and energy enhancements arising from a syn-syn LBHB in non-polar organic solvents, we synthesized the very lipophilic hexabenzyloxymethyl-XDK diacid **B2a**. At the time these studies were initiated, no examples in solution were available. Recently, Drueckhammer *et. al.* have reported values for the extra stabilization arrising from a LBHB compared to an analogous conventional hydrogen bond in enzyme-inhibitor complexes (2.0 kcal/mol for a syn-anti hydrogen bond pair)[110], and in DMSO solution (4.4 kcal/mol for an anti-anti hydrogen bond pair)[111]. Analogues of **B2a**, monoamide-monoacid **B3** which is also doubly hydrogen-bonded in the neutral state but offers a conventional hydrogen bond to the carboxylate in the anion, a diamide **B4** and *m*-phenylenediamine-bis(Kemp's triacid)imide (PDK) **B7** were also prepared as outlined in Scheme 4. Conversion of benzyloxymethyl-Kemp's anhydride-acid to the acid chloride **B5** proceeded smoothly with oxalyl chloride. This material was used to acylate diaminoxylene (generated by catalytic hydrogenation of dinitroxylene) in refluxing in pyridine to yield XDK diacid **B2a** in 70% yield. The corresponding diacid chloride **B6** was obtained by treatment of **B2a** with oxalyl chloride. When 3 equiv of ammonia was placed with diacid chloride **B6** in the presence of triethylamine (TEA) in a warm sealed tube, diamide **B4** was obtained in 78% yield. When compound **B6** was reacted with 1 equiv of ammonia under the same conditions, both XDK acid-amide **3** (6% yield) and diamide **B4** (16% yield) could be isolated. Phenylene diamine was coupled with **B5** under the same conditions described for the synthesis of **B2a**.

Spectroscopic characterization

A summary of the NMR studies of XDK derivatives **B2a**, **B2c**, **B3** and **B4**, and PDK **B7** is shown in Table B2.

Table B2. Summary of the behavior of XDK derivatives and PDK as seen by ^1H or ^2H NMR.

substrate	solvent	temperature (°C)	acid and/or amide shift (ppm)	counterion	symmetry of Kemps'
B2a	$CDCl_3$ (wet)	room temp	not observed	DABCO	lost
	$CDCl_3$	-15	18.6	Me_4N^+	present
		-15	18.44	TEA•H^+	present
	CD_2Cl_2	25	12.60	none	present
		25	18.0	TEA•H^+	present
		-70	19.2	TEA•H^+	present
		25	16.5	DPG	present
		25	19.4	Ca^{+2}	lost
B2c	CH_2Cl_2	25	11.9	none	—
		-70	17.8	TEA•H^+	—
B7	CD_2Cl_2	25	12.5	none	present
			17.9	TEA•H^+	present
B3	$CDCl_3$	25	13.8, 8.5, 6.0	none	—
		25	11.6, 6.0	TEA•H^+	—
B4	$CDCl_3$	25	8.9, 5.9	none	—

The ^1H NMR signals of silica gel chromatographed diacid **B2a** in $CDCl_3$ was somewhat peculiar. Although the diacid had been subjected to acidic work up before chromatography, the spectrum obtained suggested deprotonation of the acid (Figure E1). The spectrum indicated that the two Kemps' subunits (the cyclohexyl signals) were identical, but a plane of symmetry had been lost; specifically, the symmetry plane defined by the atoms of the xylene was lost. When HCl fumes were blown over the NMR solution using a pipet followed by shaking the tube, the symmetry plane was restored and the spectrum indicated a fully protonated molecule (Figure E2a). The xylyl proton between the two Kemp's imide-acids appeared at 6.6 ppm. From this observation, the first deprotonation of the diacid seemed extremely facile, however the LBHB signal was not observed due to exchange with reseidual water in the solvent.

Titration of diacid **B2a** with various bases could be monitored by ^1H NMR. When less than 1 equiv of 1,4-diazabicyclo[2.2.2]octane (DABCO) was added to the diacid in $CDCl_3$ pretreated with HCl fume, the appearance of the diacid signals was nearly identical to that observed after chromatography (Figure E2b). Addition of excess DABCO did not give a clean spectrum and suggested presence of multiple species. When the solution with excess DABCO was shaken with 1N HCl solution, the wet organic layer showed reappearance of the fully protonated diacid (Figure E2c). This result confirmed that excess base had not decomposed the diacid but had only deprotonated it in an unsymmetrical manner.

When diacid **B2a** was treated with 1.75 equiv of aqueous $Me_4N^+OH^-$, then freeze dried and the residue dissolved in anhydrous $CDCl_3$ at -15 °C, the spectrum showed a monodeprotonated diacid (Figure E3b), retaining a symmetry plane in the Kemp's subunits and a LBHB signal at 18.6 ppm. This LBHB signal could not be observed at room temperature due to intermediate rate of exchange with residual water. Similar treatment with 2.1 equiv of $Me_4N^+OH^-$ gave the monodeprotonated **B2a** with the LBHB signal at 18.7 and a small amount of dicarboxylate (Figure E3c).

The **B2a** • Me_4N^+ salt was then subjected to aqueous 1N HCl. The NMR in anhydrous $CDCl_3$ at -15 °C showed 0.16 equiv of remaining Me_4N^+ and fully protonated **B2a** with slightly broadened signals due to the presence of trace amounts of the monocarboxylate (Figure E4a). Addition of 0.3 equiv of triethylamine (TEA, ~0.5 equiv base including the residual Me_4N^+) yielded a spectrum with broader signals (Figure E4b). When 0.9 equiv TEA was added, the peaks were broad but very similar to that with 1.75 equiv of Me_4N^+ (Figure E4c). The Et_3NH^+ and the LBHB signals were at 9.22 and 18.44 ppm respectively. This suggested that the monodeprotonated species has a counterion dependent structure. When the counter ion is singly charged and non-chelating, such as TEA or Me_4N^+, the monoanion of **B2a** has a symmetric structure on the NMR time scale. However , with the dicationic DABCO, two molecules of **B2a** may be associated to it and give rise to the desymmetrization of the Kemp's subunits. The silica gel chromatographed **B2a**, may be forming a salt with some multicationic metal impurity in the silica.

Titration of diacid **B2a** with TEA in anhydrous CD_2Cl_2 could be conveniently monitored by ^1H NMR at 25 °C (Figure E5). The diacid signal at 12.60 ppm, characteristic of a neutral, normal hydrogen bond, was replaced by a signal at 18.0 ppm expected for a LBHB when 1 equiv of TEA was added (Figure E5c). When the same sample was cooled to -70 °C, the acid signal moved even further downfield to 19.2 ppm and suggests that the LBHB and Et_3H^+ protons are slowly exchanging at 25 °C. When less than 1 equiv of TEA was present at 25 °C, the TEA signals had broadened somewhat but the spectrum retained its symmetrical appearance (Figure E5b). When excess TEA (4 equiv) was added, the peak positions did not change beyond those observed at 1 equiv (Figure E5d). These observations indicate that the second deprotonation of the diacid does not occur under these conditions.

In benzene-d_6 at millimolar concentrations, diacid **B2a** treated with 1 equiv of diphenylguanidine (DPG) produced precipitates and NMR spectra with satisfactory resolution could not be obtained (both diacid **B2a** alone and diphenylguanidine alone were readily soluble in this medium). The precipitate obtained from treatment of diacid **B2a** with 2 equiv DPG in benzene could be filtered and dried *in vacuo* and dissolved in anhydrous CD_2Cl_2. The spectrum was broad compared to the salts formed with TEA or Me_4N^+ but similar with regard to the symmetry of the Kemp's subunits. Accordingly, all three of these salts must exist as a 1:1 acid/base salt that are not bound by chelation. Integration of the NMR spectrum of such samples confirmed a 1:1 ratio of diacid to guanidine and the signal at 16.5 ppm indicated a strongly hydrogen-bonded proton. In the less polar solvent benzene, the monoanion of the diacid is also expected to form a strong hydrogen bond.

Diacid **B7** also formed a LBHB when treated with TEA in CD_2Cl_2 at room temperature. The diacid signal at 12.5 ppm was replaced by a LBHB proton at 17.9 ppm and a TEA•H proton at 8.9 ppm. Diacid **B7** which was dried over $MgSO_4$ after acidic work up contained a small amount of material giving rise to a LBHB signal at 19.06. This is most likely a Mg complex analogous to **B1b** and **B2b**. In all the XDK derivatives (**B2**, **B3**, and **B4**) the methyl groups on the xylene subunit restrict rotation of the imide N—aryl C bond such that the two Kemp's acids are facing each other. The behavior seen with **B7** showed that restriction of rotation of the diacids is not essential to forming the LBHB in this system.

In acid-amide **B3**, the hydrogen bonds formed are of a conventional type in both the neutral and monodeprotonated form. The acid proton chemical shift was at 13.80 ppm and amide protons were observed at 8.50 and 6.03 ppm in $CDCl_3$. When approximately 1 equiv of TEA was added, the acid signal disappeared, and the downfield amide signal moved to 11.6 ppm. This signal, while unusually downfield for an amide, is far upfield from the strong hydrogen bond region (16-20 ppm). The H_E (Scheme B5) signal at 6.0 ppm moved only very slightly. In peptide helices, a much more modest shift (0.22 ppm) was recently observed for a neutral versus charged glutamine–aspartate pair. The hydrogen bond was to the H_E proton of the amide (~7.6 - 7.8 ppm) and the H_Z proton shift (~7.0 ppm) remained unchanged.[8] In diamide **B4**, the chemical shifts of the amide protons were at 8.90 and 5.86 ppm.

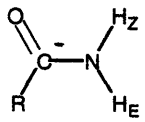

Scheme B5.

A 2:1 diacid/calcium complex **B2b** (Scheme B6) was prepared by treating **B2a** with 0.5 equiv of CaH_2. The acid NMR signal of compound **B2b** in dry CD_2Cl_2 solution was at 19.4 ppm at room temperature. The spectrum was similar to that obtained after chromatography and also with DABCO in $CDCl_3$. The loss of symmetry is consistent with the conformation determined from X-ray analysis (Figure F1-F5). Assuming that the change in chemical shift of the acid proton in these diacids correlates with the distance between the two oxygens, the carboxylate-acid hydrogen bond formed when **B2a** is treated with TEA must be slightly longer than 2.43 Å (**B1c** O—O distance) but shorter than 2.68 Å (**B1a** O—O distance).

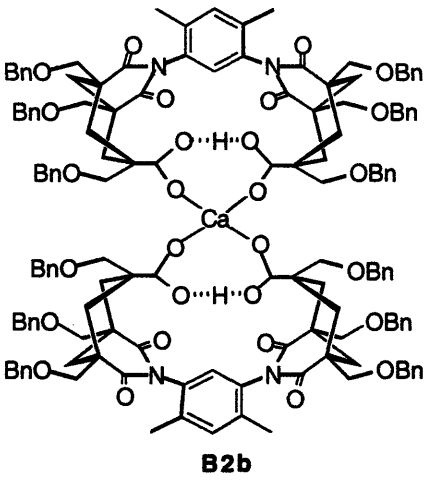

B2b

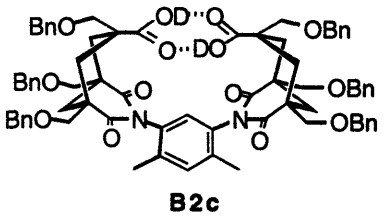

B2c

Scheme B6.

Analogous treatment of **B3** or **B4** with CaH_2 did not yield a Ca(II) complex. However, pretreatment of **B3** with $Me_4N^+OH^-$ in methanol followed by addition of 0.5 equiv $Ca(NO_3)_2$ gave the calcium complex as a mixture of two different species. Assuming that the complex adopts a similar structure to **B2b** three diastereomers can form, two enantiomeric and one achiral diastereomer. Accordingly, two signals for the hydrogen bonded H_Z amide shifts were observed in $CDCl_3$ (11.6, 11.4 ppm).

^1H NMR of **B2a** with and without TEA in 1:1 $CD_3OH/CDCl_3$ was taken with suppression of the methanol OH signal.[62,63] As anticipated, a LBHB signal was not observed in this protic medium. The acid proton signal was never observed in both the diacid and the monodeprotonated **B2a** at room temperature. TEA•H^+ signal was clearly observed.

A deuterium isotope shift experiment[118] revealed that the strong hydrogen bond in the monoanion of **B2a** was a double-well low-barrier hydrogen bond. The acid protons were exchanged with deuterium and ^2H NMR of

B2c (Scheme B6) in the neutral form and in the monoanion form were taken in dry CH_2Cl_2. The diacid signal at room temperature moved to 11.86 ppm, a $\Delta[\delta H - \delta D]$ of 0.74 ppm. The chemical shifts and the isotope shift is in the range expected for a conventional strongly hydrogen bonded system. When 1 equiv of TEA was added, an extremely broad peak spanning from 7 to 15 ppm was observed at room temperature. When this sample was cooled to -70°C, a less broad peak at 17.8 ppm for the acid deuteron was observed. An energy barrier for the deuterium transfer between the two oxygens was confirmed from the sizable positive $\Delta[\delta H - \delta D]$ value of 1.4 ppm (typically, these isotope shifts are < 1 ppm at room temperature).[118] From the chemical shift values and the isotope shifts, the diacid forms a conventional hydrogen bond, whereas the monoanion forms a LBHB, rather than a single-well, hydrogen bond (Figure B1).

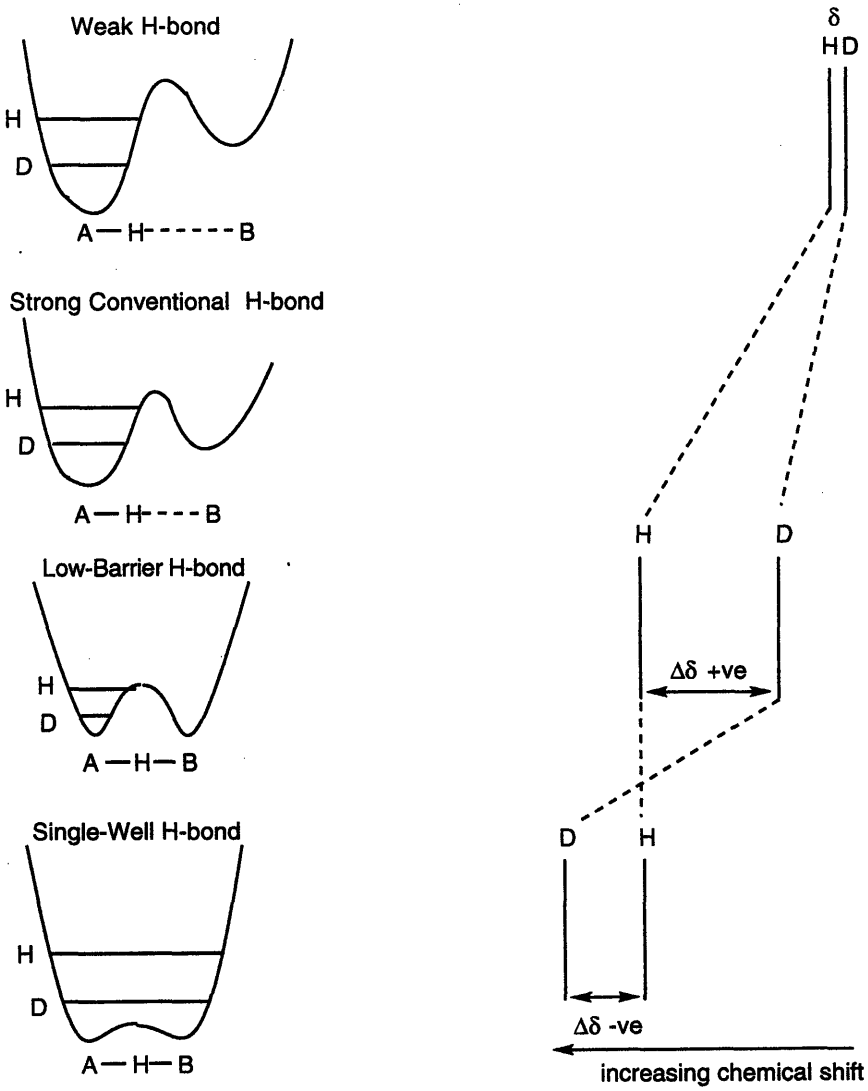

Figure B1. Different types of hydrogen bonds (where A is the hydrogen bond donor atom and B is the hydrogen bond acceptor atom), their proton transfer energy profile, and their isotopic NMR shifts $\Delta[\delta H - \delta D]$.

Crystallography

Recrystallization from CH_2Cl_2 and iso-octane yielded single crystals suitable for X-ray structure determination. A single crystal X-ray diffraction analysis performed by Dr. Leticia M. Toledo unambiguously defined the structure of **B2b** (Figure F1-F5). The overall geometry of **B2b** was analogous to that obtained earlier for **B1c**. The O—O distance of the short hydrogen bond was 2.42 Å, within the range for a LBHB. This short bond was in the same plane as the xylene atoms of **B2b**, causing the cyclohexyl rings of the Kemp's imide-acid to be tilted out of the plane of xylene . The calcium had octahedral coordination with two molecules of **B2b** positioned in the equatorial plane and two water molecules coordinated in the axial positions. The oxygen of the water molecule was coplanar with the carbonyl oxygens of the two imides, and each hydrogen of the water formed a hydrogen bond to the carbonyl oxygens of the two imides. The CH_2Cl_2 molecule filling the void cavity on the face of the xylene opposite the calcium had the two chlorine atoms in close proximity (~3.5 Å) to the acid and imide oxygens.

Equilibria and energetics

In general, direct measurement of pKa's in non-polar organic solvents is not facile,[119] but some organic soluble indicators have been devised to measure acid-base equilibria.[120-125] For the cases at hand, the deprotonation equilibria of **B2a** and **B3** with diphenyl guanidine (DPG) were determined in benzene using a well-developed procedure[120,122] involving the indicator dye bromophthalein magenta E (BME). The indicator was also applied using TEA as the base in CH_2Cl_2 at 25°C. The equilibrium constants for indicator-base complex formation and the maximum absorbance for the complex was either known or could be predetermined (Table B3).

Table B3. K_{eq}, λ_{max}, and maximum absorbance for the reaction of bromophthalein magenta E and base at 25 °C.

solvent	base	K_{eq} of complex formation	λmax of indicator-base complex	indicator concentration	absorbance$_{max}$ at 10mm cell length
benzene	diphenyl guanine[a]	2.5×10^5 M^{-1}	540 nm	2.5×10^{-5}	1.017
CH_2Cl_2	triethylamine[b]	7.0×10^4 M^{-1} ± 20%	577 nm	2.5×10^{-5}	0.98 ± 0.04

[a] Literature values[120] for K_{eq}, λ_{max}, and absorbance$_{max}$ were used. [b] K_{eq}, λ_{max}, and absorbance$_{max}$ were determined from a constant indicator UV titration.

The equilibrium constants for the deprotonation of the XDK derivatives were calculated using equation (B17).[120] The derivation of this equation is shown below (equations (B1)-(B17)).

$$I + B \xrightarrow{K_I} IB \qquad \text{I = indicator; B = base; IB = indicator-base complex} \qquad \text{(B1)}$$

$$K_I = \frac{[IB]}{[I][B]} \qquad \text{(B2)}$$

$$X + B \xrightarrow{K_X} XB \qquad X = XDK \tag{B3}$$

$$K_X = \frac{[XB]}{[X][B]} \tag{B4}$$

from equations (B2) and (B4),

$$[B] = \frac{[IB]}{[I]K_I} = \frac{[XB]}{[X]K_X} \tag{B5}$$

$$[I]_T = [IB] + [I] \qquad [I]_T = \text{total concentration of indicator} \tag{B6}$$

$$[X]_T = [XB] + [X] \qquad [X]_T = \text{total concentration of XDK} \tag{B7}$$

$$[B]_T = [IB] + [B] + [XB] \qquad [B]_T = \text{total concentration of base} \tag{B8}$$

$$[IB] = \frac{A}{A_{max}}[I]_T \qquad A = \text{observed absorbance; } A_{max} = \text{maximum absorbance at } [I]_T \tag{B9}$$

from equations (B6) and (B9),

$$[I] = [I]_T - \left(\frac{A}{A_{max}}[I]_T\right) = \left(\frac{A_{max} - A}{A_{max}}\right)[I]_T \tag{B10}$$

from equations (B5), (B9) and (B10),

$$[B] = \left(\frac{A}{A_{max}}[I]_T\right)\left(\frac{A_{max}}{A_{max} - A}\right)\left(\frac{1}{[I]_T K_I}\right) = \frac{A}{(A_{max} - A)K_I} \tag{B11}$$

from equations (B8), (B9) and (B11),

$$[XB] = [B]_T - \left(\frac{A}{A_{max}}[I]_T\right) - \left(\frac{A}{(A_{max} - A)K_I}\right) \tag{B12}$$

$$[B]_T = n[I]_T \qquad n = \text{equivalents of base wirh respect to } [I]_T \tag{B13}$$

from equations (B12) and (B13),

$$[XB] = \left(\frac{nA_{max} - A}{A_{max}}\right)[I]_T - \left(\frac{A}{(A_{max} - A)K_I}\right) \tag{B14}$$

from equations (B7) and (B14),

$$[X] = [A]_T - \left[\left(\frac{nA_{max} - A}{A_{max}}\right)[I]_T - \left(\frac{A}{(A_{max} - A)K_I}\right)\right] \tag{B15}$$

define:

$$x = \left(\frac{nA_{max} - A}{A_{max}}\right)[I]_T$$
$$y = \frac{A}{(A_{max} - A)K_I} \tag{B16}$$

from (B4), (B11), (B14), (B15) and (B16),

$$K_X = \frac{\bar{x} - y}{\{[A]_T - (x-y)\}y} \qquad \text{(B17)}$$

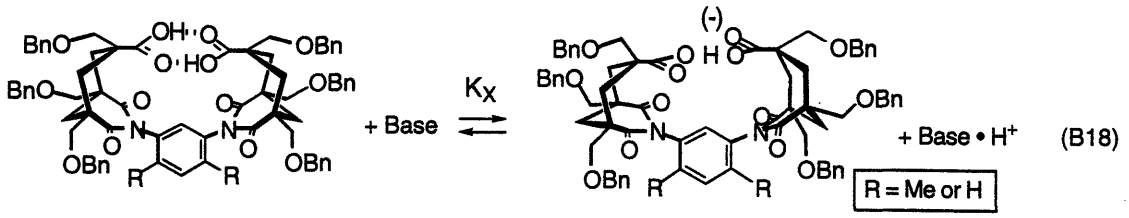

(B18)

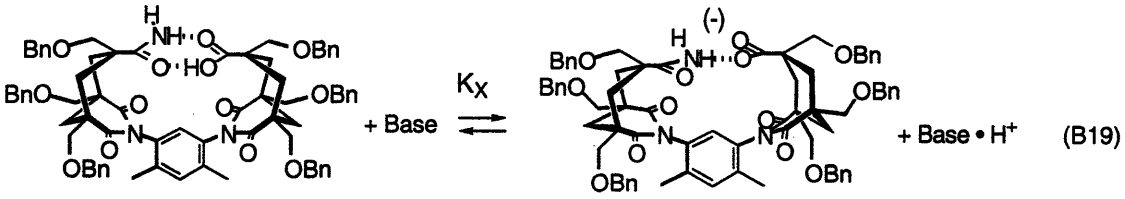

(B19)

Table B4. K_X of reactions (B18) and (B19) at 25 °C calculated from absorbance readings at the indicated base and substrate equivalents.

diphenyl guanidine (DPG) in benzene						triethylamine (TEA) in CH_2Cl_2			
Diacid **B2a**		Acid–Amide **B3**		Diacid **B7**		Diacid **B2a**		Acid–Amide **B3**	
equiv[a] DPG, **B2a**	K_X (x 10^6)	equiv[a] DPG, **B3**	K_X (x 10^4)	equiv[a] DPG, **B7**	K_X (x 10^6)	equiv[a] TEA, **B2a**	K_X (x 10^4)	equiv[a] TEA, **B3**	K_X (x 10^3)
0.5, 1	2.49	0.26, 1	3.95	0.5, 1	6.60	0.3, 2	6.36	0.2, 2	5.24
0.5, 2	2.24	0.26, 2	2.54	0.5, 2	4.65	0.5, 3	7.15	0.2, 3.2	4.42
0.5, 4	2.29	0.26, 4	1.53	0.5, 4	6.73	0.5, 4	6.99	0.2, 5.2	2.96
0.5, 6	2.23	0.5, 4	1.39	0.5, 6	2.49	0.5, 5	7.06	0.2, 7.2	2.49
1, 2	2.43	0.5, 8	2.03	1, 2	6.70	0.5, 7	6.80	0.2, 10	2.06
1, 4	2.08	0.5, 10	2.57	1, 4	4.41	0.5, 10	6.39	0.2, 1	5.78
1, 6	2.09	0.5, 15	2.41	1, 6	3.41	1, 1	6.50	0.2, 2	2.88
2, 4	2.15	1, 1	2.62	2, 4	7.03	1, 2	6.62	0.2, 5	6.71
2, 6	2.00	1, 2	1.33	2, 6	4.13	1, 6	6.24	0.2, 7	2.38
4, 5	2.54	1, 8	1.66	2, 10	3.53	1, 10	6.36	0.2, 10	3.66
		1, 10	1.36	4, 10	3.44			0.3, 2	2.28
								0.3, 4	2.48
								0.3, 6	2.33

[a]Indicator concentration (2.5 x 10^{-5} M) is taken as 1 equiv.

The change in absorbance of the indicator-base complex was monitored at constant indicator concentration (2.5 x 10^{-5} M = 1 equiv). The concentration of base (0.14 - 4 equiv) and XDK derivative (1 - 15 equiv) were varied. The concentration of diacid **B2a** was always greater than that of the base, so only the first deprotonation was

involved in the experiments (Table B4). At least 10 such measurements were made. The equilibrium constants (K_X) determined for the acid-base reaction (B18) and (B19) are summarized in Table B5.

Table B5. K_X of reaction (B18) and (B19), and ΔG of single deprotonation to form a charged hydrogen bond after statistical correction for diacid.

solvent	base	substrate	number of measurements	K_X (sd)[a]	ΔG (kcal/mol)
benzene	diphenyl guanine	**B2a**	10	2.25×10^6 (1.8×10^5)	-8.3 ± 0.1
		B3	11	2.17×10^4 (7.5×10^3)	-5.9 ± 0.3
		B7	11	4.83×10^6 (1.6×10^6)	-8.7 ± 0.2
CH_2Cl_2	triethylamine	**B2a**	10	6.65×10^4 (3.1×10^4)	-6.2 ± 0.4
		B3	13	3.51×10^3 (1.5×10^3)	-4.8 ± 0.3

The deprotonation of diacids **B2a** and **B7** were more favorable than the deprotonation of acid-amide **B3** in accord with the expected effects of a LBHB formed in reaction (B18) but not in reaction (B19). Control experiments, using various amounts of diamide **B4** and the indicator-base solution, showed that the absorbance remained constant within experimental error. This confirmed that the non-acidic portions of the molecule did not effect the equilibrium or alter the absorption of the indicator-base complex.

From the K_{eq} for equations (B18) and (B19), the energy of a single deprotonation to form a charged hydrogen bond was calculated, using a statistical correction for the two acid sites for the deprotonation of **B2a** and **B7** (Table B5). Energies of deprotonation were similar for diacids **B2a** and **B7** in benzene. This supports the earlier finding from ^1H NMR analysis that restriction of conformation of the hydrogen bonding moiety is not necessary to form a LBHB. As indicated by the NMR studies described above, the charged hydrogen bond resulting from the monodeprotonation of the diacids are LBHB's, whereas the charged hydrogen bond from deprotonation of the acid-amide is an unexceptional hydrogen bond. The difference in the free energies involved for **B2a** and **B3** can be attributed to the extra stabilization energy arising from a charged LBHB. The values in benzene and CD_2Cl_2 were determined to be -2.4 kcal/mol and -1.4 kcal/mol, respectively.

The result confirms that a stronger and shorter charged hydrogen bond can result when the pKa's are matched (i.e., the acid and base are conjugates of each other). This is in substantial agreement with the results obtained by Drueckhammer *et. al.* Comparison of enzyme-inhibitor complexes of citrate synthase showed that the complex containing one extremely short syn-anti hydrogen bond is ~2 kcal/mol more stable than the complex with a pKa mismatched hydrogen bond with a longer heteroatom distance at the analogous position.[110] Subsequent report on this enzyme-inhibitor complex showed that the binding site of this enzyme forces formation of a short hydrogen bond regardless of the pKa of the substrate.[106] Cis/trans alkene isomerization study of citraconic and mesaconic acids and their acid-amide derivatives (Figure B2) in DMSO (the first report on experimentally determined energies of LBHB in solution) showed that the slightly pKa mismatched anti-anti

LBHB formed in this system was 4.4 kcal/mol more stable than a pKa mismatched hydrogen bond formed in the analogous acid-amide derivative.[111] This energy difference is also thought to include the difference in polarization between amide-carboxylate and acid-carboxylate and its influence on the isomerization. The XDK derivatives studied in this section have no restriction of distance between the hydrogen-bonded functionalities and should allow a more accurate energy assessment of precisely pKa matched LBHB.

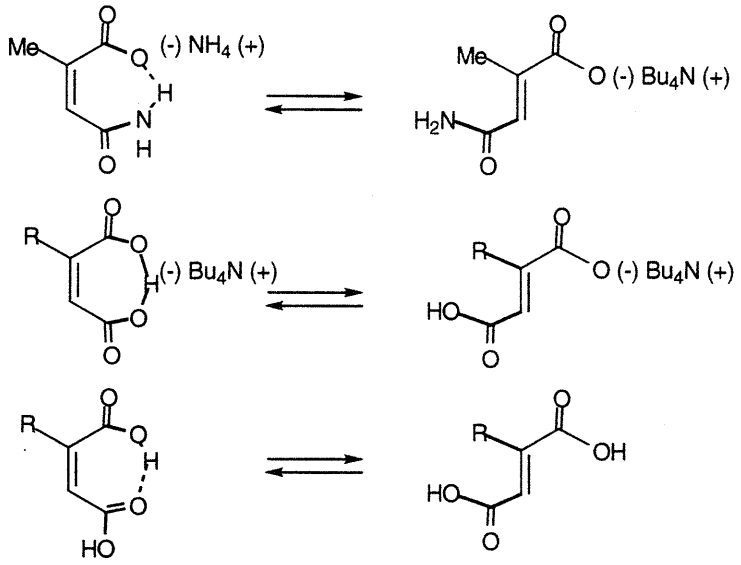

mesaconic acid citraconic acid

Figure B2. Mesaconic and citraconic acid derivatives studied by Drueckhammer *et. al.*[111]

3. KEMP'S HISTIMIDE ACID DERIVATIVES AS MODEL COMPOUNDS

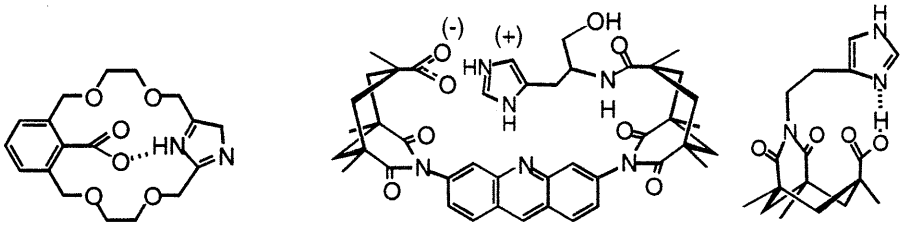

Zimmerman Rebek

Scheme B7.

Many model systems of serine proteases have been studied to elucidate its catalytic actitvity.[126-134] The arrangement of His and Asp, where the imidazole N^3 is hydrogen bonded to the syn lone pair of the carboxylate recur in active sites of enzymes such as serine proteases,[135-138] malate and lactate dehydrogenases,[139] thermolysin[140] and DNAse I,[141] and model systems with imidazole and acid precisely arranged in that orientation has been studied in the past.[127,128] Zimmerman's macrocyclic system and Kemp's triacid derivatives developed in our laboratory (Scheme B7) showed how pKa of imidazole and acid are affected by the presence

of each other in water. Presentation of the syn lone pair of the carboxylic acid to the imidazole shifted the imidazole pKa by +1.5 units, whereas presentation of the anti lone pair shfted the pKa by only < +1 unit. Conversely, presentation of imidazole to a syn lone pair shifted the carboxylic acid pKa by only -0.2 pKa units, whereas presentation to an anti lone pair shifted the acid pKa by approximately -1.5 pKa units. Another finding from the Kemp's histimide-acid derivative was that when similar pKa measurements of the imidazole and acid were repeated in an EtOH / H_2O mixture, the pKa of the imidazolium decreased and the acid increased such that the ΔpKa's were half of what it was in aqueous solution. Extrapolation of this phenomenon into a less polar environment could bring the pKa's of the functionalities closer together.

The active site triad of chymotrypsin has a low field signal in the NMR spectrum[142-144] and a recent study of the catalytic triad of serine proteases has presented spectroscopic evidence that a LBHB participates in catalysis.[92] In the low dielectric of the enzyme active site, the imidazole and acid are thought to have matched pKa's leading to the formation of a LBHB.[91,92] Observation of several complexes formed between carboxylic acids of various pKa's and methyl imidazole in solution by ^{1}H NMR has shown that as the pKa's of the acid approached that of methyl imidazole, the chemical shift for the hydrogen-bonded proton moved downfield within the LBHB range.[105] However, this bimolecular association cannot be forming a well-defined structure where the relevant syn lone pair of the acid is presented to the imidazole. Therefore, analogues of the former Kemp's histimide-acid **B8** and **B9** were prepared and examined (Scheme B8).

Synthesis

As described previously,[127] histamine was acylated with anhydride acid chloride **B5** in refluxing pyridine to yield histimide-acid **B8** (15% yield, not optimized). Analogously, *N*-methyl-4-histamine was acylated with **B5** to yield methyl histimide-acid **B9** in good yield (Scheme B8).

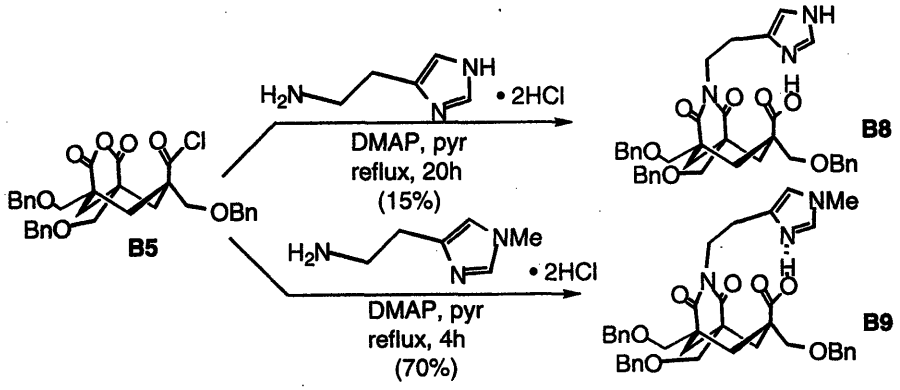

Scheme B8.

Spectroscopic Characterization

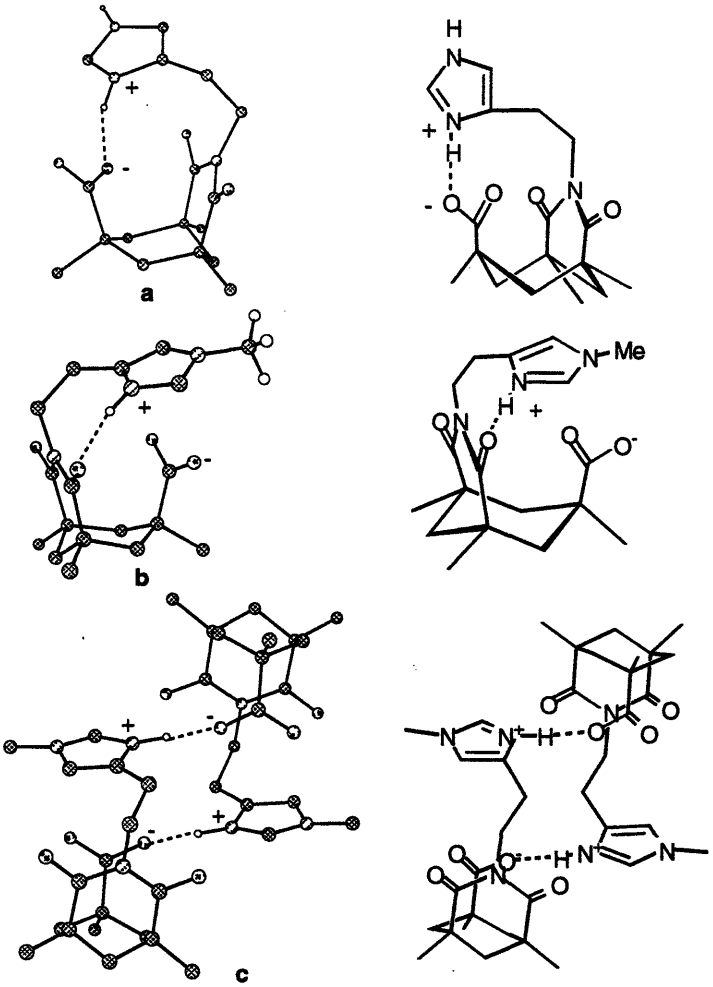

Figure B3. Probable conformations of **B8** and **B9** as minimized by macromodel.

In contrast to the XDK derivatives, these molecules have flexibility and can exist in several different conformations. Some representative conformations are shown in Figure B3. Conformation **a** with an intramolecular hydrogen bond between the imidazole and acid should keep the two sides of the Kemp's cyclohexyl ring in a similar environment and show an NMR spectrum with retention of the plane of symmetry in the Kemp's subunit. Conformation **b** with an intramolecular hydrogen bond between the imidazole and imide carbonyl will desymmetrize the Kemp's subunit and this desymmetrization should be manifested in the NMR spectrum. Dimers with conformation **c** can also form giving rise to desymmetrization of the Kemp's subunits.

The ^{1}H NMR of **B8** in $CDCl_3$ at room temperature was a very sharp spectrum. The plane of symmetry of the Kemp's subunit was lost and the three axial and equatorial protons of the cyclohexyl ring had different chemical shifts. The imidazole NH's appeared not to be hydrogen-bonded and had two signals at 7.55 and 7.70 ppm. The acid proton could not be located in the spectrum and must therefore be exchanging with residual water.

The loss of symmetry and the two shifts for the NH proton suggested the presence of two conformations, possibly **b** and **c**.

An analogous spectrum of **B9** was, in contrast, a very broad spectrum. The plane of symmetry of the Kemp's subunit was conserved. Once again, the acid proton could not be located in the spectrum. These observations suggested that this molecule was in a dynamic exchange between conformations including **a** which is most likely to yield a symmetrical set of signals for the Kemp's moiety.

In earlier studies with the XDK derivatives, anhydrous CD_2Cl_2 facilitated the observation of the exchangable protons. When **B8** was dissolved in CD_2Cl_2 at 25 °C, the spectrum was identical to that in $CDCl_3$ (Figure E6a). When this was cooled to -70 °C, the signals below 10 ppm sharpened and resolved even further (Figure E6e). Above 10 ppm, no signals were found.

When **B9** was dissolved in CD_2Cl_2 at 25 °C, the spectrum was similar to that in $CDCl_3$ below 10 ppm (Figure E7a), but an acid signal was clearly observable as an extremely broad singlet at 11 ppm (Figure E8a). At 0 °C, this broad singlet moved to 12 ppm (Figure E8b), and at -25 °C, a small broad singlet appeared at 14.2 ppm while the broad hump moved to 13.5 ppm (Figure E8c). As the sample was cooled further to -50 °C, the small singlet split into two even smaller singlets at 14.0 and 19.5 ppm and the now extremely broadened hump was centered around 16 ppm (Figure E8d). The low-intensity 19.5 ppm signal was clearly in the range for a LBHB while the 14.0 ppm was still in the range for a conventional hydrogen bond. Further cooling yielded a curious incomprehensible result. Four new peaks at 14.45, 14.42, 10.40, 10.27 ppm appeared while the 19.5 and 14.0 ppm peaks remained in place and the broadened hump moved to 18 ppm (Figure E8e). The intensity of the 19.5 ppm signal increased while the 14.0 ppm signal diminished considerably. Meanwhile, the signals below 10 ppm broadened further upon cooling (Figure E7e).

In summary, the mere presence of a methyl substituent on the imidazole altered the behavior of compounds **B8** and **B9** in solution. The symmetry features cannot be explained at this point and further studies may yield enlightening results. Perhaps the presence of the methyl group allowed formation of a LBHB in compound **B9**. If that is the case, formation of a LBHB did not eliminate formation of other non-LBHB-ing conformations, as evident from other hydrogen bonded signals above 10 ppm and the broadened signals below 10 ppm. This is in accord with the recent findings by others [110] and also from our previous experiments with XDK derivatives that LBHB provides only a moderate additional stabilization energy compared to a conventional hydrogen bond.

4 EXPERIMENTAL

4.1 General.

Air-/water-sensitive reactions were performed in flame-dried glassware under argon. Tetrahydrofuran and

dioxane were distilled from Na / benzophenone ketyl. Methylene chloride was distilled from P_2O_5. Unless otherwise stated, all other commercially available reagents were used without further purification.

NMR spectra were obtained on Bruker AC-250, Varian XL-300, Varian UN-300, and Varian VXR-500 spectrometers. All chemical shift values are reported in parts per million. Spectra taken in $CDCl_3$ were referenced to residual $CHCl_3$ (7.26). Spectra taken in DMSO-$d_6$were referenced to residual solvent (2.49). Fourier transform infrared spectra were taken on a Perkin-Elmer infrared spectrometer. UV measurements were taken on a Perkin-Elmer Lambda2 spectrophotometer. High-resolution mass spectra were obtained with a Finnegan Mat 8200 instrument. Melting points were taken on a Elctrothermal 9100 melting-point apparatus. Flash chromatography[82] was performed using Silica Gel 60 (ICN, 230-400 mesh).

4.2 Synthesis

Anhydride acid chloride B5. Oxalyl chloride(120 μL, 8 equiv) was added to a cooled (ice bath) solution of anhydride acid **A5a** (100 mg, 0.174 mmol) in CH_2Cl_2 (5 mL) and DMF (5 μL), and was stirred for 5 min. The solution was warmed to room temperature and stirred overnight. Solvent was then removed *in vacuo* and the resulting white solid was used immediately without further purification.

2,4-Bis{((cis,cis-2,4-dioxo-1,5,7-tris-((benzyloxy)methyl)-3-azabicyclo[3.3.1]non-7-carboxylic acid-*m*-xylene (B2a.). 2,4-Dinitro-*m*-xylene (176 mg, 0.897 mmol) and 10% Pd-C (18 mg) in tetrahydrofuran (4 mL) was stirred under a H_2 atmosphere at room temperature for 24h. The reaction mixture was filtered through Celite and then concentrated in vacuo to give a faintly purple crystalline solid. This was immediately treated with acid chloride **B5** (1.00 g, 1.74 mmol), and DMAP (2 mg, 0.016 mmol), dissolved in pyridine (30 mL) and the mixture was heated under reflux for 18 h under Ar. The reaction mixture was concentrated and the brownish yellow residue was taken up in EtOAc. The organic phase was washed with 1N $HCl_{(aq)}$ (2 x 50 mL) and brine (50 mL), then dried over Na_2SO_4, filtered and concentrated in vacuo. The resulting residue was purified using flash chromatography through a silica gel column (20, 30, 40% EtOAc/CH_2Cl_2) to give crude diacid **B2a** (778 mg, 70%). This was recrystallized from CH_2Cl_2/Et_2O to give 608 mg (56%) of pure **B2a** as white solid: mp 187.6-188.4 °C; IR (KBr) 3488, 2862, 1735, 1686, 1648, 1453, 1364, 1192, 1097, 737, 697 cm^{-1}; ^1H NMR (500 MHz, DMSO-d_6) δ 18.70 (br s, 1 H), 7.32-7.23 (m, 31 H), 6.982 (s, 1 H), 4.486 (s, 8 H), 4.437 (s, 4 H), 3.802 (d, 4 H, J = 8.8 Hz), 3.348 (d, 4 H, J = 8.8 Hz), 3.197 (s, 4 H), 2.588 (d, 2 H, J = 12.7 Hz), 2.343 (d, 4 H, J = 13.2 Hz), 1.792 (s, 6 H), 1.591 (d, 4 H, J = 12.2 Hz), 1.536 (d, 2 H, J = 12.7 Hz); HRMS (FAB in 3-nitrobenzyl alcohol) calcd for $C_{74}H_{77}N_2O_{14}$ (M + H), 1217.5375; found, 1217.5382.

Deuterated Diacid B2b. Diacid **B2a** was dissolved in CH_2Cl_2 and washed with 1N DCl in D_2O (3 x 8 mL). The organic phase was separated, concentrated, and dried in a vacuum desiccator.

Diacid Calcium Complex B2c. Diacid **B2a** (30 mg, 0.025 mmol) and CaH_2 (0.5 mg, 0.5 equiv) were placed in dry benzene (1 mL) and stirred at room temperature for 1 h. The solution was filtered through glass wool and concentrated in vacuo: mp 200.9-203.2 °C; IR (KBr) 3488, 2862, 1735, 1686, 1648, 1453, 1364, 1192, 1097, 737, 697 cm^{-1}; ^1H NMR (300 MHz, CD_2Cl_2) δ 19.4 (br s, 2 H), 7.36-7.12 (m, 62 H), 7.028 (s, 2 H), 4.58-4.47 (m, 16 H), 4.394 (d, 4 H, J = 12.2 Hz), 4.281 (d, 4 H, J = 11.7 Hz), 3.964 (d, 4 H, J = 8.8 Hz), 3.912 (d, 4 H, J = 9.3 Hz), 3.51-3.44 (m, 12 H), 3.349 (d, 4 H, J = 8.3 Hz), 2.769 (d, 4 H, J = 13.2 Hz), 2.676 (d, 4 H, J = 13.2 Hz), 2.590 (d, 4 H, J = 14.2 Hz), 1.91-1.84 (m, 16 H), 1.702 (d, 4 H, J = 12.7 Hz), 1.629 (d, 4 H, J = 13.2 Hz).

Single Crystal X-ray Diffraction Analysis of Diacid Calcium Complex B2c. Compound **B2c** crystallized as clear rods from slow diffusion of iso-octane into CH_2Cl_2 containing **B2c**. X-ray diffraction analysis of **B2c** was performed by Dr. Leticia M. Toledo. A specimen with approximate dimensions 0.4 x 0.3 x 0.3 x mm was selected for analysis and was mounted on a fiber embedded in a matrix of Paraton N. Data were collected at -66 °C on a Siemens CCD diffractometer (equipped with an automated 3 circle goniometer and a solid state generator) using graphite-monochromatized Mo, K_α (0.710690 Å) by the ω scan method operating under the program SMART.[145] A total of 15 frames at 20 seconds measured at 0.3 ° increments of ω at three different values of 2θ and φ were collected, and after least squares, a preliminary unit cell was obtained. For data collection three sets of frames of 20 second exposure were collected. Data were collected in three distinct shells. For the first shell, 606 frames were collected with values of φ = 0° and ω = -26°. For the second shell, 435 frames were collected with φ = 88° and ω = -21°, and for the third shell, values of φ = 180° and ω = -23° were used to collect 230 frames. At the end of the data collection, the first 50 frames of the first shell were recollected to correct for any crystal decay, but no anomalies were observed. The data were integrated using the program SAINT.[146] The integrated intensities of the three shells were merged into one reflection file. Thbe data were filtered to reject outliers based on the agreement of the intensityu of the reflection and the average of the symmetry equivalents to which the reflection belongs. A total of 26381 reflections were measured, ($2\theta_{max}$ = 46.6°) of which 9955 (R_{int} for averaged reflections = 0.06).

Systematic extinctions and crystal density were consistent with monoclinic space group $P2_1/n$ with half the molecule, one CH_2Cl_2 and one water of composition $C_{75}H_{80}N_2O_{15}Cl_2Ca_{0.5}$ forming the asymmetric unit. The unit cell dimensions were a=16.631(1), b=23.990(2), and c=17.267(1) Å, β=95.9645(1)°, V=6852.0(6) $Å^3$ with Z=4. The structure was solved using the direct methods program Sir92 of the TeXsan[147] crystallographic package of the Molecular Structure Corporation. The final full-matrix least-squares refinements with 4477 reflections (2.7°<2θ<40.9°, I>3σ) with anisotropic thermal parameters for all nonhydrogen atoms, and located and riding isotropic hydrogens converged smoothly to a final R = 0.072, Rw = 0.085. A computer-generated perspective model of the final model is given in Figure F1.

Diacid chloride B6. Oxalyl chloride (100 μL, 14 equiv) was added to diacid **B2a** (100 mg, 0.082 mmol) dissolved in CH_2Cl_2 (15 mL) and DMF (5 μL) and cooled in an ice bath. After stirring for 10 min, the bath was removed and stirred for 3 h at room temperature. The clear solution gradually became cloudy. Concentration *in vacuo* yielded the diacid chloride as a white solid, and this material was used without further purification: ^{1}H NMR (250 MHz, $CDCl_3$) δ 7.4-7.2 (m, 31 H), 7.047 (d, 1 H, J = 6.1 Hz), 4.572 (d, 4 H, J = 12.0 Hz), 4.494 (s, 4 H), 4.483 (d, 4 H, J = 12.0 Hz), 3.889 (d, 4 H, J = 9.0 Hz), 3.518 (s, 4 H), 3.502 (d, 4 H, J = 7.7 Hz), 2.724 (d, 6 H, J = 14.2 Hz), 1.907 (s, 6 H), 1.717 (d, 2 H, J = 12.7 Hz), 1.662 (d, 4 H, J = 14.4 Hz).

Acid-Amide B3. Triethylamine (250 μL) was added to diacid chloride **B6** (0.103 mmol) dissolved in dioxane (20 mL) and the flask was sealed with a septum. Ammonia (0.5 M in dioxane, 205 μL, 1 equiv) was added through the septum and the slightly cloudy mixture was stirred at room temperature for 20 h. An aqueous solution of 1N HCl (1 mL) was added to quench the reaction. Solvent was removed at reduced pressure, and the residue was taken up in CH_2Cl_2 (20 mL) and washed with 1N $HCl_{(aq)}$ (2 x 20 mL) and brine (20 mL). The organic layer was dried over Na_2SO_4, filtered and concentrated *in vacuo*. The crude material was purified by flash chromatography through a silica gel column (5,7,20% acetone/CH_2Cl_2) to give a mixture of acid-amide **3** and diamide **B4** (30 mg). Diacid was recovered (26.6 mg, 22%). Rechromatography of the mixture (4, 8% acetone/CH_2Cl_2) yielded pure acid-amide **3** (7 mg, 6%) and diamide **B4** (20 mg, 16%) as white solids: for **B3**; mp 86.1-87.5 °C; IR (KBr) 3421, 3179, 2860, 1700, 1453, 1400, 1365, 1193, 1101, 737, 698 cm^{-1}; ^{1}H NMR (300 MHz, $CDCl_3$) δ 13.80 (br s, 1 H), 8.495 (br s, 1 H), 7.35-7.19 (m, 30 H), 7.095 (s, 1 H), 6.828 (2, 1 H), 6.030 (br s, 1 H), 4.59-4.43 (m, 12 H), 3.892 (t, 4 H, J = 9.9 Hz), 3.467 (dd, 4 H, J = 2.7, 8.8 Hz), 3.397 (s, 2 H), 3.311 (s, 2 H), 2.747 (t, 2 H, J = 12.2 Hz), 2.570 (d, 2 H, J = 13.7 Hz), 2.434 (d, 2 H, J = 14.4 Hz), 1.935 (s, 3 H), 1.927 (s, 3 H), 1.73-1.59 (m, 6 H); HRMS (FAB in 3-nitrobenzyl alcohol)calcd for $C_{74}H_{78}N_3O_{13}$ (M + H), 1216.5535; found, 1216.55215.

Diamide B4. Acid chloride **B6**(0.0821 mmol) dioxane (3 mL), TEA (200 μL, 17 equiv) were combined in a round bottom flask then sealed with a septum. Ammonia solution (0.5 M in dioxane, 500 μL, 3 equiv) was added through the septum and the suspension was stirred for 24h. The reaction mixture was concentrated, taken up in CH_2Cl_2 (20 mL) and washed with 1N HCl (20 mL). The layers were separated, the organic layer was washed with 1N HCl (2 x 10 mL) and with brine (10 mL), then dried over Na_2SO_4, filtered and concentrated. The crude white solid was purified by flash chromatography through a silica gel column (5, 10% acetone/$CHCl_3$) to give diamide **B4** (78.2 mg) in 78% yield: mp 88.4-89.7 °C; IR (KBr) 3477, 3168, 2859, 1735, 1694, 1496, 1453, 1400, 1365, 1194, 1100, 736, 697 cm^{-1}; ^{1}H NMR (300 MHz, $CDCl_3$) δ 8.903 (br s, 2 H), 7.35-7.24 (m, 30 H), 7.079 (s, 1 H), 7.015 (s, 1 H), 5.856 (br s, 2 H), 4.572 (d, 4 H, J = 12.32 Hz), 4.490 (d, 4 H, J = 11.2 Hz), 4.471 (s, 4 H), 3.889 (d, 4 H, J = 9.4 Hz), 3.475 (d, 4H, J = 8.5 Hz), 3.323 (s, 4 H), 2.767 (d, 2 H, J = 13.0 Hz), 2.404 (d, 4 H, J = 14.3 Hz), 1.917 (s, 6 H), 1.689 (d, 2 H, J = 13.0 Hz), 1.618 (d, 4 H, J = 14.9 Hz); HRMS (FAB in 3-nitrobenzyl alcohol)calcd for $C_{74}H_{79}N_4O_{12}$ (M + H), 1215.5694; found, 1215.5704.

Diacid B7. Phenylene diamine (37.3 mg, 0.345 mmol), anhydride acid chloride **B5** (405 mg, 0.70 mmol), and DMAP (1 mg, 0.008 mmol) dissolved in pyridine was heated to reflux for 20h. Solvent was removed by reduced pressure and the resulting residue was taken up in CH_2Cl_2 (50 mL). This was washed with 1N HCl (3 x 30 mL) and concentrated *in vacuo* to yield 151 mg (37%) of **B7**: mp 169.8-170.2 °C; IR (KBr) 3474, 2859, 1736, 1686, 1646, 1453, 1364, 1190, 1099, 736, 696 cm^{-1}; ^1H NMR (500 MHz, $CDCl_3$) δ 7.46-7.00 (m, 33 H), 6.869 (s, 1 H), 4.561 (d, 4 H, J = 11.7 Hz), 4.503 (d, 4 H, J = 12.2 Hz), 4.458 (s, 4 H), 3.825 (d, 4 H, J = 8.8 Hz), 3.494 (d, 4 H, J = 9.3 Hz), 3.380 (s, 4 H), 2.602 (d, 2 H, J = 15.1 Hz), 2.565 (d, 4 H, J = 14.7 Hz), 1.742 (d, 2 H, J = 13.7 Hz), 1.709 (d, 4 H, J = 14.2 Hz); HRMS (FAB in 3-nitrobenzyl alcohol)calcd for $C_{72}H_{73}N_2O_{14}$ (M + H), 1189.5062; found, 1189.5074.

Histimide Acid B8. Histamine dihydrochloride (33 mg, 0.18 mmol) and acid chloride **B5** (100 mg, 0.174 mmol) were dissolved in pyridine (10 mL) and the mixture was heated to reflux for 20h. The resulting residue was concentrated, dissolved in CH_2Cl_2 (10 mL) and washed with 1N HCl (2 x 10 mL). The CH_2Cl_2 layer was dried over Na_2SO_4, filtered and concentrated *in vacuo*. The resulting residue was purified by flash chromatography through a silica gel column (5, 8, 12 % MeOH/$CHCl_3$) to give **B8** (17 mg 15%): mp 65.6-66.1 °C; IR (CH_2Cl_2) 3054, 2986, 2305, 1721, 1684, 1422, 1265, 1099, 896, 735, 706 cm^{-1}; ^1H NMR (300 MHz, $CDCl_3$) δ 8.206 (s, 1 H), 7.37-7.20 (m, 15 H), 6.868 (s, 1 H), 4.57-4.42 (m, 6H), 4.054 (dt, 1 H, J = 4.3, 12.7 Hz), 3.93-3.87 (m, 1 H), 3.759 (d, 1 H, J = 9.1 Hz), 3.648 (d, 1 H, J = 8.4 Hz), 3.606 (d, 1 H, J = 0.3 Hz), 3.476 (d, 1 H, J = 9.2 Hz), 3.386 (d, 1 H, J = 9.2 Hz), 3.365 (d, 1 H, J = 8.4 Hz), 3.185 (dt, 1 H, J = 5.1, 12.8 Hz), 2.79-2.64 (m, 3 H), 2.332 (d, 1 H, J = 13.5 Hz), 1.824 (d, 1 H, J = 14.9 Hz), 1.750 (d, 1 H, J = 13.6 Hz), 1.490 (d, 1 H, J = 13.4 Hz); HRMS (FAB in 3-nitrobenzyl alcohol)calcd for $C_{38}H_{42}N_3O_7$ (M + H), 652.3023; found 652.3022.

Methyl-Histimide Acid B9. 1-Methyl-4-histamine dihydrochloride (25 mg, 0.13 mmol), acid chloride **5** (81 mg, 0.14 mmol) and DMAP (2 mg, catalytic) were dissolved in pyridine (8 mL) and the mixture was refluxed for 4 h under Ar. The resulting residue was concentrated dissolved in $CHCl_3$ (8 mL) and washed with 1N HCl (10 mL), water (10 mL) and brine (10 mL). The $CHCL_3$ layer was dried over Na_2SO_4, filtered and concentrated *in vacuo*. The residue was purified by flash chromatography through a silica gel column (2-15 % MeOH/CH_2Cl_2) to give **B9** (59 mg, 70 %): mp 165.5-167.0 °C; 3426, 3029, 2857, 1724, 1675, 1587, 1452, 1363, 1152, 1101, 1027, 738, 698 cm^{-1}; ^1H NMR (300 MHz, $CDCl_3$) δ 7.532 (br s, 1 H), 7.35-7.23 (m, 15 H), 6.637 (br s, 1 H), 4.59-4.45 (m, 6H), 3.90-3.83 (m, 4 H), 3.619 (br s, 3 H), 3.42-3.36 (m, 4 H), 2.988 (br s, 2H), 2.551 (d, 2 H, J = 13.3 Hz), 2.432 (d, 1 H, J = 11.7 Hz), 1.65-1.54 (m, 3H); HRMS (FAB in 3-nitrobenzyl alcohol) calcd for $C_{39}H_{44}N_3O_7$ (M + H), 666.3179; found 666.3171.

4.3 Determination of Equilibrium Constants by UV

Reagent grade benzene, dried over 4A molecular sieves and subsequently stored over fresh 4A molecular sieves, and anhydrous methylene chloride stored over 4A molecular sieves, were used as solvent. Teflon

stoppered quartz cuvettes (10 mm cell length) were dried in a vacuum desiccator prior to use. 3',3",5',5"-The tetrabromophenolphthalein ethyl ester (Bromophthalein magenta E), diphenyl guanidine, and substrates **B2a**, **B3**, **B4**, and **B7** were stored in a desiccator prior to use. TEA was dried over 4A molecular sieves.

Stock solutions of bromophthalein magenta E (BME) indicator (2.5×10^{-4} M, 5×10^{-4} M) and substrates **B2a** (2.5×10^{-4} M, 5×10^{-4} M) and **B3** (2.5×10^{-4} M, 1.25×10^{-3} M, 1.0×10^{-3} M) were prepared in both benzene and CH_2Cl_2. Solutions of diphenyl guanidine in benzene (5×10^{-4} M), triethylamine in CH_2Cl_2 (5×10^{-4} M), diamide **B4** (5×10^{-4} M) and diacid **B7** (1.25×10^{-3}) in benzene were prepared. Aliquots of indicator, base, and substrate (**B2a**, **B3**, **B4**, or **B7**) were added to the cuvette and diluted with either benzene or CH_2Cl_2 to 1.00 mL such that the indicator was 2.5×10^{-5} M, the base concentrations were 0.14-4.0 equiv, and the substrate concentration was in the range of 1-15 times that of the indicator. The solutions were capped immediately, and were mixed well using a vortex mixer. The cuvettes were placed in a temperature-controled cell holder at 25 °C and were equilibrated for 15-20 minutes before taking the absorbance measurements. Absorbances were read using as reference a cuvette containing 1 mL of solvent. The changes in absorbance that accompanied the conversion of BME to its diphenylguanidinium salt (540 nm in benzene) or triethylammonium salt (577 nm in CH_2Cl_2) were recorded.

A literature value for the equilibrium constant for the reaction of BME and diphenyl guanine forming the salt complex in benzene at 25 °C was used.[120] The equilibrium constant of BME and TEA in CH_2Cl_2 at 25 °C was determined from a constant indicator UV titration: aliquots of a solution of 2.5×10^{-4}, 1.0×10^{-3}, 2.5×10^{-3} M TEA in 2.5×10^{-5} M BME were added to a 2.5×10^{-5} M BME solution. The resultingcurve (18 point) obtained by following the absorbance of the indicator-TEA salt was fitted to the 1:1 binding isotherm.[64] Nonlinear least-squares regression was used to curve-fit the experimental data with the Simplex algorithm as implemented in Systat 5.2.[84] Equilibrium constants of deprotonation of the substrate were calculated as described by Davis et al.[120] At least 10 reliable measurements were taken and averaged to obtain the value for each equilibrium constant.

C. RECEPTORS FOR NUCLEOTIDE DERIVATIVES

1. INTRODUCTION

Molecular recognition of nucleic acid components has attracted considerable attention in recent years, and all of the naturally-occuring nucleosides were the focus of such studies. Adenosine in particular has attracted considerable attention and a large variety of synthetic receptors were designed including macrocycles,[17,22] tweezers,[18,148] and clefts.[15,16,56,57,72,149-152] Successful strategies in organic solvents typically employ receptor surfaces that simultaneously interact with the target through hydrogen bonding and aromatic stacking. Additional salt bridge interactions lead to stronger binding of phosphates and other oxyanion derivatives.[19,29,31-34,40,46,47,49,51,54,153-155] This laboratory has developed generations of adenine receptors and has reported an evolved and improved one with exceptionally high affinity to adenine.[58] The interactions involved simultaneous formation of Watson-Crick and Hoogsteen type hydrogen bonding combined with aromatic stacking on both faces of the adenine surface. Further modifications including attachment of a guanidinium unit and providing a salt bridge to the phosphate have yielded organic soluble cAMP[47] and ApA receptors[46,156] as well as water soluble receptors.[39,40,72] Some changes in the design and method of obtaining such receptors now yield 5'-AMP, ApA and a library of potential nucleotide receptors.

2. WATER SOLUBLE 5'-AMP RECEPTOR

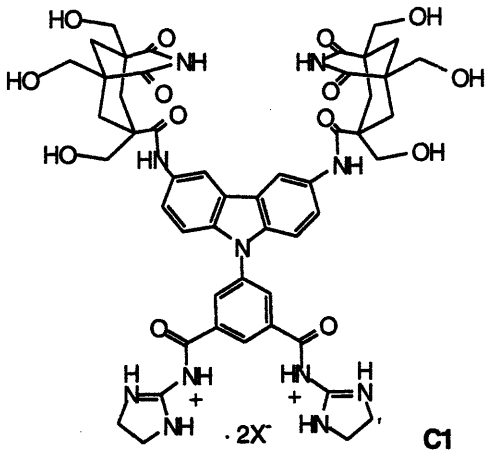

C1

Scheme C1.

Non-enzymatic approaches to phosphodiester cleavage has attracted much attention,[48,157-168] and numerous receptors have been designed based on Staphyloccal Nuclease (SNase)[48,164,169] which has two guanidinium moieties in the active site. One guanidinium is required for recognition of the phosphodiester and the second guanidinium for catalyzing hydrolysis.[170] Several successful receptors mimicing the active site structure of SNase have been studied.[48,164] Combination of such a bis-guanidinium motif with an adenine recognition system by Dr. M. Morgan Conn, yielded a design for a 5'-AMP receptor **C1**.

Synthesis

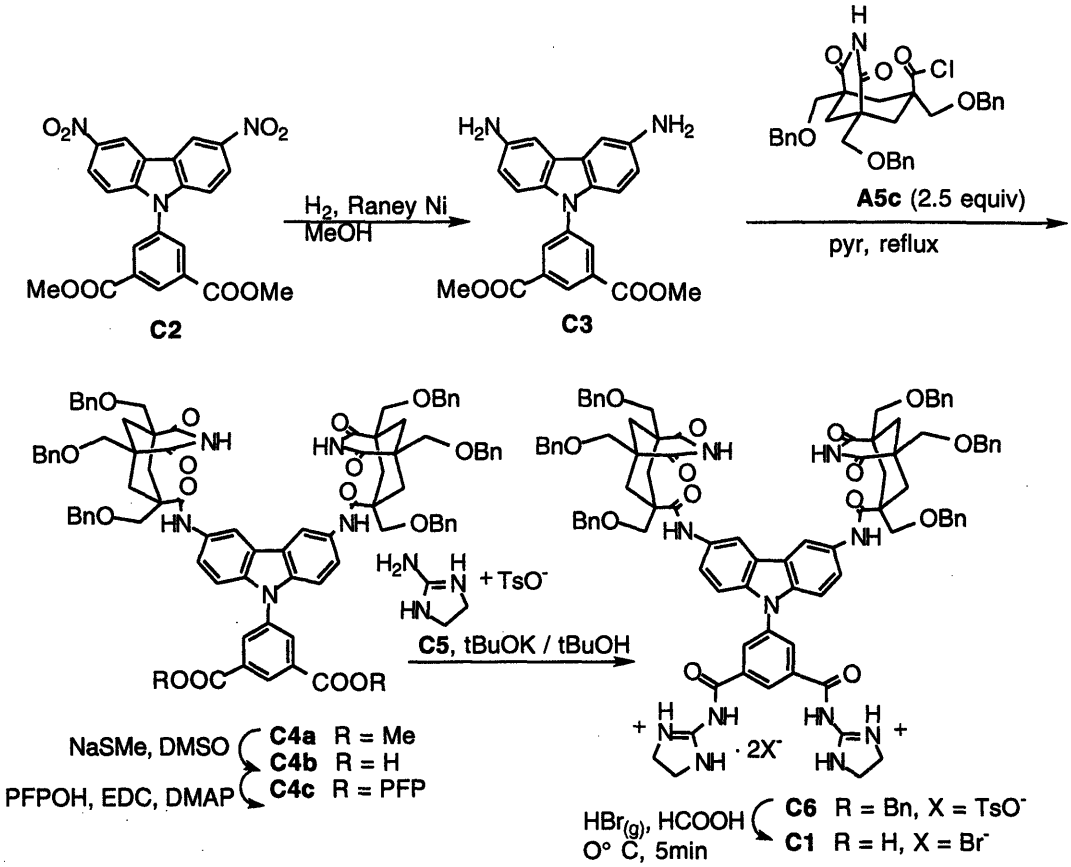

Scheme C2.

The synthesis of the receptor is outlined in Scheme C2. Dinitro **C2** was hydrogenated in the presence of Raney Ni to diamine **C3** (diamine **C3** was previously synthesized in our group from **C2** using Pd-C as a catalyst).[58] Acylation of diamine **C3** with Kemp's imide-acid chloride proceeds as usual to give the bis-imide receptor **C4a**. Treatment of the methylester with sodium thiomethoxide displaced the methyl groups and yields the diacid. The isophthalic acid portion of **C4b** was converted to pentafluorophenol (PFP) esters by EDC mediated coupling. These activated esters were reacted with guanidinium **C5** pretreated with *t*-BuOK to give the isophthaloyl acyl guanidinium receptor **C6**. Removal of the benzyl protecting groups under HBr / HCOOH conditions, yielded the desired receptor **C1**.

Titrations

In unbuffered or acidic water, receptor **C1** is readily soluble. However, at pH > 4, **C1** is completely insoluble. Conversion of the bromide salt to the chloride salt, by passing receptor **C1** through an ion exchange column, did not improve its solubility. Both cacodylate and bis-tris buffered solutions were examined to make certain the insolubility was not being caused by buffers. The insolubility can be explained if at around pH4, at least one of

the two guanidiniums is deprotonated to the neutral guanidine. However, a pKa near 4 seemed extremely low, even for acyl guanidiniums which have lower pKa's (~8) than alkyl guanidiniums (~14).[169] If the two guanidiniums were positioned closer together, the reduced pKa might suggest LBHB formation because deprotonating one of the guanidiniums can result in a pKa matched hydrogen bond donor and acceptor pair. However, in this system, the two guanidiniums are too distant from each other. ^{1}H NMR of **C6** under anhydrous conditions did not show any LBHB signal. The remaining explanation for the low pKa might be the extended conjugation of the guanidine with the carbazole phenyl group. Crude titrations of **C1** with 5'-AMP at pH3 (monosodium phosphate buffer) and 4 (acetic acid buffer) under conditions otherwise identical to all the previously described aqueous ^{1}H NMR titrations (section A4.3) gave Ka's of 140 M^{-1} and 170 M^{-1} respectively. These association constants showed that contribution to binding from the guanidinium component in **C1** is practically non-existent when compared to association results obtained with receptors **A1** and **A2** (section A2).

Investigation of this system was halted at this point. Future improvement to this system should include attachment of alkyl guanidiniums instead of acyl guanidiniums. This will elevate the pKa of the guanidinium, allow the receptor to stay dissolved at neutral pH, and may form a salt bridge with the phosphate portion of the 5'-AMP guest at neutral pH.

3. WATER AND ORGANIC SOLUBLE NUCLEOTIDE RECEPTORS

Extension of the previously described water soluble cAMP receptor **A1** with another adenine recognizing function could yield a water soluble ApA recognition system analogous to the ApA receptor previously reported from this laboratory.[46] Neccessary modifications were to attach functionalities to impart water solubility, increase the stacking surface of the adenine recognizing unit, and modify the ester linkage between the adenine recognition unit and the bicyclic guanidinium to a more robust and hydrophyllic amide linkage. Of the three major modifications to be made, the first two had been worked out.[39,40] The third modification required synthesis of a diamino bicyclic guanidinium compound. A route to diamino-guanidinium was developed in de Mendoza's laboratory, and an alternate route, allowing differentiation of the two sides of the bicyclic guanidinium, was recently reported by Schmidtchen.[54]

Synthesis

Using the protocol developed by the de Mendoza group, the diamino guanidinium was synthesized as summarized in Scheme C3. The dihydroxy guanidinium **C7** was chlorinated by treatment with thionyl chloride to dichloride **C8**. Treating dichloride **C8** with NH_4OH in a biphasic mixture with Hünig's base gives diamino guanidinium **C9a** in good yield. An alternate route converts the dichloride to diiodide **C10** using Finkelstein conditions and subsequently treats it with NH_4OH to give diamino guanidinium but in a lower yield.

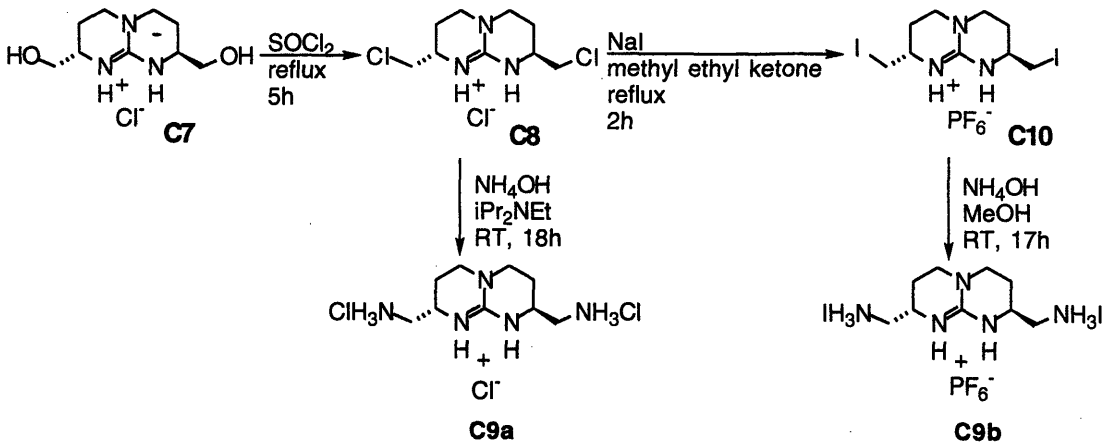

Scheme C3.

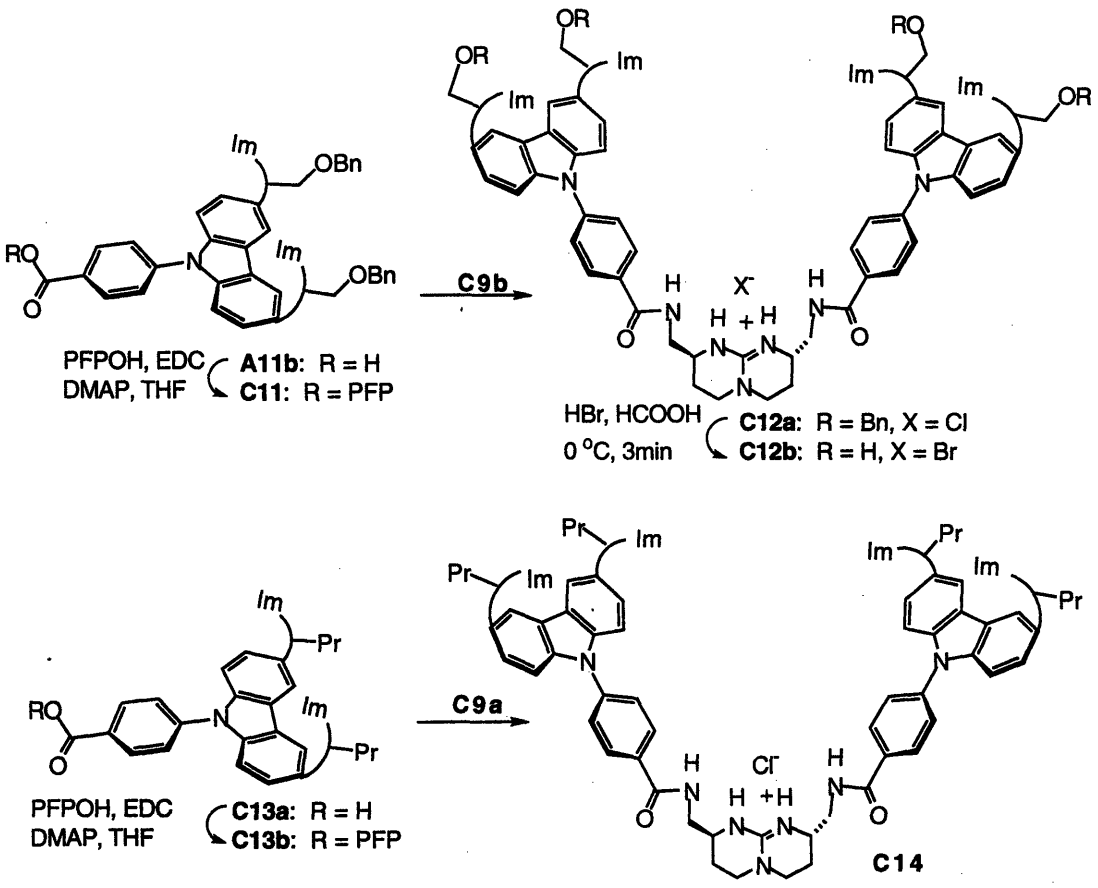

Scheme C4.

Using this diamino guanidinium, both organic soluble (propylated Kemp's subunits) and water soluble (hydroxymethylated Kemp's subunits) ApA receptors were synthesized. The simple route via acid chloride was unsuccessful and an activated ester had to be made. The PFP esters **C11** and **C13b** were obtained from the corresponding acids using EDC as a coupling agent. These activated esters were used to doubly acylate the

diamino guanidinium to yield organic soluble ApA receptors **C12a** and **C14**. The desired amide linkage with the guanidinium subunit was confirmed by ^{1}H NMR of the propylated receptor **C14** with an unobscured downfield region. The benzyloxy groups of receptor **C12a** were removed under HBr / HCOOH conditions to yield hydroxymethyl receptor **C12b**. Surprisingly, this receptor containing 12 hydroxyls and one guanidinium is insoluble in water at millimolar concentrations, rendering aqueous NMR studies an impractical option.

Receptor **C12b** was given to Dr. Nassim Ussman at Ribozyme Pharmaceutical Inc. for cellular membrane transport studies. Liquid membrane transport studies on receptor **C14** was performed entirely by Dr. Cecilia Andreu.

Nucleotide Transport

Numerous studies on nucleotide transport across liquid membrane have been performed using receptors with quaternary ammonium groups[171-175] and expanded porphyrin derivatives.[149,176,177]

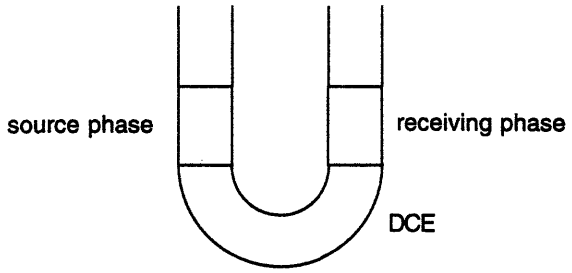

Figure C1. U-tube apparatus for liquid membrane transport studies.

Imide-based receptors[178] and imide-based receptors in combination with phosphate binding guanidinium subunits[156] have enabled transport of nucleoside derivatives and later nucleotides through liquid membranes. The U-tube (Figure C1) method was used for studying the transport properties of receptor **C14**. In our set up, the aqueous source phase contains the nucleotide, the aqueous receiving phase is a salt (NaCl) solution, and the oranic phase is dichloroethane (DCE) and contains the carrier. The nucleotides in this system are unable to difuse to the receiving phase without the assistance of the carrier molecules. The rate of this facilitated transport observed in the presence of the carrier is measured by monitoring the concentrations of nucleotide in the source and receiving phase over time by UV/Vis spectroscopy. The resulting graph from such data points is shown in Figure C2. This system has two concentration gradients — one is the nucleotide gradient and the other is the salt gradient in the source and receiving phases. At the source/DCE interphase, the positively charged carrier exchanges its negative couterion for the nucleotide and at the receiving/DCE interphase, the converse occurs. After the nucleotide concentration is balanced between the source and receiving phase, it is the chloride ion gradient that enables the continuing transport of nucleotides against the concentration gradient.

This portion of the transport phenomenon is termed active transport. The rates of initial and active transport are approximated from the most linear data points immediately after time zero and equivalence, respectively.

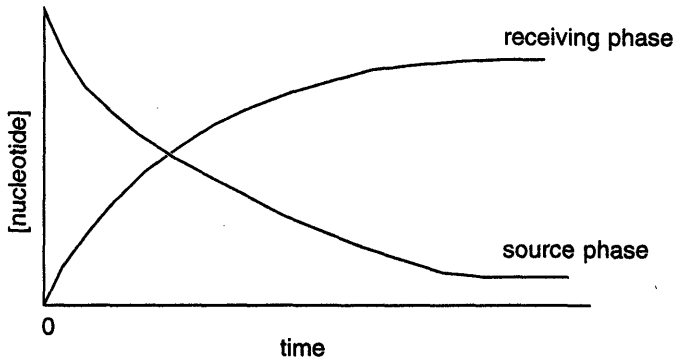

Figure C2. Mock liquid membrane transport concentration profile.

The results from the U-tube study for **C14** are summarized in Table C1. Every dinucleotide that contained adenosine was transported. The selectivity of the nucleotides being transported was such that A » T > G > C. Nucleotides with A on the first position was transported at higher rates than those with A at the second position. Compared to the dinuceleotide receptor **C15** with a carbazole-methylene spacer,[156] similar rates with **C14** were achieved with lower concentration of the carrier but with a larger salt (NaCl) concentration in the receiving phase. For the transport of d(AA), the affinity between the carrier and substrate was so high that it was necessary to keep the concentration of carrier low and to use extremely large salt concentration in the receiving phase to enable release of the nucleotide. Another finding was that d(ApC) and d(GpG) which could not be transported with **C15** were now being transported by **C14**.

Table C1. Liquid membrane transport results.[a]

[carrier][b] (μM)	nucleotide (10 μM)	receiving phase [NaCl] (mM)	initial rate (pmol/h-cm^2)	active transport (pmol/h-cm^2)
2	d(ApA)	10000	.82 ± .02	.50 ±.01
5	dApT	500	1.13 ± .02	.62 ±.03
12	TpdA	10	.97 ±.04	.62 ± .02
8	d(ApG)	500	1.342 ± .001	.64 ± .06
20	GpA	10	.66 ± .02	.357 ± .001
10	d(ApC)	500	1.39 ± .03	.72 ± .02
20	TpT	10	.88 ± .04	.68 ± .06
20	d(GpG)	10	.617 ± .007	.44 ± .02
20	d(CpC)	10	0	0

[a]Spectrophotometrical conversion for determining the concentration of nucleotide was 1un $A_{260}$of RNA = 40 μg/mL; 1 un A_{260} DNA single strand = 33 μg/mL; for mixed dinucleotides (dXpX' or XpdX') 1un A_{260} = 36.5 μg/mL. [b]The carrier was receptor **C2b**.

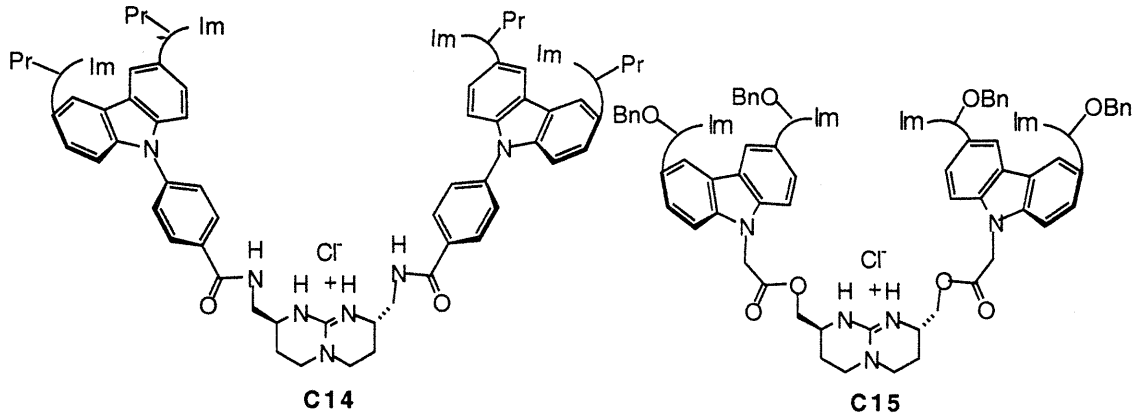

C14 **C15**

Scheme C5.

In summary, the increased aromatic surface in receptor **C14** made it, in general, a better carrier for a larger variety of nucleotides. Development of an improved nucleotide transporter will require attenuation of receptor **C14**'s strong affinity towards adenosine derivatives.

4. A LIBRARY OF NUCLEOTIDE RECEPTORS

Combinatorial chemistry has emerged as an excellent tool for generating a large number of related compounds. Modern analytical methods enable screening of such a pool of molecules to identify those with desireable properties.[179] In the early stages of combinatorial chemistry, the libraries were made by solid phase synthesis and the types of molecules were limited to peptides[180-183] and oligonucleotides.[184-186] Lately, the method has been extended to small molecule libraries in the solution phase.[187,188]

The bicyclic guanidinium diol seemed suitable for a core molecule in the production of a library of nucleotide receptors in solution. The differential protection of the diol provides separate "addresses" for the two diversifiable alcohol groups, facilitating the deconvolution of the library to find the receptor of interest. The alcohol functionality is easily diversified by reaction with isocyanates. Carbamates are a popular linkage in the field of combinatorial libraries;[189-192] the resulting carbamate library should be less prone to hydrolysis than an ester library, and should be stable towards amidases.

In creating the library, a sub-library approach was taken rather than making a single large library with all components in one mixture. The sub-libraries were constructed such that each contained molecules with homogeneous functionalization on alcohol site **A** and diversified functionalization on alcohol site **B** as outlined in Scheme C6.

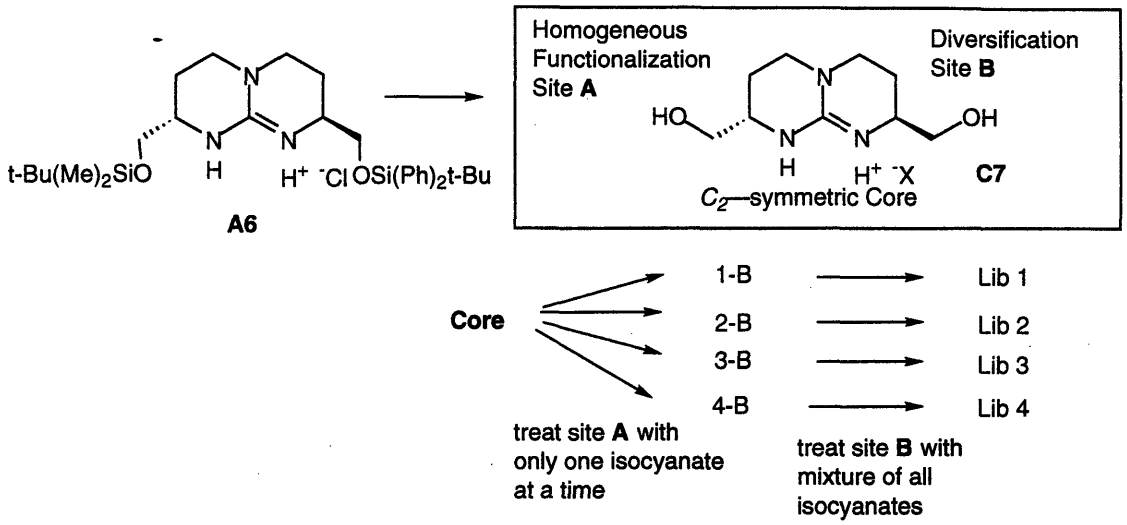

Scheme C6.

The C_2 symmetry of the bicyclic guanidinium core facilitates identification of the compound which made a hit. If Lib 1 is active, then the active compound could only be 1-1 (where both site A and B are from isocyanate 1). If Lib 2 and 4 are active, the active compound(s) must be one or more of 2-4, 2-2 and 4-4 (Figure C3). If Lib 1,2 and 4 are active, the active compound(s) are one or more of 1-1, 2-2, 4-4, 1-2, 1-4, and 2-4.

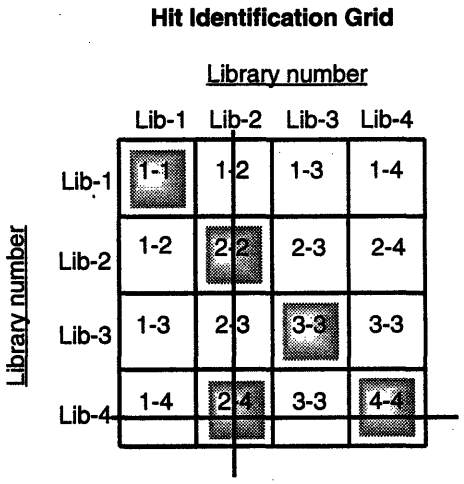

Figure C3. Hit determination grid when Lib 2 and 4 are active. The grey boxes with lines running through are possible hits.

Synthesis

Twelve readily available alkyl and aryl isocyanates (Scheme C7) of various shapes were chosen to construct a library of 78 compounds with each of the 12 sub-libraries containing 12 compounds. The syntheses of the libraries were carried out as outlined in Scheme C8. The $(Bu)_2Sn(OAc)_2$ catalyzed carbamate formation proceeded quickly (30 min - 1 h) in nearly quantitative yield.

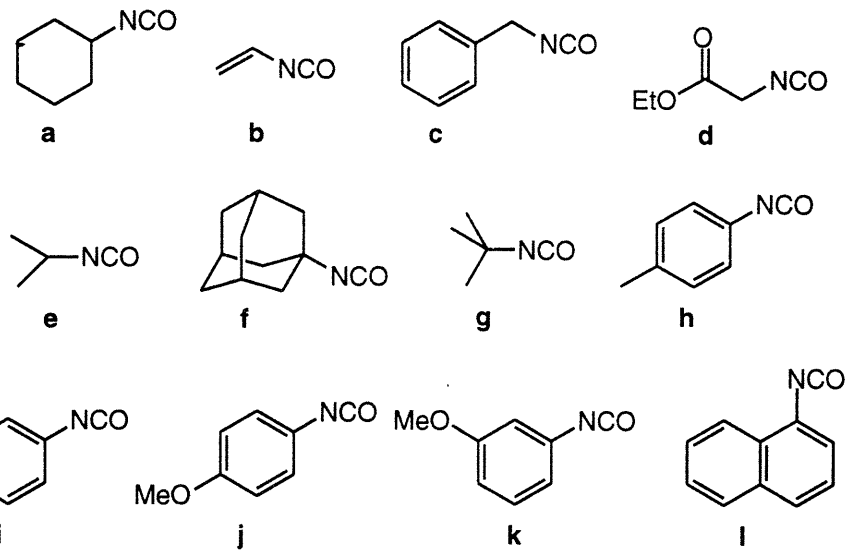

Scheme C7.

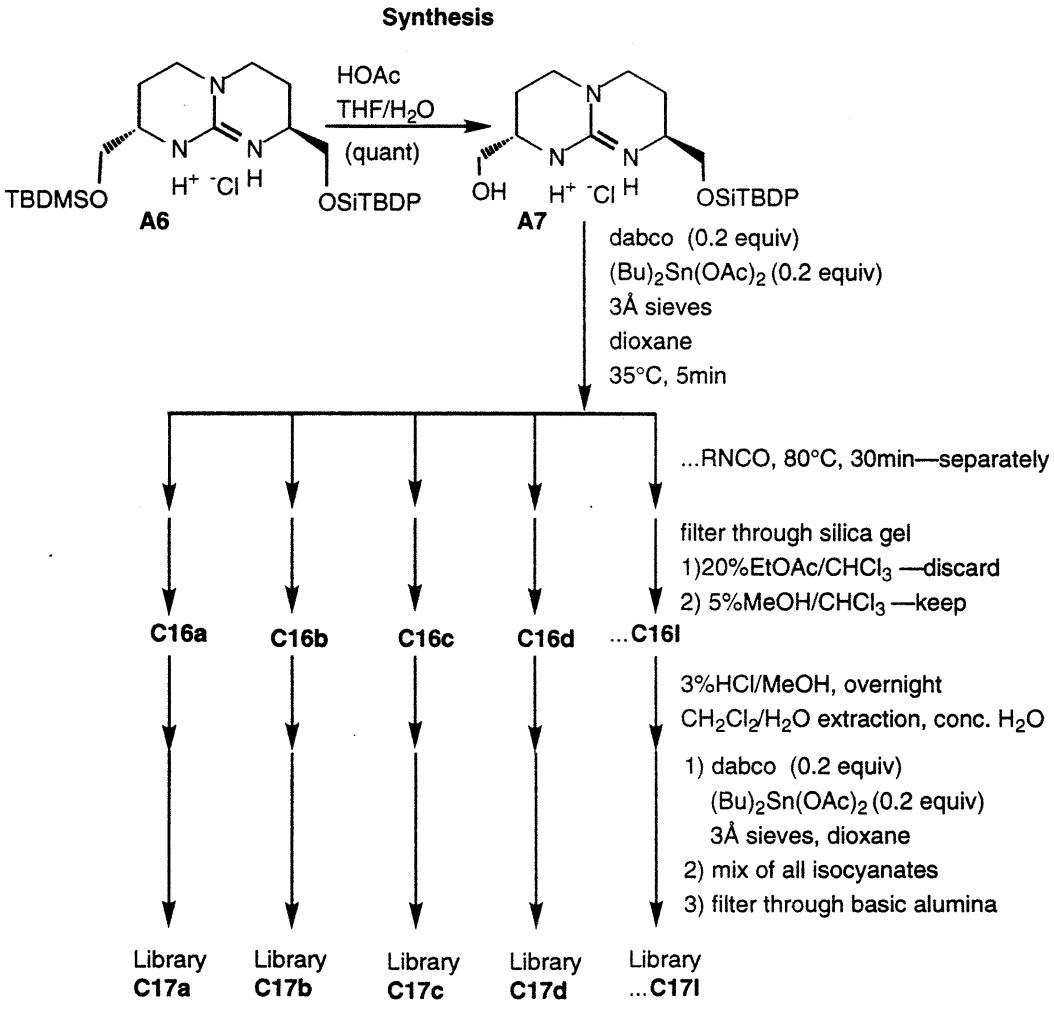

Scheme C8.

These libraries were not assayed nor used for recognition studies due to their insolubility in water and sparse solubility (1×10^{-5} M) in <10% DMSO/H_2O. It is waiting to be assayed in a system which can tolerate > 10% DMSO/H_2O.

The problem with this library lies in the limited variety (mostly lipophylic) of commercialy available isocyanates. A better approach is to activate the core molecule. The recent report of the synthesis of mono- and di-aminobicyclic guanidinium[153] should facilitate conversion of these amino groups to the reactive isocyanates. This in turn should enable the creation of a truely diverse library using alcohols, amines, and amino acids — not just a simple library of alkyl and aryl derivatives.

5. EXPERIMENTAL

5.1 Synthesis

***N*-(3,5-Bis(methoxycarbonyl)phenyl)-3,6-diaminocarbazole (C3).** Dinitro **C2** (795 mg, 1.769 mmol) was hydrogenated at balloon pressure in THF (20 mL) and MeOH (5 mL) with Raney Ni (2 mL susp in neutral water) for 20h. Filteration through Celite, followed by evaporation of solvent under reduced pressure gave an unstable yellow solid which was used immediately without further purification.

Benzyloxymethyl-bis(Kemp's imide)carbazole-*N*-isophalic acid methyl ester C4a. Diamine **C3** (790 mg, 1.769 mmol) and benzyloxy Kemp's imide acid chloride **A5c** (2.0 g, 3.5 mmol) with catalytic DMAP (5 mg) were heated in refluxing pyridine (100 mL) for 20h. The solvent was removed under reduced pressure and the residue was taken up in CH_2Cl_2 (100 mL). The solution was washed with 1N HCl (100 mL) and brine (100 mL), dried over $MgSO_4$, filtered and concentrated *in vacuo*. Flash chromatography (5, 10, 20% EtOAc/$CHCl_3$) gave the desired compound (750 mg, 28% yield from **C2**): ^{1}H NMR (300 MHz, DMSO-d_6) δ 10.629 (s, 2 H), 9.424 (s, 2 H), 8.534 (s, 1 H), 8.329 (s, 2 H), 8.304 (s, 2 H), 7.51-7.23 (m, 34 H), 4.51-4.46 (m, 12 H), 3.930 (s, 6 H), 3.781 (d, 4 H, J = 9.13 Hz), 3.463 (s, 4 H), 3.413 (d, 4 H, J = 9.3 Hz), 2.576 (d, 4 H, J = 13.8 Hz), 2.342 (d, 2 H, J = 12.1 Hz), 1.613 (d, 6 H, J = 14.4 Hz).

Benzyloxymethyl-bis(Kemp's imide)carbazole-*N*-isophalic acid C4b. Methylester **C4a** (191 mg, 0.130 mmol) and NaSMe (100.6 mg, 1.44 mmol) were dissolved in DMSO (5.5 mL) and stirred at 75 °C for 1.5 h. Upon cooling to room temperature, $CHCl_3$ (10 mL) and 1N HCl (10 mL) were added and stirred well for 30 min. The organic layer was separated and washed with 1N HCl (10 mL), water (3 x 10 mL), and brine (10 mL) and dried over Na_2SO_4, filtered and concentrated *in vacuo* to give the crude **C4b** (quant): ^{1}H NMR (300 MHz, DMSO-d_6) δ 10.634 (s, 2 H), 9.431 (s, 2 H), 8.531 (s, 1 H), 8.301 (s, 2 H), 8.288 (s, 2 H), 7.52-7.21 (m, 34 H), 4.51-4.46 (m, 12 H), 3.781 (d, 4 H, J = 9.6 Hz), 3.461 (s, 4 H), 3.412 (d, 4 H, J = 9.3 Hz), 2.339 (d, 2 H, J = 11.5 Hz), 1.611 (d, 6 H, J = 13.6 Hz).

Benzyloxymethyl-bis(Kemp's imide)carbazole-*N*-isophalic acid pentafluorophenyl ester C4c. Diacid **C4b** (0.115 mmol), pentafluorophenol (150 mg, 0.817 mmol), EDC (155.0, 0.809 mmol) and DMAP (9.5 mg, 0.078 mmol) were placed in THF (4 mL). The cloudy suspension was stirred for 4 h. The yellow reaction mixture was concentrated *in vacuo* and was purified by flash cromatography (5, 10% EtOAc/$CHCl_3$) to obtain the desired activated ester **C4c** (140 mg, 70% from **C4a**) which was used immediately.

Benzyloxymethyl-bis(Kemp's imide)carbazole-*N*-isophalyl-bis(guanidinium)amide dichloride C6. Guanidinium **C5** (173.8 mg, 0.675 mmol) was added to a suspension of *t*-BuOK (74.3 mg, 0.663 mmol) and *t*-BuOH at 60 °C and stirred for 10 min. After cooling to room temperature, the activated ester **C4c** (115 mg, 0.65 mmol) was added and the reaction mixture was heated in refluxing *t*-BuOH for 4h. The reaction mixture was taken up in MeOH (2 mL) and CH_2Cl_2 (5 mL) and filtered. The resulting yellow solution was concentrated under reduced pressure. The concentrated residue was dissolved in CH_2Cl_2 (15 mL), washed with 1N HCl (15 mL), and brine (15 mL), dried over $MgSO_4$, filtered, and concentrated under reduced pressure. The crude product was flash chromatographed (5, 10% MeOH/$CHCl_3$) to give clean **C6** (34.9 mg, 32.6%) as a white powder: mp 188.3-189.0 °C; IR (KBr) 3374, 2862, 1701, 1591, 1517, 1496, 1468, 1395, 1203, 1100, 1006, 738, 697 cm^{-1}; ^1H NMR (300 MHz, DMSO-d_6) δ 10.641 (s, 2 H), 9.430 (s, 2 H), 8.860 (s, 1 H), 8.33-8.26 (m, 8 H), 7.34-7.24 (m, 34 H), 4.51-4.46 (m, 12 H), 3.781 (d, 4 H, J = 8.5 Hz), 3.535 (s, 8 H), 3.460 (s, 4 H), 3.412 (d, 4 H, J = 8.9 Hz), 2.339 (d, 2 H, J = 12.0 Hz), 1.612 (d, 6 H, 13.8 Hz); HRMS (FAB in 3-nitrobenzyl alcohol) calcd for $C_{92}H_{93}N_{11}O_{14}$ $(M - 2Cl)^{+2}$, 1575.6904; found, 1575.6914.

Hydroxymethyl-bis(Kemp's imide)carbazole-*N*-isophalyl-bis(guanidinium)amide dibromide C1. HBr gas was bubbled for 4 min through the benzylated cleft **C1** (30 mg, 0.0182 mmol) in formic acid (1.5 mL) at 0 °C, followed by Ar for 5 min. The solution was concentrated *in vacuo* to give orange solids which upon trituration in THF (1.5 mL) with 3 drops of MeOH gave a yellow solid (20 mg, 0.0167 mmol, 90%): IR (KBr) 3415, 3154, 1685, 1400 cm^{-1}; ^1H NMR (300 MHz, DMSO-d_6) δ 12.4 (br s, 2 H), 10.350 (s, 2 H), 9.271 (s, 2 H), 8.86 (br s, 4 H), 8.577 (s, 1 H), 8.442 (s, 2 H), 8.376 (s, 2 H), 7.522 (d, 2 H, J = 9.3 Hz), 7.455 (d, 2 H, J = 9.0 Hz), 4.0-3.3 (br m, 30 H), 2.407 (d, 4 H, J = 14.0 Hz), 2.207 (d, 2 H, J = 12.9 Hz), 1.491 (d, 4 H, J = 14.0 Hz), 1.350 (d, 2 H, J = 13.0 Hz); HRMS (FAB in 3-nitrobenzyl alcohol) calcd for $C_{50}H_{57}N_{11}O_{14}$ $(M - 2Br)^{+2}$, 1035.4087; found, 1035.4109.

Bicyclic guanidinium dichloride C8. Diol **C7** (64.3 mg, 0.273 mmol) was heated in refluxing $SOCl_2$ (2.9 mL) for 3.5 h and then concentrated *in vacuo*. The resulting residue was flash chromatographed (20% EtOH/CH_2Cl_2) to yield the dichloride (66.5 mg, 89%): mp 78-79 °C; IR (KBr) 3496, 3410, 3187, 3008, 1621, 1440, 1398, 1315, 725, 693 cm^{-1}; ^1H NMR (250 MHz, $CDCl_3$) δ 9.12 (s, 2 H), 3.72 (m, 4 H), 3.57 (m, 2 H), 3.42 (m, 4 H), 2.16 (m, 4 H); HRMS (FAB in 3-nitrobenzyl alcohol) calcd for $C_9H_{16}N_3Cl_2$ $(M)^+$, 236.0721; found, 236.07182.

Bicyclic guanidinium diiodide C10. NaI (116.7 mg, 0.779 mmol) was heated in refluxing methyl ethyl ketone (1.5 mL) for 1h; dichloride **C8** (30.4 mg, 0.110 mmol) was added and heating was continued for 24 h. Solvent was removed under reduced pressure and the residue was taken up in CH_2Cl_2 (10 mL) / saturated KPF_6 (10 mL). The aqueous layer was washed with CH_2Cl_2 (2 x 10 mL). The combined organics were dried over $MgSO_4$, filtered and concentrated under reduced pressure. The resulting yellow solid was recrystallized from CH_2Cl_2 and Et_2O to yield 38.6 mg (61%) of clean **C10**: mp decomp; IR (KBr) 3413, 3142, 1659, 1628, 1517, 1400, 1309, 839, 557 cm^{-1}; MS (FAB in 3-nitrobenzyl alcohol) calcd for $C_9H_{16}N_3I_2$ $(M)^+$, 419.94; found 419.9.

Bicyclic guanidinium diamine C9

Cl^- salt C9a. Dichloride **C8**(115 mg, 6.422 mmol), NH_4OH (3.5 mL, 30% NH_3 solution) and Hünig's base (2.5 mL) were stirred vigorously for 20h such that the two phases were well mixed. CH_2Cl_2 (5 mL) was added and the organic layer separated. The aqueous layer was washed with CH_2Cl_2 (2 x 10 mL), then concentrated *in vacuo* to yield a pale yellow solid (118 mg, 87%).

PF_6^- salt C9b. Diiodide **C10** (323.1 mg, 0.572 mmol) and MeOH (600 μL) were stirred and gave a dark orange solution. NH_4OH (40 mL) was added and the solution instantly cleared. This was stirred over night at room temperature, then concentrated *in vacuo* to give brown solids which were triturated in acetone to give beige solids (280 mg, 81.7%): mp decomp 217 °C; IR (KBr) 3157, 1614, 1469, 1352, 1302, 1230, 1202, 1087, 1025, 990, 849, 668, 557 cm^{-1}; ^1H NMR (300 MHz, DMSO-d_6) δ 7.972 (br s, 6 H), 7.847 (br s, 2 H), 3.667 (m, 2 H), 2.967 (m, 4 H), 2.10-1.82 (m, 4 H); HRMS (FAB in 3-nitrobenzyl alcohol) calcd for $C_9H_{20}N_5$ $(M)^+$, 198.1719; found, 198.1721.

Benzyloxymethyl-bis(Kemp's imide)carbazolephenyl-*p*-pentafluorophenyl ester C11. A11b(448 mg, 0.285 mmol), EDC (3.6 eq), DMAP (0.4 eq) and pentafluorophenol (3.4eq) were placed in THF (16.5 mL). The suspension was stirred at room temperature for 22h. Solvent was removed and the residue was flash chromatographed (2, 5, 12% EtOAc/$CHCl_3$) yielding **C11** (470 mg) in quantitative yield. This material was used immediately.

Benzyloxymethyl ApA receptor C12a. Diamine **C9b** (70.4 mg, 0.118 mmol) and **C11** (2.4 eqiv) were placed with DMF (11 mL) and freshly distilled TEA (270 μL, 16 equiv). The suspension gradually cleared and was stirred at room temperature for 22h. Solvent was removed under reduced pressure and the orange residue was flash chromatographed (5, 10% MeOH/$CHCl_3$) to give 336.9 mg (92%) of receptor **C12a**: IR (KBr) 3378, 3154, 1700, 1653, 1534, 1517, 1465, 1399, 1200, 1100, 995, 740, 678 cm^{-1}; ^1H NMR (300 MHz, DMSO-d_6) δ 10.608 (s, 4 H), 9.411 (s, 4 H), 8.872 (br s, 2 H), 8.288 (d, 4 H, J = 1.80 Hz), 8.161 (d, 4 H, J = 8.40 Hz), 7.756 (d, 4 H, J = 8.40 Hz), 7.626 (s, 2 H), 7.502 (dd, 4 H, J = 9.00, 1.50 Hz), 7.19-7.21 (m, 64 H), 4.508 (s, 16 H), 4.458 (s, 8 H), 3.778 (d, 8 H, J = 8.40 Hz), 3.642 (s, 2 H), 3.46-3.30 (m, 24 H), 2.574 (d, 8 H, J = 13.2 Hz), 2.344 (d, 4 H, J = 12.71 Hz), 2.02 (m, 2 H), 1.82 (m, 2 H), 1.602 (d, 12 H, J = 11.57 Hz).

Hydroxymethyl ApA receptor C12b. HBr gas was bubbled through a solution of **C12a** (100 mg, 0.0324 mmol) in formic acid (9.5 mL) at 0°C for 3min. The solvent was removed under reduced pressure to give an orange film which was triturated in THF. Solids were separated from the orange solution by centrifugation, then dried *in vacuo* to give **C12b** in 95% yield: IR (KBr) 3378, 1696, 1647, 1507, 1465, 1400, 1320, 1200, 1057 cm^{-1}; ^1H NMR (300 MHz, DMSO-*d6*) δ 10.374 (s, 4 H), 9.246 (s, 4 H), 8.856 (s, 2 H), 8.338 (d, 4 H, J = 0.90 Hz), 8.158 (d, 4 H, J = 8.47 Hz), 7.751 (d, 4 H, J = 8.40 Hz), 7.584 (s, 2 H), 7.505 (d, 4 H, J = 8.96 Hz), 7.348 (d, 8 H, J = 8.80 Hz), 5.10 (br s, 4 H), 4.77 (br s, 8 H), 3.774 (d, 8 H, J = 9.94 Hz), 3.70-3.30 (m, 26 H), 2.405 (d, 8 H, J = 13.80 Hz), 2.242 (d, 4 H, J = 11.10 Hz), 1.754 (d, 4 H, J = 9.90 Hz), 1.482 (d, 8 H, J = 13.68 Hz).

Propyl-bis(Kemp's imide)carbazolephenyl-*p*-pentafluorophenyl ester C13b. Acid **C13a** (384 mg, 0.414 mmol), EDC (3.2 eq), DMAP (0.4 eq), pentafluorophenol (3.3 eq) and THF (24 mL) were stirred at room temperature for 18h. Solvent was removed under reduced pressure and the residue was flash chromatographed (2, 4, 6, 10, 15% EtOAc in $CHCl_3$) yielding **C13b** (463 mg) in quantitative yield. The material was taken immediately to the next step.

Propyl ApA receptor C14. Diamine **C9a** (41.6 mg, 0.136 mmol), **C13b** (3 eqiv), DMF (10 mL) and freshly distilled TEA (330 μL, 17 equiv) were stirred at room temperature for 22h. The suspension gradually cleared. The reaction mixture was concentrated *in vacuo* and the orange residue was flash chromatographed (10, 15% MeOH/$CHCl_3$) to give 219.3 mg (78.5%) of receptor **C14**: IR (KBr) 3381, 3178, 2959, 2871, 1700, 1653, 1506, 1465, 1399, 1308, 1196 cm^{-1}; ^1H NMR (300 MHz, DMSO-d_6) δ 10.311 (s, 4 H), 9.242 (s, 4 H), 8.903 (s, 2 H), 8.281 (s, 4 H), 8.174 (d, 4 H, J = 8.38 Hz), 7.742 (d, 6 H, J = 7.91 Hz), 7.506 (d, 4 H, J = 8.75 Hz), 7.344 (d, 4 H, J = 8.75 Hz), 3.7-3.4 (m, 10 H), 2.671 (d, 12 H, J = 17.29 Hz), 2.013 (d, 4 H, J = 12.47), 1.9-1.7 (m, 12 H), 1.6-0.7 (m, 84 H); MS (Plasma Desorption) calc'd for $C_{119}H_{154}N_{15}O_{14}$ $(M)^+$, 2017.2, found 2018.7.

Preparation of mono(carbamate)-mono(*t*-butyl-diphenyl-silylether)bicyclicguanidiniums C16a - C16l. Alcohol **A7** (50 mg, 0.10 mmol), DABCO (3 mg, 0.03 mmol) and dioxane (1 mL) over 3 Å sieves were warmed to 80 °C. Once this was homogeneous, $(Bu)_2Sn(OAc)_2$ (7.6 μL) was added and stirred for 5 min. The isocyanate (**a, b, c...** or **l**, 1.1 equiv) was added and the solution was stirred at 70 °C for 30min - 1 h. Solvent was removed under reduced pressure and the resulting residue was filtered through silica gel (20% EtOAc/$CHCl_3$, 5% MeOH/$CHCl_3$). The desired carbamates were obtained from the MeOH/$CHCl_3$ elution.

Mono(cyclohexylcarbamate)-mono(*t*-butyl-diphenyl-silylether)bicyclicguanidinium C16a: ^1H NMR (300 MHz, $CDCl_3$) δ 9.134 (s, 1 H), 8.782 (s, 1 H), 7.64-7.58 (m, 4 H), 7.43-7.34 (m, 6 H), 5.953 (d, 1 H, J = 7.8 Hz), 4.318 (d, 1 H, J = 6.4 Hz), 3.83-3.12 (m, 10 H), 2.05-1.67 (m, 10 H), 1.30-1.06 (m, 4 H), 1.046 (s, 9 H).

Mono(allylcarbamate)-mono(*t*-butyl-diphenyl-silylether)bicyclicguanidinium C16b: ^1H NMR (300 MHz, $CDCl_3$) δ 9.229 (s, 1 H), 8.767 (s, 1 H), 7.619 (m, 4 H), 7.407 (m, 6 H), 6.139 (br t, 1 H, J = 5.8 Hz), 5.83-5.24 (m, 1 H), 5.25-5.10 (m, 1 H), 5.075 (d, 1 H, J = 10.26 Hz), 4.358 (dd, 1 H, J = 9.6, 3.3 Hz), 3.82-3.50

(m, 5 H), 3.27-3.13 (m, 4 H), 2.04-1.73 (m, 4 H), 1.049 (s, 9 H).

Mono(benzylcarbamate)-mono(*t*-butyl-diphenyl-silylether)bicyclicguanidinium C16c: ^{1}H NMR (300 MHz, $CDCl_3$) δ 9.300 (s, 1 H), 8.773 (s, 1 H), 7.627 (m, 4 H), 7.43-7.20 (m, 11 H), 6.464 (t, 1 H, J = 5.9 Hz), 4.39-4.33 (m, 3 H), 3.83-3.50 (m, 5 H), 3.26-3.11 (m, 4 H), 2.04-1.73 (m, 4 H), 1.058 (s, 9 H).

Mono(ethoxyacetylcarbamate)-mono(*t*-butyl-diphenyl-silylether)bicyclicguanidinium C16d: ^{1}H NMR (300 MHz, $CDCl_3$) δ 9.205 (s, 1 H), 8.725 (s, 1 H), 7.626 (m, 4 H), 7.46-7.35 (m, 6 H), 6.395 (t, 1 H, J = 6.1 Hz), 4.336 (dd, 1 H, J = 4.5, 10.7 Hz), 4.170 (q, 2 H, J = 7.2 Hz), 3.97-3.50 (m, 7H), 3.28-3.14 (m, 4 H), 2.17-1.77 (m, 4 H), 1.253 (m, 3 H, J = 7.1 Hz), 1.056 (s, 9 H).

Mono(isopropylcarbamate)-mono(*t*-butyl-diphenyl-silylether)bicyclicguanidinium C16e: ^{1}H NMR (300 MHz, $CDCl_3$) δ 9.200 (s, 1 H), 8.835 (s, 1 H), 7.632 (m, 4 H), 7.47-7.36 (m, 6 H), 5.858 (d, 1 H, J = 7.7 Hz), 4.339 (dd, 1 H, J = 9.6, 3.2 Hz), 3.85-3.57 (m, 6 H), 3.27-3.14 (m, 4 H), 2.08-1.70 (m, 4 H), 1.21-1.12 (m, 6 H), 1.066 (s, 9 H).

Mono(adamantylcarbamate)-mono(*t*-butyl-diphenyl-silylether)bicyclicguanidinium C16f: ^{1}H NMR (300 MHz, $CDCl_3$) δ 9.232 (s, 1 H), 8.880 (s, 1 H), 7.625 (m, 4 H), 7.47-7.36 (m, 6 H), 5.835 (br s, 1 H), 8.582 (d, 1 H, J = 6.2 Hz), 3.853 (d, 1 H, J = 6.2 Hz), 3.706 (s, 5 H), 3.64-3.51 (m, 4 H), 3.25-3.10 (m, 4 H), 2.06-1.25 (m, 14 H), 1.065 (s, 9 H).

Mono(*t*-butylcarbamate)-mono(*t*-butyl-diphenyl-silylether)bicyclicguanidinium C16g: ^{1}H NMR (300 MHz, $CDCl_3$) δ 9.201 (s, 1 H), 8.847 (s, 1 H), 7.625 (m, 4 H), 7.47-7.36 (m, 6 H), 5.954 (br s, 1 H), 4.303 (d, 1 H, J = 6.4 Hz), 3.848 (d, 1 H, J = 6.0 Hz), 3.70-3.51 (m, 4 H), 3.28-3.14 (m, 4 H), 2.07-1.73 (m, 4 H), 1.32-1.30 (m, 9 H), 1.065 (s, 9 H).

Mono(*p*-tolylcarbamate)-mono(*t*-butyl-diphenyl-silylether)bicyclicguanidinium C16h: ^{1}H NMR (300 MHz, $CDCl_3$) δ 9.311 (s, 1 H), 8.661 (br s, 1 H), 8.554 (s, 1 H), 7.66-7.61 (m, 4 H), 7.44-7.38 (m, 8 H), 7.060 (d, 2 H, J = 8.2 Hz), 4.475 (d, 1 H, J = 6.2 Hz), 3.84-3.53 (m, 5 H), 3.28-3.13 (m, 4 H), 2.274 (s, 3 H), 2.06-1.75 (m, 4 H), 1.069 (s, 9 H).

Mono(phenylcarbamate)-mono(*t*-butyl-diphenyl-silylether)bicyclicguanidinium C16i: ^{1}H NMR (300 MHz, $CDCl_3$) δ 9.381 (br s, 1 H), 8.850 (br s, 1 H), 8.621 (br s, 1 H), 7.66-7.61 (m, 4 H), 7.521 (d, 2 H, J = 7.5 Hz), 7.47-7.23 (m, 8 H), 7.004 (t, 1 H, J = 7.3 Hz), 4.490 (d, 1 H, J = 6.2 Hz), 3.84-3.53 (m, 5 H), 3.29-3.10 (m, 4 H), 2.12-1.74 (m, 4 H), 1.070 (s, 9 H).

Mono(*p*-methoxyphenylcarbamate)-mono(*t*-butyl-diphenyl-silylether)bicyclicguanidinium C16j: ^{1}H NMR (300 MHz, $CDCl_3$) δ 9.288 (br s, 1 H), 8.668 (br s, 1 H), 8.565 (br s, 1 H), 7.66-7.60 (m, 4 H), 7.46-7.35 (m, 8 H), 6.801 (d, 2 H, J = 9.0 Hz), 4.454 (d, 1 H, J = 6.4 Hz), 3.83-3.52 (m, 8 H), 3.27-3.12 (m, 4 H), 2.06-1.73 (m, 4 H), 1.063 (s, 9 H).

Mono(*m*-methoxyphenylcarbamate)-mono(*t*-butyl-diphenyl-silylether)bicyclicguanidinium C16k: ^{1}H NMR (300 MHz, $CDCl_3$) δ 9.417 (br s, 1 H), 8.743 (br s, 1 H), 8.612 (br s, 1 H), 7.66-7.61 (m, 4 H), 7.44-7.37 (m, 6 H), 7.20-7.05 (m, 3 H), 6.59-6.56 (m, 1 H), 4.505 (d, 1 H, J = 6.2 Hz), 3.86-3.56 (m, 8 H), 3.32-3.14 (m, 4 H), 2.08-1.77 (m, 4 H), 1.070 (s, 9 H).

Mono(1-naphthylcarbamate)-mono(*t*-butyl-diphenyl-silylether)bicyclicguanidinium C16l: ^{1}H NMR (300 MHz, $CDCl_3$) δ 9.728 (br s, 1 H), 8.700 (br s, 1 H), 8.652 (br s, 1 H), 8.477 (d, 1 H, J = 8.6 Hz), 7.92-7.40 (m, 16 H), 4.584 (d, 1 H, J = 6.4 Hz), 3.88-3.56 (m, 6 H), 3.34-3.15 (m, 4 H), 2.10-1.73 (m, 4 H), 1.077 (s, 9H).

Preparation of bis-carbamate bicyclicguanidinium libraries C17a - l. Silylether **C16a...or C16l** (0.05 mmol) was stirred in a 3% HCl/MeOH solution (500 - 800μL) at room temperature overnight. The solvent was removed, and the residue was taken up in CH_2Cl_2(2 mL) and water (2 mL). The aqueous layer was washed with CH_2Cl_2 (3 x 2 mL) and was concentrated *in vacuo*. The deprotected alcohol was converted to the carbamate using an equimolar mixture of 12 isocyanates under the same conditions described for the synthesis of **C16**'s. Filtration of library **C17**'s was through basic alumina using 20% MeOH/CH_2Cl_2.

5.2 Transport

Transport studies were preformed by Dr. Cecilia Andreu using a U-tube with dichloroethane separating the aqueous source and receiving solutions (2 mL). The source phase was a solution of the nucleotide and the receiving phase was an NaCl (10 mM) solution unless otherwise noted. The surface area of contact between aqueous and organic phases was 1.468 cm^2.

The rate of transport was followed by monitoring the concentration of nucleotide in aliquots from both aqueous phases by UV/visible spectroscopy. Experiments were performed at least in duplicate.

D. BIBLIOGRAPHY

(1) Fersht, A. R.; Shi, J.-P.; Knill-Jones, J.; Lowe, D. M.; Wilkson, A. J.; Blow, D. M.; Brick, P.; Carter, P.; Wayne, M. M. Y.; Winter, G. *Nature* **1985**, *314*, 235-238.

(2) Wells, T. N. C.; Fersht, A. R. *Nature* **1985**, *316*, 656-657.

(3) Fersht, A. R. *Trends Biochem. Sci.* **1987**, *12*, 301-304.

(4) Serrano, L.; Kellis, J. T.; Cann, P.; Matouschek, A.; Fersht, A. R. *J. Mol. Biol.* **1992**, *224*, 783-804.

(5) Williams, D. H. *Aldrichimica Acta* **1991**, *24*, 71-80.

(6) Williams, D. H. *Aldrichimica Acta.* **1992**, *25*, 9.

(7) Searle, M. S.; Williams, D. H. *Anal. Quim.* **1993**, *89*, 17-26.

(8) Huyghues-Despointes, B. M. P.; Klingler, T. M.; Baldwin, R. L. *Biochemistry* **1995**, *34*, 13267-13271.

(9) Thorson, J. S.; Chapman, E.; Murphy, E. C.; Schultz, P. G. *J. Am. Chem. Soc.* **1995**, *117*, 1157-1158.

(10) Thorson, J. S.; Chapman, E.; Schultz, P. G. *J. Am. Chem. Soc.* **1995**, *117*, 9361-9362.

(11) Rebek J., J. *Science* **1987**, *235*, 1437-1444.

(12) Schneider, H.-J. *Angew. Chem. Int. Ed. Engl.* **1991**, *30*, 1417-1436.

(13) Seel, C.; Galán, A.; de Mendoza, J. *Top. Curr. Chem.* **1995**, *175*, 101-132.

(14) Rebek, J. *Angew. Chem. Int. Ed. Engl.* **1990**, *29*, 245-255.

(15) Williams, K.; Askew, B.; Ballester, P.; Buhr, C.; Jeong, K. S.; Jones, S.; Rebek, J., Jr. *J. Am. Chem. Soc.* **1989**, *111*, 1090-1094.

(16) Adrian, J. C.; Wilcox, C. S. *J. Am. Chem. Soc.* **1989**, *111*, 8055-8057.

(17) Goswami, S.; Hamilton, A. D. *J. Am. Chem. Soc.* **1989**, *111*, 3425-3426.

(18) Zimmerman, S. C.; Wu, W.; Zeng, Z. *J. Am. Chem. Soc.* **1991**, *113*, 196-201.

(19) Galán, A.; Pueyo, E.; Salmerón, A.; de Mendoza, J. *Tetrahedron Lett.* **1991**, *132*, 1827-1830.

(20) Kurihara, K.; Ohto, K.; Honda, Y.; Kunitake, T. *J. Am. Chem. Soc.* **1991**, *113*, 5077-5079.

(21) Nowick, J. S.; Chen, J. S. *J. Am. Chem. Soc.* **1993**, *115*, 7637-7644.

(22) Schall, O. F.; Gokel, G. W. *J. Am. Chem. Soc.* **1994**, *116*, 6089-6100.

(23) Böhmer, V.; Vogt, W.; Goldmann, H. *J. Org. Chem.* **1990**, *55*, 2569-2570.

(24) Breslow, R.; Canary, J. W.; Varney, M.; Waddell, S. T.; Yang, D. *J. Am. Chem. Soc.* **1990**, *112*, 5212-5219.

(25) Deiderich, F. *J. Chem. Ed.* **1990**, *67*, 813-320.

(26) Hosseini, M. W.; Blacker, A. J.; Lehn, J.-M. *J. Am. Chem. Soc.* **1990**, *112*, 3896-3904.

(27) Tucker, J. A.; Knobler, C. B.; Goldberg, I.; J., C. D. *J. Org. Chem.* **1989**, *54*, 5460-5482.

(28) Schneider, H.-J. *Angew. Chem. Int. Ed. Engl.* **1989**, *28*, 753-754.

(29) Schneider, H.-J.; Blatter, T.; Palm, B.; Pfingstag, U.; Rüdiger, V.; Theis, I. *J. Am. Chem. Soc.* **1992**, *114*, 7704-7708.

(30) Schneider, H.-J.; Blatter, T. *Angew. Chem. Int. Ed. Engl.* **1992**, *31*, 1207-1208.

(31) Schneider, H.-J.; Schiestel, T.; Zimmermann, P. *J. Am. Chem. Soc.* **1992**, *116*, 7698-7703.

(32) Schneider, H.-J.; Theis, I. *J. Org. Chem.* **1992**, *57*, 3066-3070.

(33) Schneider, H.-J.; Blatter, T.; Eliseev, A.; Rüdiger, V.; Raevsky, O. *Pure & Appl. Chem.* **1993**, *65*, 2329-2334.

(34) Eliseev, A. V.; Schneider, H.-J. *J. Am. Chem. Soc.* **1994**, *116*, 6081-6088.

(35) Poh, B.-L.; Tan, C. M. *Tetrahedron* **1994**, *50*, 3453-3462.

(36) Poh, B.-L.; Tan, C. M. *Tetrahedron* **1995**, *51*, 953-958.

(37) Hunter, C. A.; Sanders, J. K. M. *J. Am. Chem. Soc.* **1990**, *112*, 5525-5534.

(38) Smithrud, D. B.; Diederich, F. *J. Am. Chem. Soc.* **1990**, *112*, 339-343.

(39) Rotello, V.; Viani, E.; Deslonchamps, G.; Murray, B.; Rebek, J. *J. Am. Chem. Soc.* **1993**, *115*, 797-798.

(40) Kato, Y.; Conn, M. M.; Rebek, J., Jr. *J. Am. Chem. Soc.* **1994**, *114*, 3279-3284.

(41) Thornton, J. S. J. M.; Snarey, M.; Campbell, S. F. *FEBS Letters* **1987**, *224*, 161-171.

(42) Echavarren, A.; Galán, A.; de Mendoza, J.; Salmerón, A.; Lehn, J.-M. *Helvetica Chimica Acta* **1988**, *71*, 685-693.

(43) Müller, G.; Riede, J.; Schmidtchen, F. P. *Angew. Chem. Int. Ed. Engl.* **1988**, *27*, 1516-1518.

(44) Echavarren, A.; Galán, A.; Lehn, J.-M.; de Mendoza, J. *J. Am. Chem. Soc.* **1989**, *111*, 4994-4995.

(45) Schmidtchen, F. P. *Tetrahedron Lett.* **1989**, *30*, 4493-4496.

(46) Galán, A.; de Mendoza, J.; Toiron, C.; Bruix, M.; Deslongchamps, G.; Rebek, J. *J. Am. Chem. Soc.* **1991**, *113*, 9424-9425.

(47) Deslongchamps, G.; Galán, A.; de Mendoza, J.; Rebek, J. *Angew. Chem. Int. Ed. Engl.* **1992**, *31*, 61-63.

(48) Göbel, M. W.; Bats, J. W.; Dürner, G. *Angew. Chem. Int. Ed. Engl.* **1992**, *31*, 207-209.

(49) Schmidtchen, F. P.; Schießl, P. *Tetrahedron Lett.* **1993**, *34*, 2449-2452.

(50) Russell, V. A.; Etter, M. C.; Ward, M. D. *J. Am. Chem. Soc.* **1994**, *116*, 1941-1952.

(51) Schiessl, P.; Schmidtchen, F. P. *J. Org. Chem.* **1994**, *59*, 509-511.

(52) Albert, J. S.; Goodman, M. S.; Hamilton, A. D. *J. Am. Chem. Soc.* **1995**, *117*, 1143-1144.

(53) Perreault, D. M.; Chen, X.; Anslyn, E. V. *Tetrahedron* **1995**, *51*, 353-362.

(54) Peschke, W.; Schiessl, P.; Schmidtchen, F. P.; Bissinger, P.; Schier, A. *J. Org. Chem.* **1995**, *60*, 1039-1043.

(55) Saenger, W. In *Principles of Nucleic Acid Structure* Springer-Verlag: New York, 1984.

(56) Tjivikua, T.; Deslongchamps, G.; Rebek, J., Jr. *J. Am. Chem. Soc.* **1990**, *112*, 8408-8414.

(57) Conn, M. M.; Deslongchamps, G.; de Mendoza, J.; Rebek, J. *J. Am. Chem. Soc.* **1993**, *115*, 3548-3557.

(58) Conn, M. M. Ph. D. Thesis, Massachusetts Institute of Technology, 1994.

(59) Kurzmeier, H.; Schmidtchen, F. P. *J. Org. Chem.* **1990**, *55*, 3749-3755.

(60) Lindley, J. *Tetrahedron* **1984**, *40*, 1433-1456.

(61) Springs, B.; Haake, P. *Bioorg. Chem.* **1977**, *6*, 181-190.

(62) Hore, P. J. *J. Magn. Reson.* **1983**, *54*, 283-300.

(63) Hore, P. J. *J. Magn. Reson.* **1983**, *54*, 539-542.

(64) Connors, K. A. *Binding Constants*; John Wiley & Sons, Inc.: New York, 1987.

(65) Marquesse, S.; Baldwin, R. L. *Proc. Natl. Acad. Sci. USA* **1987**, *84*, 8898-8902.

(66) Williams, D. H. ;. C., J. P. L.; Doig, A. J.; Gardner, M.; Gerhard, U.; Kaye, P. T.; Lal, A. R.; Nicholls, I. A.; Salter, C. J.; Mitchell, R. C. *J. Am. Chem. Soc.* **1991**, *113*, 7020-7030.

(67) Doig, A., J.; Williams, D. H. *J. Am. Chem. Soc.* **1992**, *114*, 338-343.

(68) Searle, M. S.; Williams, D. H.; Gerhard, U. *J. Am. Chem. Soc.* **1992**, *114*, 10697-10704.

(69) Page, M. I.; Jencks, W. P. *Proc. Natl. Acad. Sci. U.SA.* **1971**, *68*, 1678-1683.

(70) Jencks, W. P. *Proc. Natl. Acad. Sci. U.S.A.* **1981**, *78*, 4046-4050.

(71) Gerhard, U.; Searle, M. S.; Williams, D. H. *Bioorg. Med. Chem. Lett.* **1993**, *3*, 803-808.

(72) Kato, Y.; Conn, M. M.; Rebek, J., Jr. *Proc. Nat. Acad. Sci. USA* **1995**, *92*, 1208-1212.

(73) Jeffrey, G. A. *Hydrogen Bonding in Biological Structures*; Springer-Verlag: Berlin, 1991.

(74) Whitesides, G. M.; Mathias, J. P.; Seto, C. T. *Science* **1991**, *254*, 1312-1319.

(75) Bass, B. L.; Cech, T. R. *Nature* **1984**, *308*, 820-826.

(76) Jorgensen, W.; Severance, D. L. *J. Am. Chem. Soc.* **1991**, *113*, 209-216.

(77) Ts'o, P. O. P. In *Basic Principles in Nucleic Acid Chemistry*; P. O. P. Ts'o, Ed.; Academic Press: New York, 1974; Vol. I; pp Chapter 6.

(78) Newcomb, L. F.; Gellman, S. H. *J. Am. Chem. Soc.* **1994**, *116*, 4993-4994.

(79) Newcomb, L. F.; Haque, T. S.; Gellman, S. H. *J. Am. Chem. Soc.* **1995**, *117*, 6509-6519.

(80) Doig, A. J.; Williams, D. H. *Biochemistry* **1992**, *31*, 9371-9375.

(81) Searle, M. S.; Westwell, M. S.; Williams, D. H. *J. Chem. Soc. Perkin Trans. 2* **1995**, 141-151.

(82) Still, W. C.; Kahn, M.; Mitra, A. *J. Org. Chem.* **1978**, *43*, 2923-2925.

(83) Askew, B.; Ballester, P.; Buhr, C.; Jeong, K. S.; Jones, S.; Parris, K.; Williams, K.; Rebek, J., Jr. *J. Am. Chem. Soc.* **1989**, *111*, 1082-1090.

(84) *Systat 5.2*; 5.2 ed.; Systat Inc: Evanston, IL, 1992.

(85) Mohamadi, F.; Richards, N. G.; Guida, W. C.; Liskamp, R.; Lipton, M.; Caufield, C.; Chang, G.; Hendrickson, T.; Still, W. C. *J. Comput. Chem.* **1990**, *11*, 440-467.

(86) Ponder, J. W.; Richards, F. M. *J. Comput. Chem.* **1987**, *8*, 1016-1024.

(87) McDonald, D. Q.; Still, W. C. *Tetrahedron Lett.* **1992**, *33*,

(88) Still, W. C.; Tempczyk, A.; Hawley, R. C.; Hendrickson, T. *J. Am. Chem. Soc.* **1990**, *112*, 6127-6129.

(89) Gerlt, J. A.; Gassman, P. G. *Biochemistry* **1993**, *32*, 11943-11952.

(90) Gerlt, J. A.; Gassman, P. G. *J. Am. Chem. Soc.* **1993**, *115*, 11552-11568.

(91) Cleland, W. W.; Kreevoy, M. M. *Science* **1994**, *264*, 1887-1890.

(92) Frey, P. A.; Whitt, S. A.; Tobin, J. B. *Science* **1994**, *264*, 1927-1930.

(93) McGaw, B. L.; Ibers, J. A. *J. Chem. Phys.* **1963**, *39*, 2677-2684.

(94) Hamilton; Ibers *Hydrogen Bonding in Solids*; W. A. Benjamin, Inc.: 1968, pp 94-.

(95) Emsley, J. *Chem. Soc. Revs.* **1980**, *9*, 91-124.

(96) Emsley, J.; Jones, D. J.; Lucas, J. *Reviews in Inorganic Chemistry* **1981**, *3*, 104-140.

(97) Hibbert, F.; Emsley, J. *Advances in Physical Organic Chemistry* **1990**, *26*, 255-379.

(98) Gilli, P.; Bertolasi, V.; Ferretti, V.; Gilli, G. *J. Am. Chem. Soc.* **1994**, *116*, 909-915.

(99) Guthrie, J. P.; Kluger, R. *J. Am. Chem. Soc.* **1993**, *115*, 11569-11572.

(100) Warshel, A.; Papazyan, A.; Kollman, P. A.; Cleland, W. W.; Kreevoy, M. M.; Frey, P. A. *Science* **1995**, *269*, 102-106.

(101) Scheiner, S.; Kar, T. *J. Am. Chem. Soc.* **1995**, *117*, 6970-6975.

(102) Alagona, G.; Ghio, C.; Kollman, P. A. *J. Am. Chem. Soc.* **1995**, *117*, 9855-9862.

(103) Mock, W. L.; Chua, D. C. Y. *J. Chem. Soc. Perkin Trans. 2* **1995**, 2069-2074.

(104) Brzezinski, B.; Maciejewska-Urjasz, H.; Zundel, G. *J. of Molecular Structure* **1994**, *319*, 177-182.

(105) Tobin, J. B.; Whitt, S. A.; Cassidy, C. S.; Frey, P. A. *Biochemistry* **1995**, *34*, 6919-6924.

(106) Schwartz, B.; Drueckhammer, D. G.; Usher, K. C.; Remington, S. J. *Biochemistry* **1995**, *34*, 15459-15466.

(107) Staab, H. A.; Saupe, T. *Angew. Chem. Int. Ed. Engl.* **1988**, *27*, 865-879.

(108) Einspahr, H.; Robert, J.-B.; Marsh, R. E.; Roberts, J. D. *Acta Crystallogr., Sect. B* **1973**, *29*, 1611.

(109) Truter, M. R.; Vickery, B. L. *J. C. S. Dalton* **1972**, 395.

(110) Usher, K. C.; Remington, S. J.; Martin, D. P.; Drueckhammer, D. G. *Biochemistry* **1994**, *33*, 7753-7759.

(111) Schwartz, B.; Drueckhammer, D. G. *J. Am. Chem. Soc.* **1995**, *117*, 11902-11905.

(112) Watton, S. P.; Masschelein, A.; Rebek, J., Jr.; Lippard, S. J. *J. Am. Chem. Soc.* **1994**, *116*, 5196-5205.

(113) Parris, K. D. Ph.D. Thesis, University of Pittsburgh, 1988.

(114) Yun, J.; Lippard, S. J. unpublished results.

(115) Rebek, J., Jr.; Duff, R. J.; Gordon, W. E.; Parris, K. *J. Am. Chem. Soc.* **1986**, *108*, 6068-6069.

(116) Perrin, C. L.; Thoburn, J. D. *J. Am. Chem. Soc.* **1992**, *114*, 8559-8565.

(117) Perrin, C. L. *Science* **1994**, *266*, 1665-1668.

(118) Altman, L. J.; Laungani, D.; Gunnarsson, G.; Wennerström, H.; Forsén, S. *J. Am. Chem. Soc.* **1978**, *100*, 8264-8266.

(119) Frant, M. S. *Today's Chemist at Work* **1995**, 39-42.

(120) Davis, M. M.; Hetzer, H. B. *Journal of Research of the National Bureau of Standards* **1958**, *60*, 569-592.

(121) Kucharsky, J.; Safarik, L. *Titrations in Non-aqueous Solvents*; Elsevier Publishing Co.: Amsterdam, 1965.

(122) Davis, M. M.; Paabo, M. *J. Org. Chem.* **1966**, *31*, 1804-1810.

(123) Gyenes, I.; Cohen, D.; Millar, I. T. *Titration in Non-aqueous Media*; Iliffe Books Ltd.: Princeton, 1967.

(124) Huber, W. *Titrations in Nonaqueous Solvents*; Academic Press: New York, 1967.

(125) Davis, M. M. *Acid-Base Behavior in Aprotic Organic Solvents*; U. S. National Bureau of Standards: Washington D. C., 1968; Vol. Monograph 105.

(126) Zhou, G. W.; Guo, J.; Huang, W.; Fletterick, R. J.; Scanlan, T. S. *Science* **1994**, *256*, 1059-1064.

(127) Huff, J. B.; Askew, B.; Duff, R. J.; Rebek, J., Jr. *J. Am. Chem. Soc.* **1988**, *110*, 5908-5909.

(128) Zimmerman, S. C.; Cramer, K. D. *J. Am. Chem. Soc.* **1988**, *110*, 5906-5908.

(129) Breslow, R.; Trainor, G.; Ueno, A. *J. Am. Chem. Soc.* **1983**, *105*, 2739-2744.

(130) Lehn, J.-M.; Sirlin, C. *J. Chem. Soc.: Chem. Commun.* **1978**, 949.

(131) Cram, D. J.; Lam, P. Y.; Ho, S. P. *J. Am. Chem. Soc.* **1986**, *108*, 839-841.

(132) D'Souza, V. T.; Bender, M. L. *Acc. Chem. Res.* **1987**, *20*, 146-152.

(133) Kunitake, T.; Okahata, Y.; Sakamoto, T. *J. Am. Chem. Soc.* **1976**, *98*, 7799-7806.

(134) Menger, F. M.; Whitesell, L. G. *J. Am. Chem. Soc.* **1985**, *107*, 707-708.

(135) Blow, D. M.; Birktoft, J. J.; Hartley, B. S. *Nature* **1969**, *221*, 337.

(136) Kraut, J. *Ann. Rev. Biochem.* **1977**, *46*, 331.

(137) Singer, P. T.; Smalås, A.; Carty, R. P.; Mangel, W. F.; Sweet, R. M. *Science* **1993**, *259*, 669-673.

(138) Perona, J. J.; Craik, C. S.; Fletterick, R. J.; Singer, P. T.; Smalås, A.; Carty, R. P.; Mangel, W. F.; Sweet, R. M. *Science* **1993**, *261*, 620-621.

(139) *J. Biol. Chem.* **1983**, *258*, 472.

(140) Weaver, L. H.; Kester, W. R.; Matthews, B. W. *J. Mol. Biol.* **1977**, *114*, 119.

(141) Suck, D.; Oefner, C. *Nature* **1986**, *321*, 620.

(142) Robillard, G.; Shulman, R. G. *J. Mol. Biol.* **1972**, *71*, 507-512.

(143) Bachovchin, W. W. *Proc. Natl. Acad. Sci. U. S. A.* **1985**, *82*, 7948-7951.

(144) Markley, J. L. *Biochemistry* **1978**, *17*, 4646-4656.

(145) *SMART, V. 4.0*; 4.0 ed.; Siemens Industrial Automation, Inc.: Madison, WI, 1994.

(146) *SAINT, V. 4.0*; 4.0 ed.; Siemens Industrial Automation, Inc.: Madison, WI, 1995.

(147) *TeXsan Single Crystal Analysis Package, V. 1.7-1*; 1.7-1 ed.; Molecular Structure Corporation: The Woodlands, TX, 1995.

(148) Zimmerman, S.; Wu, W. *J. Am. Chem. Soc.* **1989**, *111*, 8054-8055.

(149) Král, V.; Sessler, J. L. *Tetrahedron* **1995**, *51*, 539-554.

(150) Würthner, F.; Rebek, J., Jr. *Angew. Chem. Int. Ed. Engl.* **1995**, *34*, 446-448.

(151) Pieters, R. J.; Huc, I.; Rebek, J., Jr. *Tetrahedron* **1995**, *51*, 485-488.

(152) Chen, C.-T.; Siegel, J. S. *J. Am. Chem. Soc.* **1994**, *116*, 5959-5960.

(153) Worm, K.; Schmidtchen, F. P. *Angew. Chem. Int. Ed. Engl.* **1995**, *34*, 65-66.

(154) Ariga, K.; Anslyn, E. V. *J. Org. Chem.* **1992**, *57*, 417-419.

(155) Dixon, R. P.; Gelb, S. J.; Hamilton, A. D. *J. Am. Chem. Soc.* **1992**, *114*, 365-366.

(156) Andreu, C.; Galán, A.; Kobiro, K.; de Mendoza, J.; Park, T. K.; Rebek, J., Jr.; Salmerón, A.; Usman, N. *J. Am. Chem. Soc.* **1994**, *116*, 5501-5502.

(157) Kirby, A. J.; Marriott, R. E. *J. Am. Chem. Soc.* **1995**, *117*, 833-834.

(158) Kimura, E.; Kodama, Y.; Koike, T.; Shiro, M. *J. Am. Chem. Soc.* **1995**, *117*, 8304-8311.

(159) Linkletter, B.; Chin, J. *Angew. Chem. Int. Ed. Engl.* **1995**, *34*, 472-474.

(160) Lehr, S.; Schütz, K.; Bauch, M.; Göbel, M. W. *Angew. Chem. Int. Ed. Engl.* **1994**, *33*, 984-986.

(161) Breslow, R.; Xu, R. *Proc. Natl. Acad. Sci. USA* **1993**, *90*, 1201-1207.

(162) Breslow, R. *Proc. Natl. Acad. Sci. USA* **1993**, *90*, 1208-1211.

(163) Breslow, R. *Supramol. Chem.* **1993**, *1*, 111.

(164) Anslyn, E. V.; Smith, J.; Kneeland, D. M.; Ariga, K.; Chu, F. *Supramol. Chem.* **1993**, *1*, 201-208.

(165) Schneider, H.-J.; Rammo, J.; Hettich, R. *Angew. Chem. Int. Ed. Engl.* **1993**, *32*, 1716.

(166) Vance, D. H.; Czarnik, A. W. *J. Am. Chem. Soc.* **1993**, *115*, 12165.

(167) Pratviel, G.; Duarte, V.; Bernadou, J.; Meunier, B. *J. Am. Chem. Soc.* **1993**, *115*, 7939-7943.

(168) Morrow, J. R.; Buttrey, L. A.; Shelton, V. M.; Berback, K. A. *J. Am. Chem. Soc.* **1992**, *114*, 1903.

(169) Jubian, V.; Dixon, R. P.; Hamilton, A. D. *J. Am. Chem. Soc.* **1992**, *114*, 1120-1121.

(170) Serpersu, E. H.; Shortle, D.; Mildvan, A. S. *Biochemistry* **1987**, *26*, 1289-1300.

(171) Tabushi, I.; Imuta, J.; Seko, N.; Kobuke, Y. *J. Am. Chem. Soc.* **1978**, *100*, 6287-6288.

(172) Tabushi, I.; Kobuke, Y.; Imuta, J. *J. Am. Chem. Soc.* **1980**, *102*, 1744-1745.

(173) Tabushi, I.; Kobuke, Y.; Imuta, J. *J. Am. Chem. Soc.* **1981**, *103*, 6152-6157.

(174) Li, T.; Diederich, F. *J. Org. Chem.* **1992**, *57*, 3449-3454.

(175) Li, T.; Krasne, S. J.; Persson, B.; Kaback, H. R.; Diederich, F. *J. Org. Chem.* **1993**, *58*, 380-384.

(176) Král, V.; Sessler, J. L.; Furuta, H. *J. Am. Chem. Soc.* **1992**, *114*, 8704-8705.

(177) Sessler, J. L.; Furuta, H.; Král, V. *Supramol. Chem.* **1993**, *1*, 209-220.

(178) Benzing, T.; Tjivikua, T.; Wolfe, J.; Rebek, J., Jr. *Science* **1988**, *242*, 266-268.

(179) Jung, G.; Beck-Sickinger, A. G. *Angew. Chem. Int. Ed. Engl.* **1992**, *31*, 367-383.

(180) Geysen, H. M.; Rodda, S. J.; Mason, T. J.; Tribbick, G.; Schoofs, P. G. *J. Immunol. Methods* **1987**, *102*, 259-274.

(181) Houghten, R. A.; Pinilla, C.; Blondelle, S. E.; Appel, J. R.; Dooley, C. T.; Cuervo, J. H. *Nature* **1991**, *354*, 84-86.

(182) Furka, A.; Sebestyén, F.; Asgedom, M.; Dibó, G. *J. Pept. Protein Res.* **1991**, *37*, 487-493.

(183) Lam, K. S.; Salmon, S. E.; Hersh, E. M.; Hurby, V. J.; Kazmierski, W. M.; Knapp, R. J. *Nature* **1991**, *354*, 82-84.

(184) Tuerk, C.; Gold, L. *Science* **1990**, *24*, 505-510.

(185) Beaudry, A. A.; Joyce, G. F. *Science* **1992**, *257*,

(186) Bartel, D. P.; Szostak, J. W. *Science* **1993**, *261*, 1411-1417.

(187) Carell, T.; Wintner, E. A.; Bashir-Hashemi, A.; Rebek, J., Jr. *Angew. Chem. Int. Ed. Engl.* **1994**, *33*, 2059-2061.

(188) Carell, T.; Wintner, E. A.; Sutherland, A. J.; Rebek, J., Jr.; Dunayevskiy, Y. M.; Vouros, P. *Chem. & Biol.* **1995**, *2*, 171-183.

(189) Fodor, S. P. A.; Read, J. L.; Pirrung, M. C.; Stryer, L.; Lu, A. T.; Solas, D. *Science* **1991**, *251*, 767-773.

(190) Rozsnyai, L. F.; Benson, D. R.; Fodor, S. P. A.; Schultz, P. G. *Angew. Chem. Int. Ed. Engl.* **1992**, *31*, 759-761.

(191) Cho, C. Y.; Moran, E. J.; Cherry, S. R.; Stephans, J. C.; Fodor, S. P. A.; Adams, C. L.; Sundaram, A.; Jacobs, J. W.; Schultz, P. G. *Science* **1993**, *261*, 1303-1305.

(192) Pirrung, M. C.; Chen, J. *J. Am. Chem. Soc.* **1995**, *117*, 1240-1245.

E. SPECTRA

Figure E1. NMR of **B2a** in $CDCl_3$ at room temperature after silica gel chromatography.

Figure E2. NMR of **B2a** in $CDCl_3$ at room temperature a) after treatment with HCl gas, b) after addition of 1equiv of DABCO, and c) after washing with 1N HCl.

Figure E3. NMR of **B2a** with a) 0 equiv, b) 1.75 equiv, and c) 2 equiv of Me_4N^+ in $CDCl_3$ at -15 °C.

Figure E4. NMR of **B2a** with 0.16 equiv of Me_4N^+ and a) 0 equiv, b) 0.3 equiv, and c) 0.9 equiv of TEA in $CDCl_3$ at -15 °C.

Figure E5. NMR of **B2a** in CD_2Cl_2 at room temperature with a) 0 equiv, b) <1 equiv, c) 1 equiv, and d) 4 equiv of TEA.

Figure E6. NMR of **B8** in CD_2Cl_2 at a) 25 °C, b) 0 °C, c) -25 °C, d) -50 °C, and e) -70 °C from 0 to 10 ppm.

Figure E7. NMR of **B9** in CD_2Cl_2 at a) 25 °C, b) 0 °C, c) -25 °C, d) -50 °C, and e) -70 °C from 0 to 10 ppm.

Figure E8. NMR of **B9** in CD_2Cl_2 at a) 25 °C, b) 0 °C, c) -25 °C, d) -50 °C, and e) -70 °C from 10 to 20 ppm.

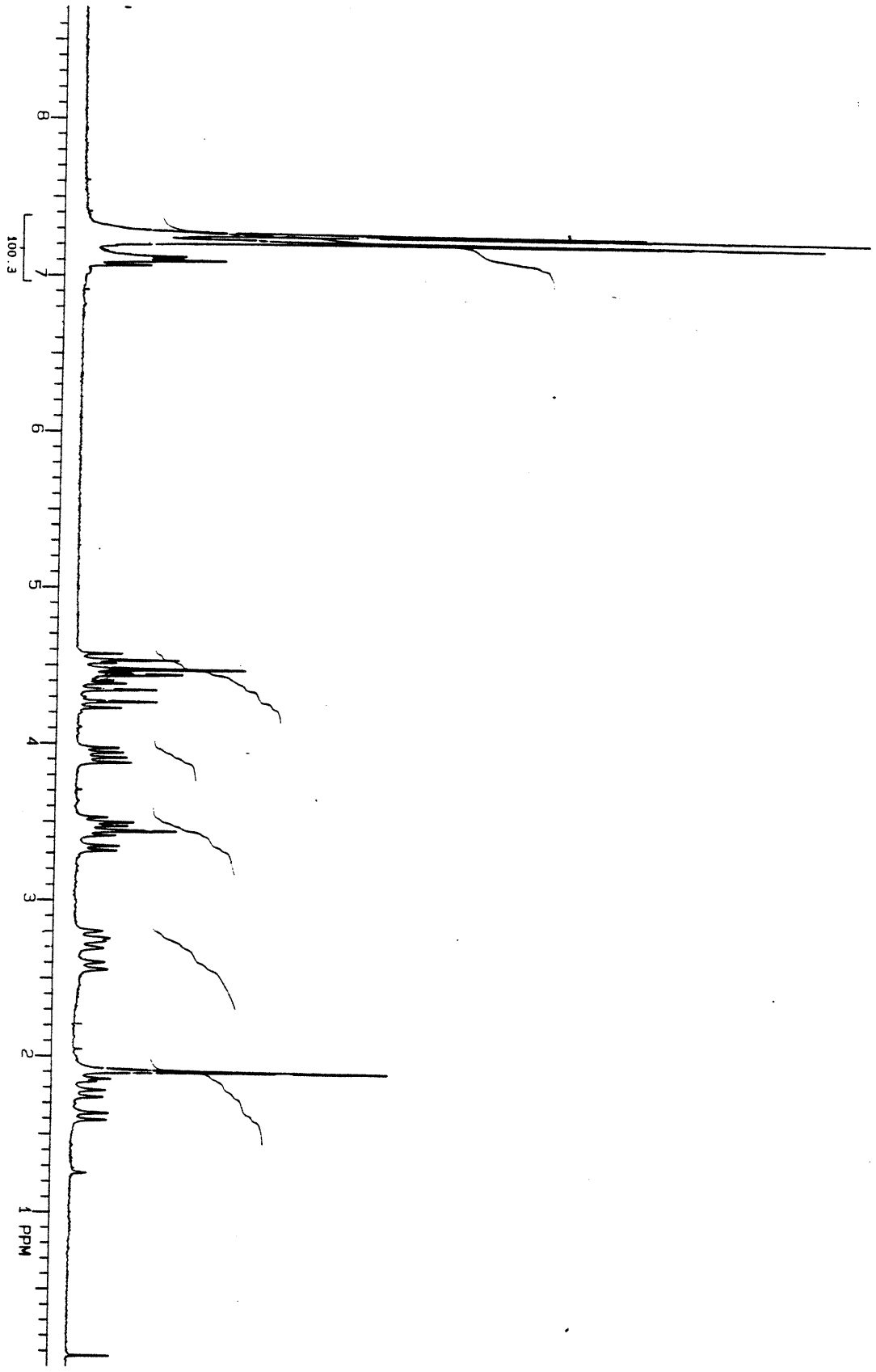

Figure E1. NMR of **B2a** in $CDCl_3$ at room temperature after silica gel chromatography.

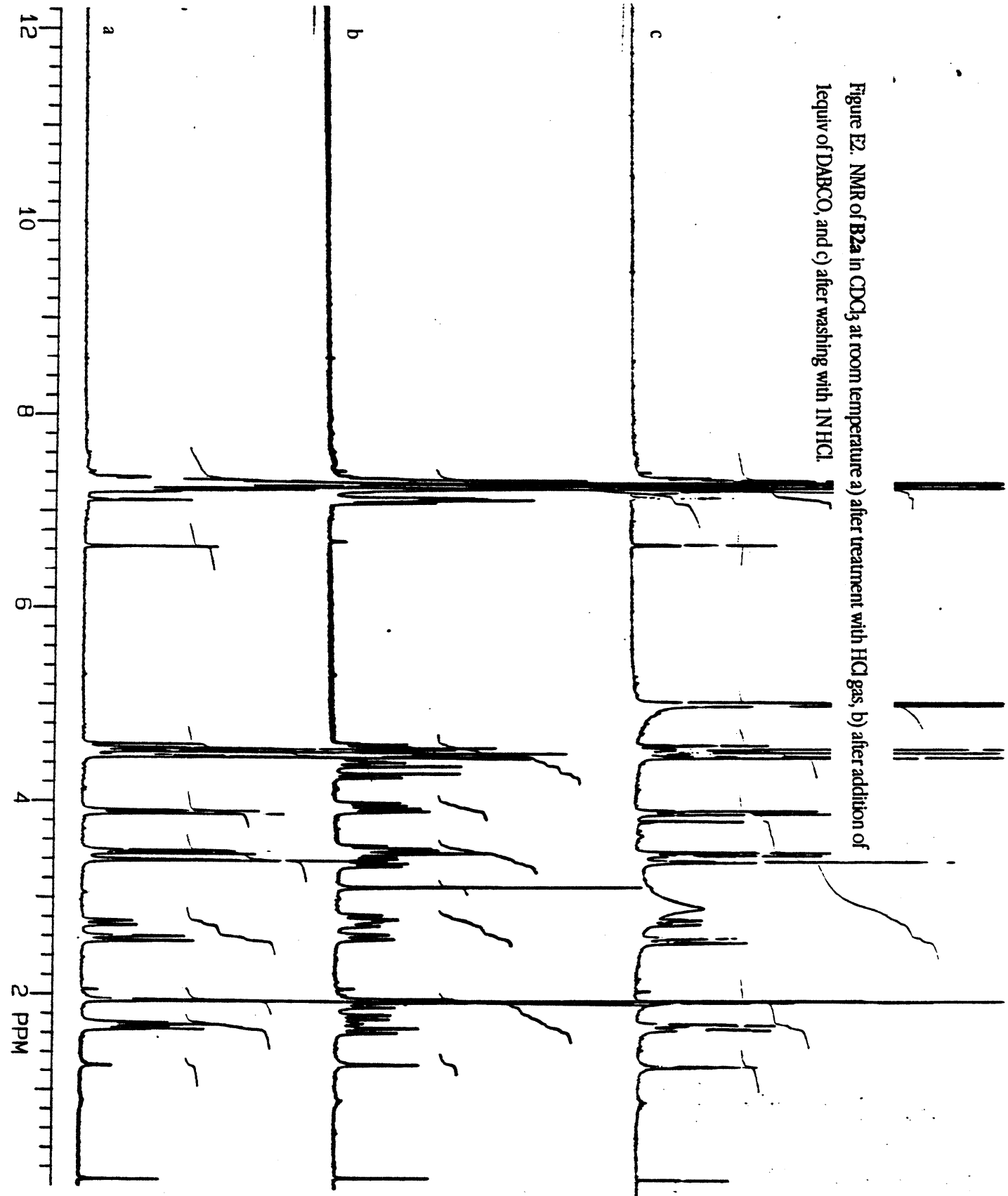

Figure E2. NMR of **B2a** in $CDCl_3$ at room temperature a) after treatment with HCl gas, b) after addition of 1equiv of DABCO, and c) after washing with 1N HCl.

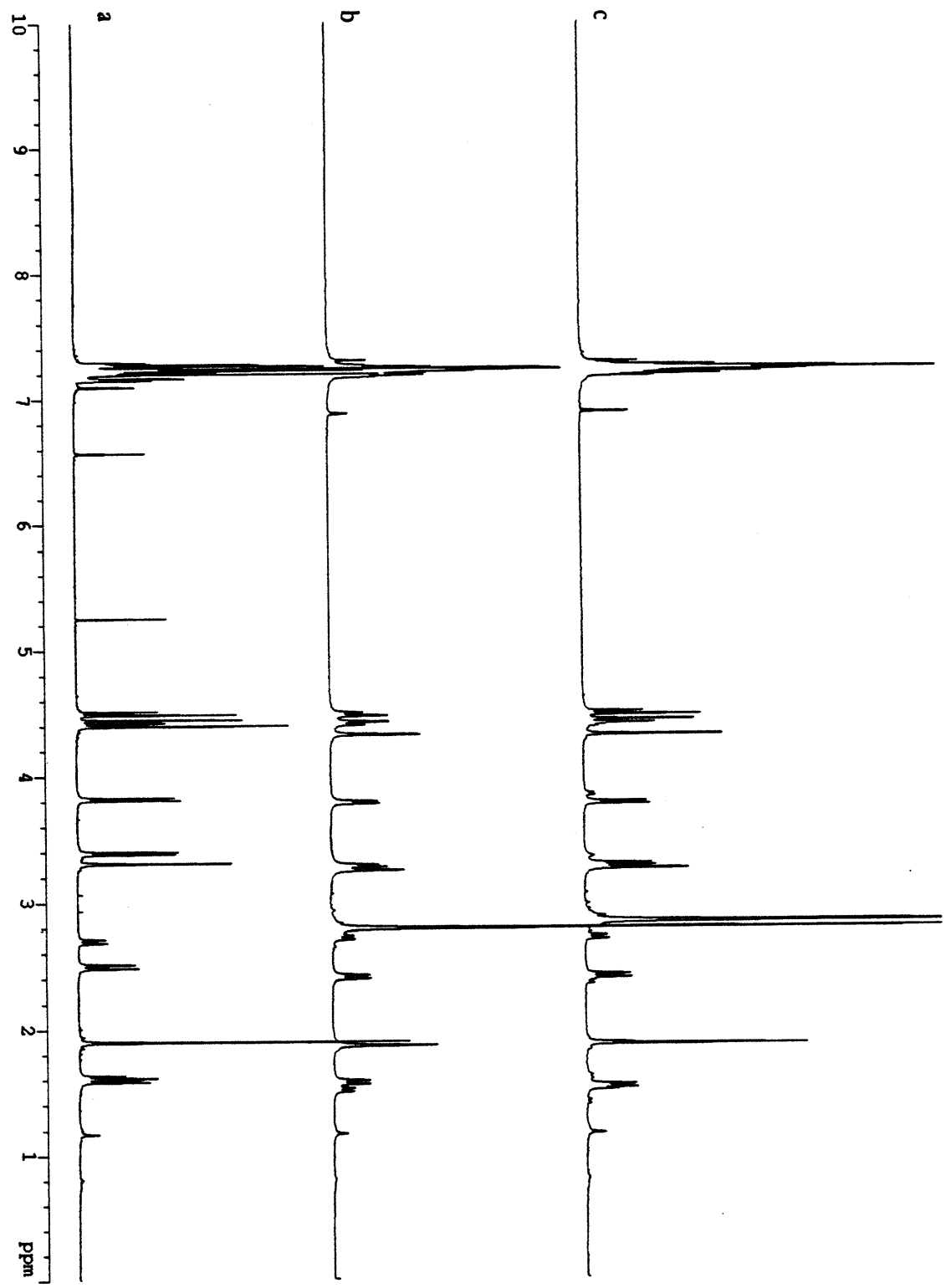

Figure E3. NMR of **B2a** with a) 0 equiv, b) 1.75 equiv, and c) 2 equiv of Me_4N^+ in $CDCl_3$ at -15 °C.

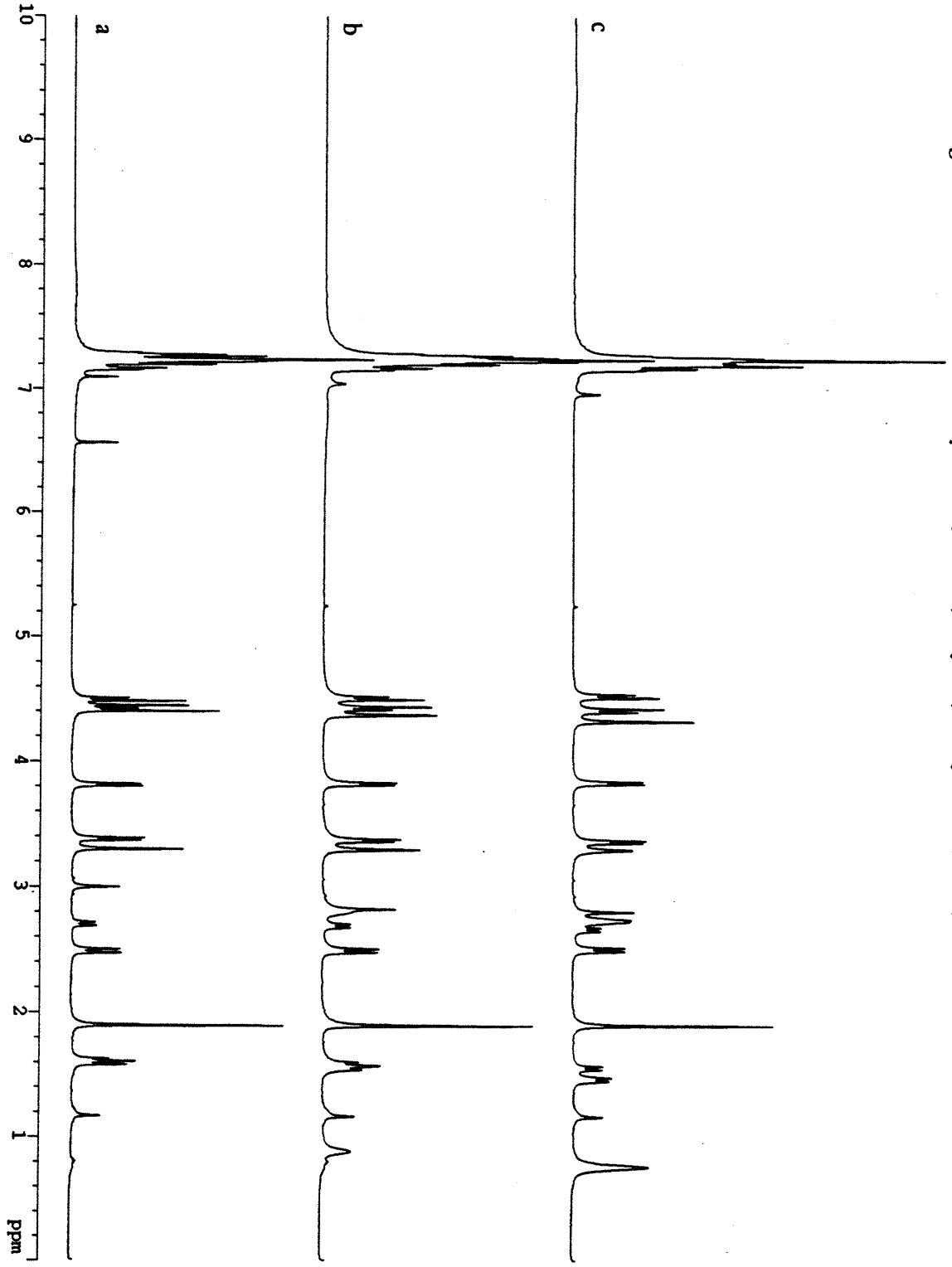

Figure E4. NMR of **B2a** with 0.16 equiv of Me_4N^+ and a) 0 equiv, b) 0.3 equiv, and c) 0.9 equiv of TEA in $CDCl_3$ at -15 °C.

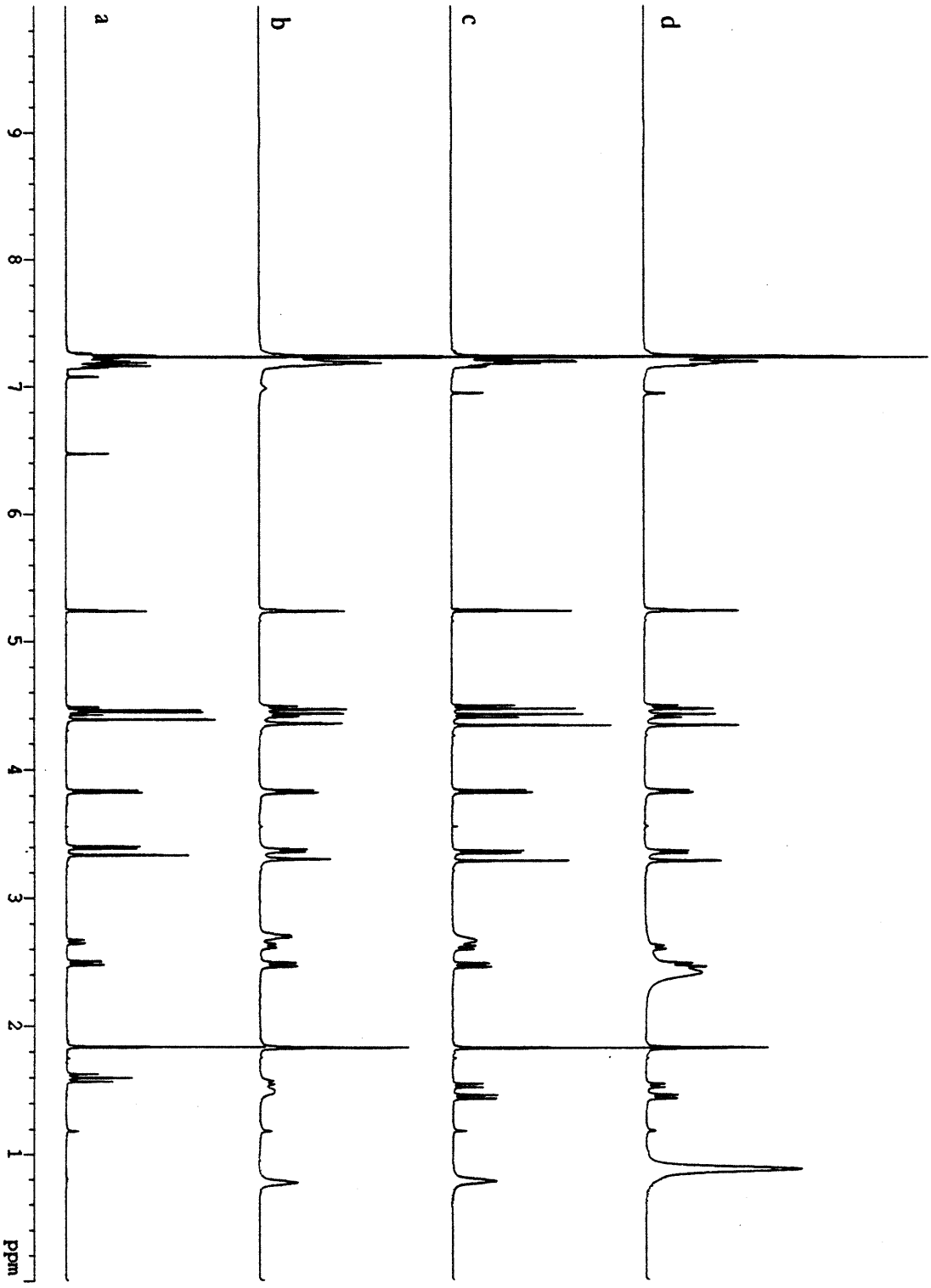

Figure E5. NMR of **B2a** in CD_2Cl_2 at room temperature with a) 0 equiv, b) <1 equiv, c) 1 equiv, and d) 4 equiv of TEA.

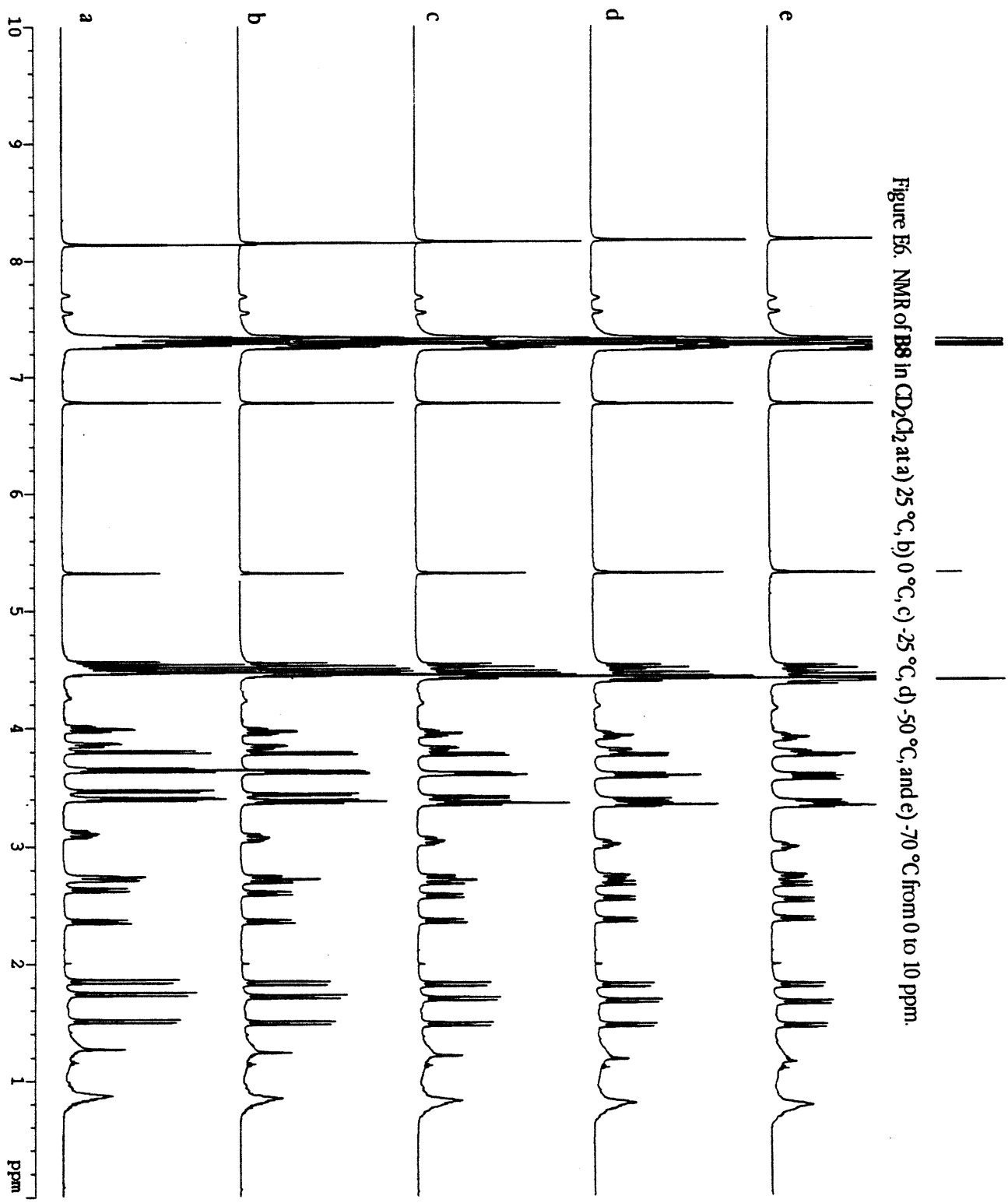

Figure E6. NMR of **B8** in CD_2Cl_2 at a) 25 °C, b) 0 °C, c) -25 °C, d) -50 °C, and e) -70 °C from 0 to 10 ppm.

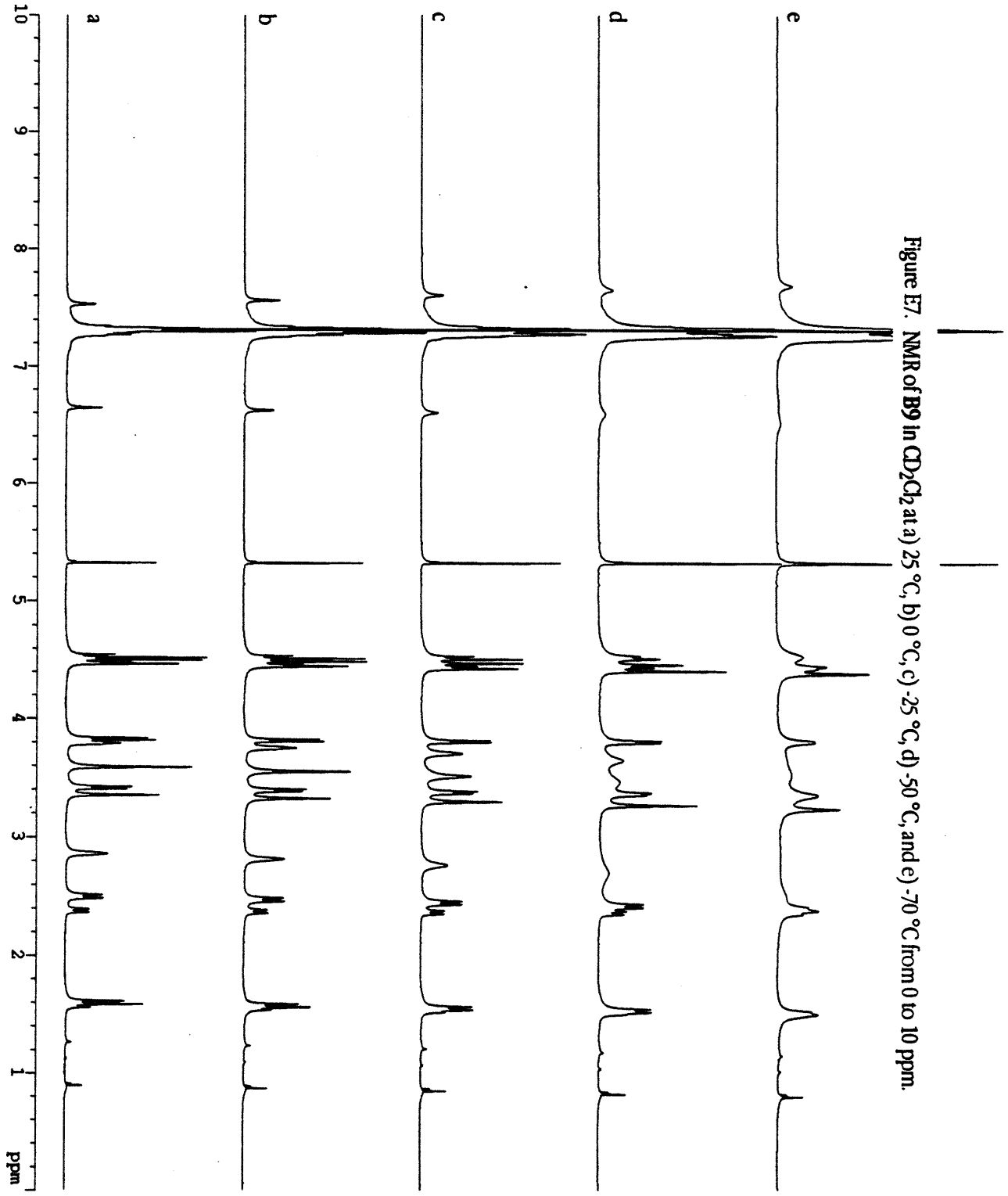

Figure E7. NMR of **B9** in CD_2Cl_2 at a) 25 °C, b) 0 °C, c) -25 °C, d) -50 °C, and e) -70 °C from 0 to 10 ppm.

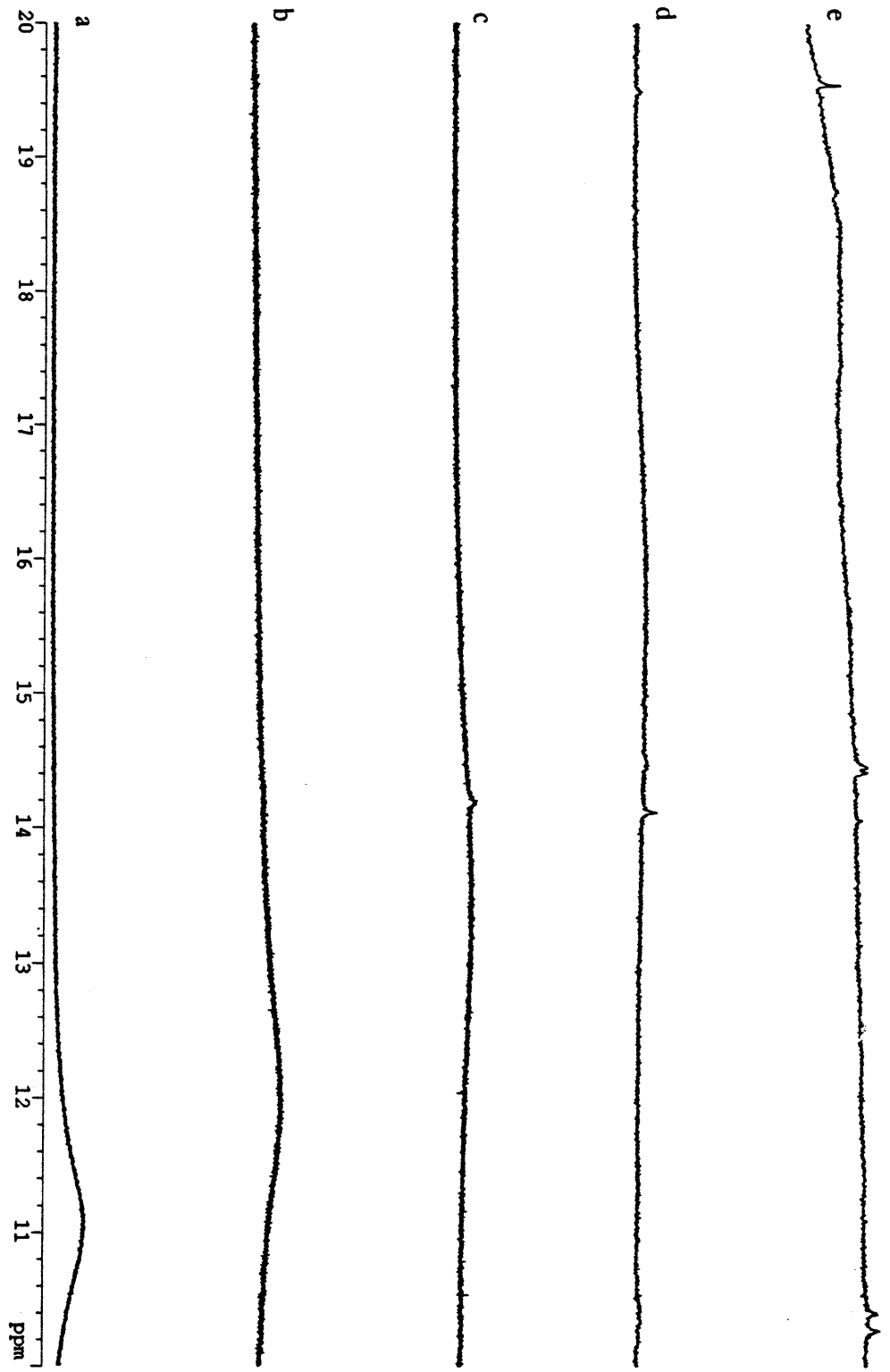

Figure E8. NMR of **B9** in CD_2Cl_2 at a) 25 °C, b) 0 °C, c) -25 °C, d) -50 °C, and e) -70 °C from 10 to 20 ppm.

F. CRYSTALLOGRAPHIC DATA

Table F1. Crystallographic Parameters for **B2b**.

Formula	C75H79Ca0.5Cl2N2O15
a (Å)	13.924(3)
b (Å)	15.314(3)
c (Å)	18.094(4)
β (deg)	98.65(3)
Volume ($Å^3$)	3366(2)
space group,	$P2_1/n$
Z	4
ρ_{calc} (g/cm^3)	1.41
μ (cm^{-1})	1.11
radiation, λ (Å)	Mo, Kα (0.710690)
2θ limit (deg)	46
temperature (°C)	-66
total / unique reflections	12856 / 8853
no. observations ($I>3\sigma$),	5716
no. of parameters	904
R	0.072
Rw	0.091

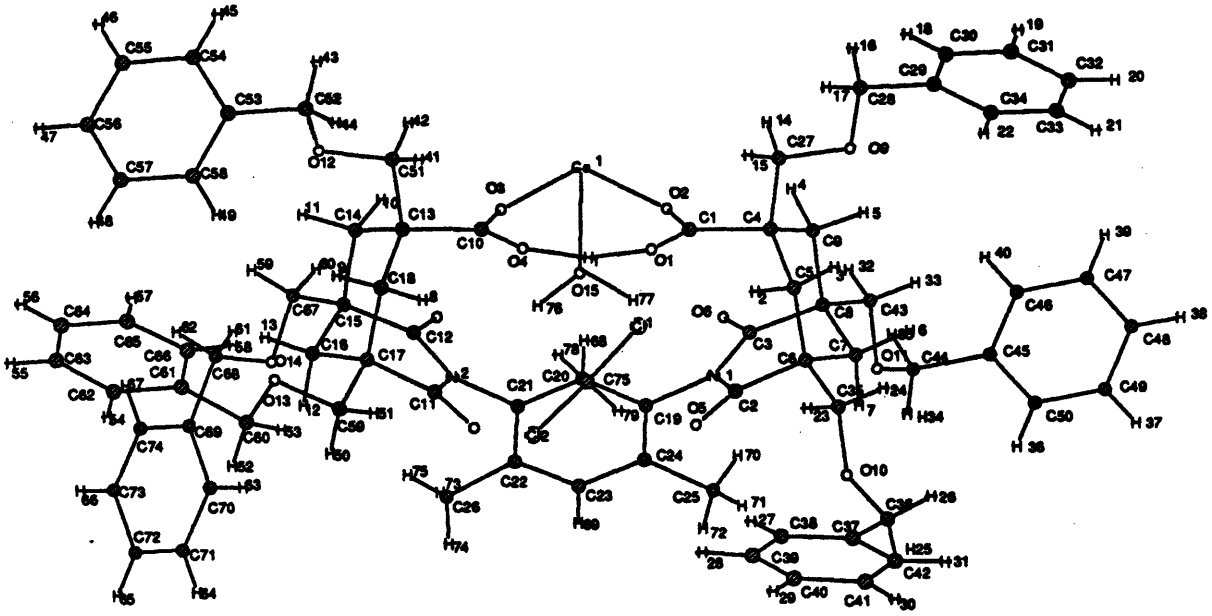

Figure F1. A computer-generated perspectiveof the final model for crystal structure of **B2b**. Only the asymmetric unit is shown (i.e., half of complex **B2b**).

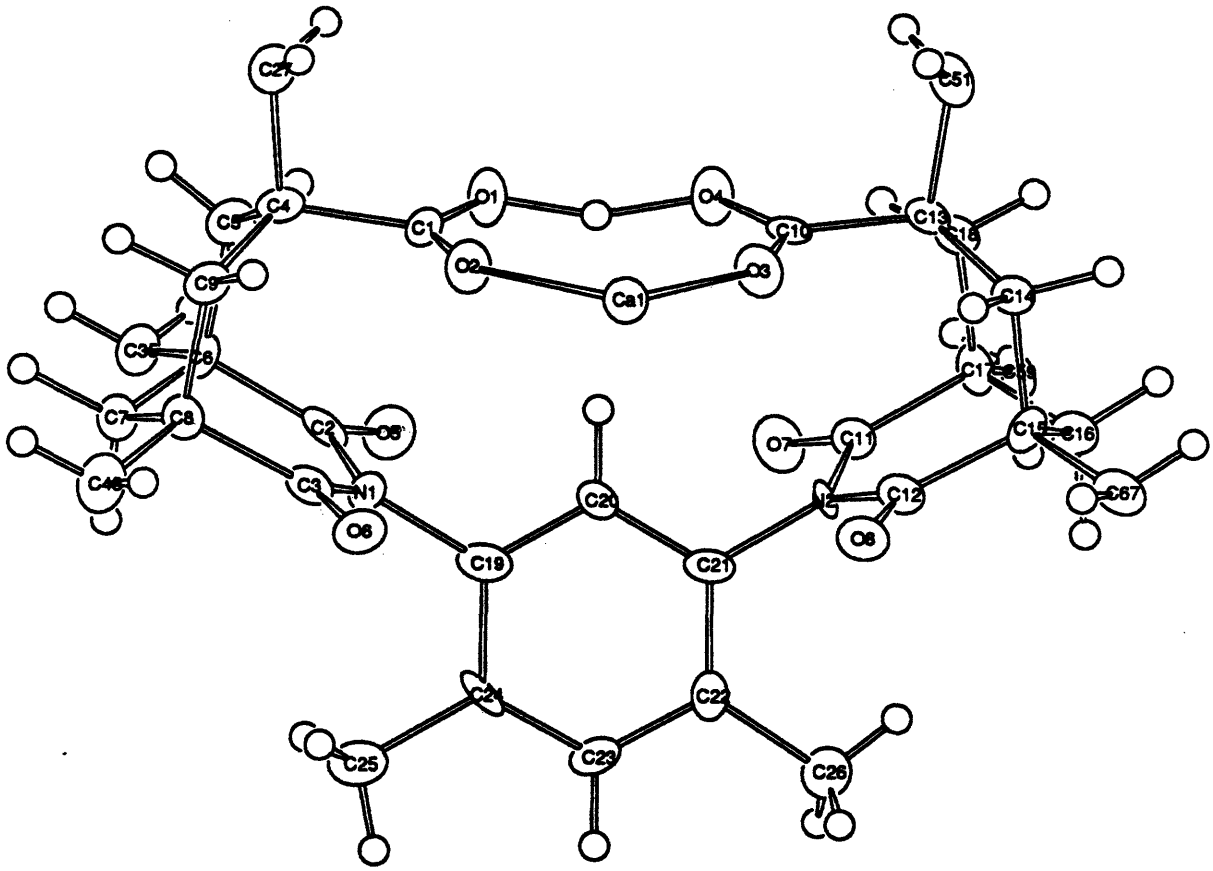

Figure F2. Crystal structure of half of **B2b** with the benzyloxy groups, CH_2Cl_2 and H_2O omitted for clarity.

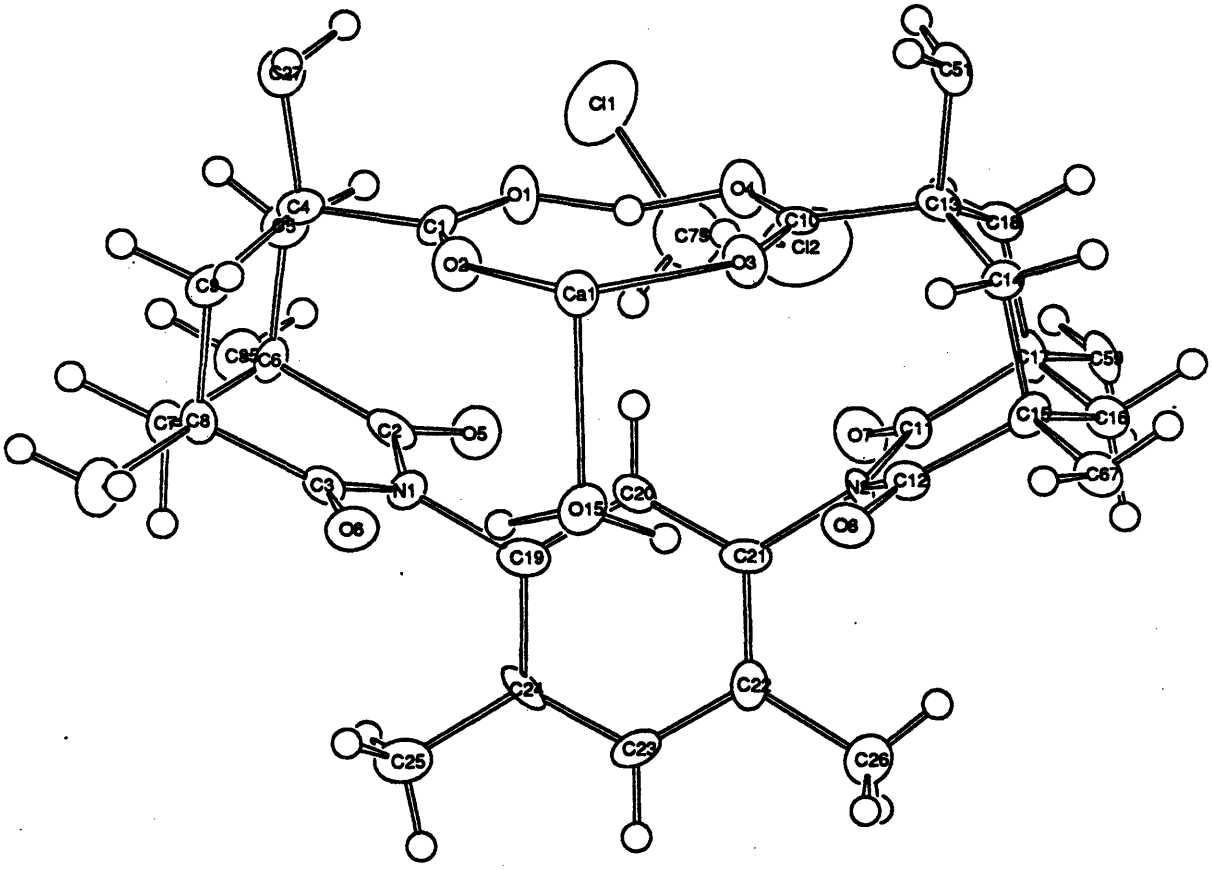

Figure F3. Crystal structure of half of **B2b** with benzyloxy groups omitted for clarity. Water coordinated to calcium is hydrogen-bonded to the imide carbonyls.

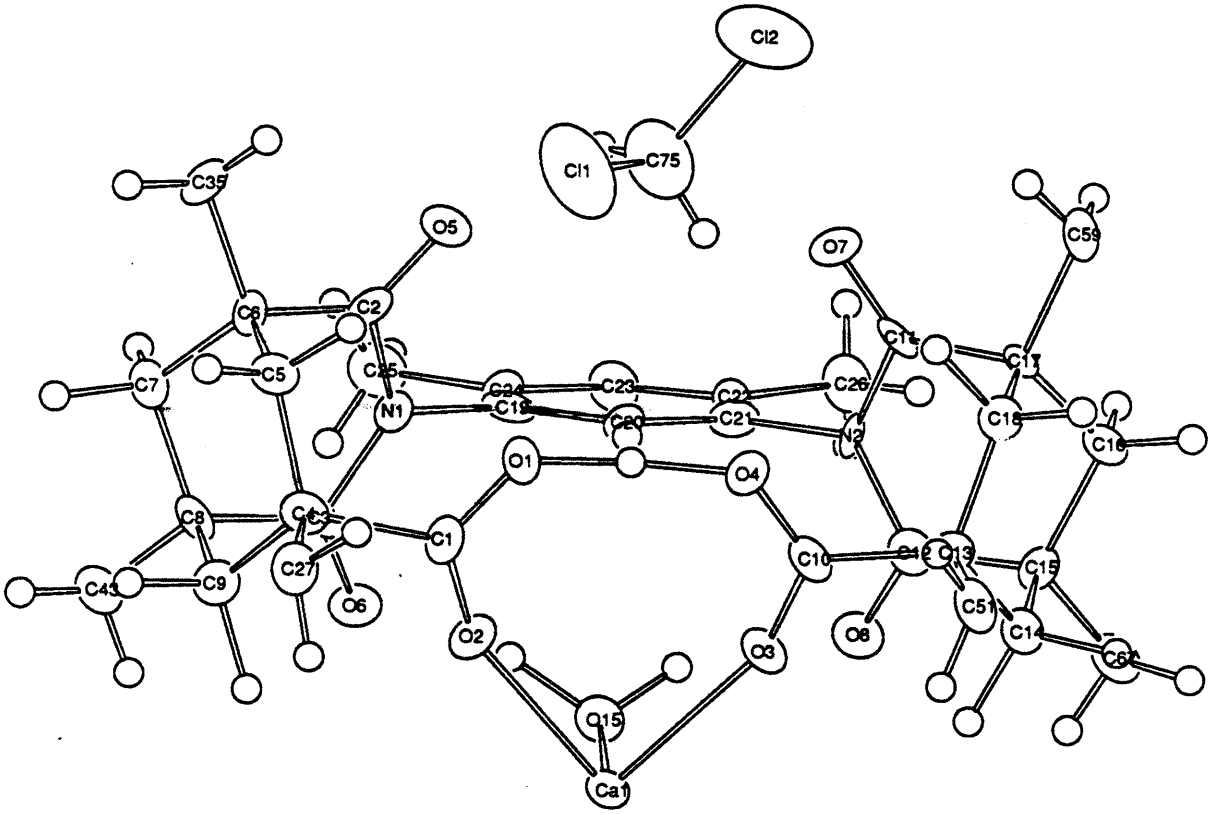

Figure F4. Top view of half molecule of **B2b** as determined from single crystal X-ray analysis. Benzyloxy groups are omitted for clarity.

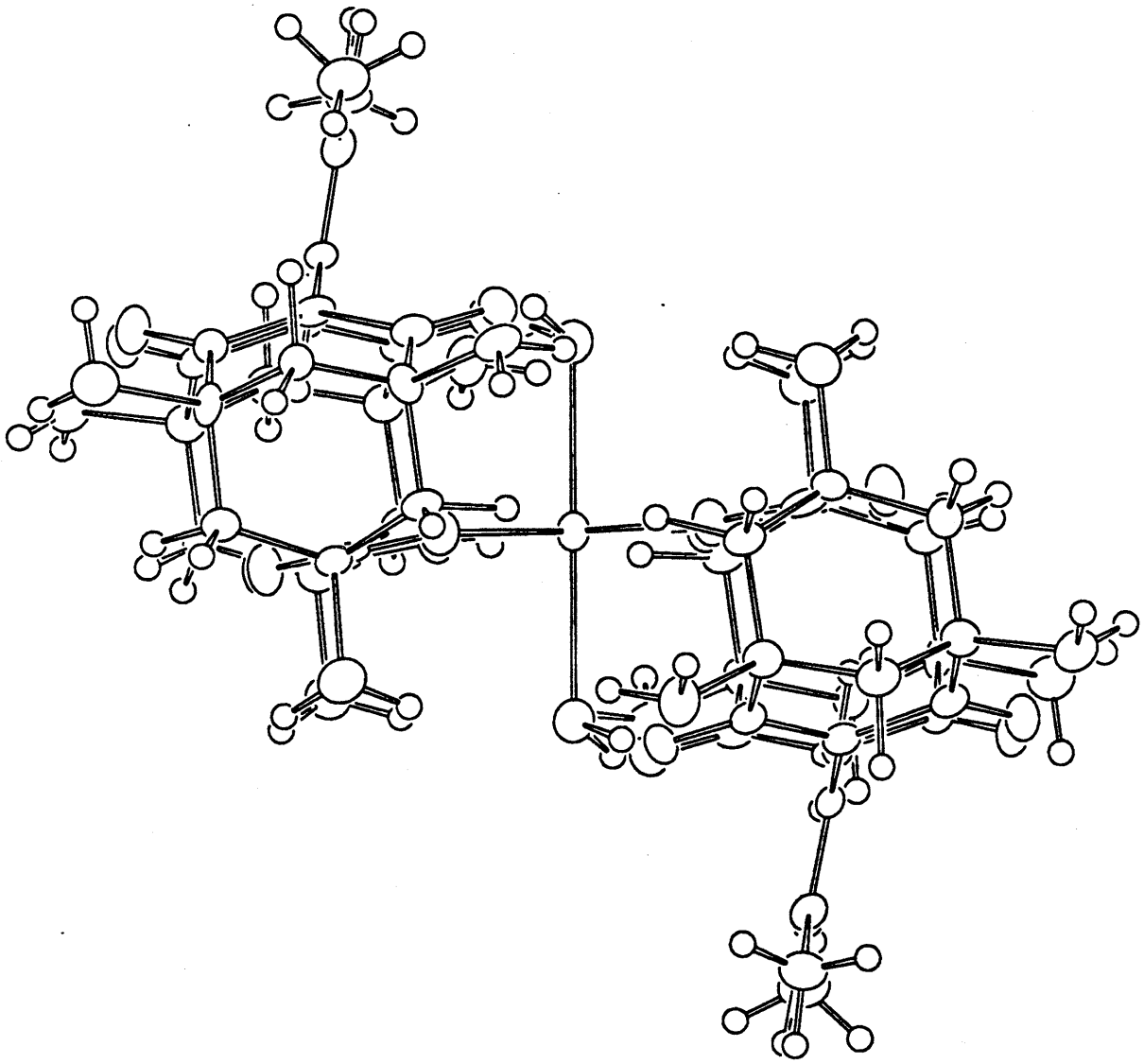

Figurre F5. Structure of **B2b** as determined by single crystal X-ray analysis. CH_2Cl_2 molecules and benzyloxy groups omitted for clarity.

Table F2. Positional Parameters and B(eq) for **B2b**.

atom	x	y	z	B(eq)
Ca(1)	1.000000	0.000000	1.000000	2.12(6)
Cl(1)	0.7019(2)	0.1524(1)	1.2107(2)	8.4(1)
Cl(2)	0.5509(2)	0.1093(1)	1.1391(2)	7.63(6)
O(1)	0.8665(4)	0.0766(2)	1.1504(3)	2.7(2)
O(2)	0.9697(3)	0.0239(2)	1.1210(3)	2.7(2)
O(3)	0.8754(4)	0.0361(2)	0.9565(3)	2.7(2)
O(4)	0.7946(3)	0.0877(2)	1.0224(3)	2.8(2)
O(5)	0.7451(4)	-0.0090(2)	1.2479(3)	2.8(2)
O(6)	0.9683(3)	-0.0983(2)	1.1794(3)	2.5(2)
O(7)	0.6198(3)	0.0045(2)	1.0269(4)	2.9(2)
O(8)	0.8088(4)	-0.0782(2)	0.8941(3)	2.6(2)
O(9)	1.0492(3)	0.1265(2)	1.3251(3)	3.1(2)
O(10)	0.7754(4)	-0.0294(2)	1.4201(4)	3.7(2)
O(11)	1.0150(4)	-0.1390(3)	1.3461(3)	3.7(2)
O(12)	0.7571(3)	0.1553(2)	0.7921(3)	3.2(2)
O(13)	0.5104(3)	0.0854(2)	0.8337(3)	3.1(2)
O(14)	0.6831(3)	-0.0932(2)	0.7399(3)	2.8(2)
O(15)	0.9449(3)	-0.0908(2)	1.0126(3)	2.8(1)
N(1)	0.8567(4)	-0.0580(3)	1.2181(4)	1.9(2)
N(2)	0.7093(4)	-0.0396(3)	0.9585(4)	1.7(2)
C(1)	0.9325(6)	0.0505(4)	1.1673(5)	2.2(3)
C(2)	0.8158(6)	-0.0197(3)	1.2659(5)	2.2(2)
C(3)	0.9390(5)	-0.0705(4)	1.2272(5)	2.0(3)
C(4)	0.9687(5)	0.0560(3)	1.2533(5)	2.1(2)
C(5)	0.9041(5)	0.0614(3)	1.3097(5)	2.4(2)
C(6)	0.8671(5)	0.0058(3)	1.3336(4)	2.0(2)
C(7)	0.9336(5)	-0.0349(3)	1.3640(5)	2.4(2)
C(8)	0.9886(5)	-0.0465(3)	1.2991(5)	2.2(2)
C(9)	1.0285(5)	0.0085(3)	1.2760(4)	2.4(2)
C(10)	0.8153(5)	0.0666(4)	0.9602(5)	1.9(2)
C(11)	0.6477(5)	0.0003(3)	0.9659(6)	1.9(2)
C(12)	0.7511(6)	-0.0465(4)	0.8919(5)	2.4(3)
C(13)	0.7636(5)	0.0814(3)	0.8853(5)	1.9(2)
C(14)	0.7734(5)	0.0409(3)	0.8189(5)	2.1(2)
C(15)	0.7218(5)	-0.0128(3)	0.8205(5)	2.1(2)
C(16)	0.6331(5)	0.0024(3)	0.8207(5)	2.2(2)
C(17)	0.6242(5)	0.0357(3)	0.8951(4)	2.0(2)
C(18)	0.6744(5)	0.0894(3)	0.8972(4)	2.2(2)
C(19)	0.8072(5)	-0.0832(4)	1.1522(5)	2.1(2)
C(20)	0.7815(5)	-0.0507(3)	1.0878(5)	1.7(2)
C(21)	0.7350(5)	-0.0742(4)	1.0247(5)	2.0(2)
C(22)	0.7125(5)	-0.1300(4)	1.0252(5)	2.0(2)
C(23)	0.7414(5)	-0.1621(3)	1.0894(5)	2.6(2)
C(24)	0.7880(5)	-0.1402(4)	1.1530(5)	2.1(2)

Positional Parameters and B(eq) for **B2b** (cont'd).

atom	x	y	z	B(eq)
C(25)	0.8144(5)	-0.1760(3)	1.2239(5)	3.3(2)
C(26)	0.6572(5)	-0.1567(4)	0.9612(5)	3.3(2)
C(27)	1.0148(5)	0.1108(4)	1.2498(5)	2.9(2)
C(28)	1.0839(5)	0.1802(4)	1.3283(5)	3.4(3)
C(29)	1.1091(5)	0.1985(4)	1.4109(5)	2.8(3)
C(30)	1.1064(6)	0.2532(4)	1.4327(6)	3.9(3)
C(31)	1.1279(8)	0.2702(4)	1.5064(7)	5.8(4)
C(32)	1.1533(7)	0.2313(5)	1.5629(6)	5.3(3)
C(33)	1.1570(6)	0.1759(5)	1.5413(6)	4.5(3)
C(34)	1.1356(5)	0.1596(4)	1.4671(7)	3.4(3)
C(35)	0.8134(5)	0.0201(4)	1.3980(5)	2.8(2)
C(36)	0.7347(6)	-0.0229(4)	1.4877(6)	4.4(3)
C(37)	0.6617(6)	0.0148(4)	1.4791(7)	3.6(3)
C(38)	0.6185(7)	0.0265(5)	1.4095(7)	5.2(4)
C(39)	0.5516(8)	0.0601(6)	1.4051(8)	6.7(4)
C(40)	0.5254(8)	0.0818(6)	1.469(1)	7.4(5)
C(41)	0.566(1)	0.0703(5)	1.5394(8)	7.4(5)
C(42)	0.6345(8)	0.0381(5)	1.5447(7)	5.6(4)
C(43)	1.0533(5)	-0.0887(4)	1.3264(5)	3.1(3)
C(44)	1.0707(6)	-0.1836(4)	1.3634(6)	4.6(3)
C(45)	1.1226(6)	-0.1783(3)	1.4372(6)	2.6(3)
C(46)	1.0910(7)	-0.1856(4)	1.5055(8)	4.5(3)
C(47)	1.139(1)	-0.1815(5)	1.5731(8)	7.1(5)
C(48)	1.221(1)	-0.1703(5)	1.573(1)	8.1(5)
C(49)	1.2522(8)	-0.1633(5)	1.506(1)	6.8(4)
C(50)	1.2034(8)	-0.1669(4)	1.4381(7)	4.6(3)
C(51)	0.7973(5)	0.1382(4)	0.8645(5)	3.0(2)
C(52)	0.7539(5)	0.2131(4)	0.7830(5)	3.4(3)
C(53)	0.6952(5)	0.2293(4)	0.7130(5)	2.3(2)
C(54)	0.7085(6)	0.2753(4)	0.6689(6)	3.7(3)
C(55)	0.6539(8)	0.2898(4)	0.6058(6)	5.2(3)
C(56)	0.5865(8)	0.2590(5)	0.5880(6)	5.9(4)
C(57)	0.5724(6)	0.2132(5)	0.6300(7)	5.1(3)
C(58)	0.6267(6)	0.1978(4)	0.6950(5)	3.8(3)
C(59)	0.5355(5)	0.0515(4)	0.8998(5)	2.8(2)
C(60)	0.4295(6)	0.1022(5)	0.8344(7)	6.1(4)
C(61)	0.4065(5)	0.1429(5)	0.7681(6)	3.4(3)
C(62)	0.4062(6)	0.2001(5)	0.7808(7)	4.6(3)
C(63)	0.3819(7)	0.2364(5)	0.7205(9)	5.3(4)
C(64)	0.3595(7)	0.2178(6)	0.6467(9)	6.1(4)
C(65)	0.3604(7)	0.1624(8)	0.6340(6)	6.5(4)
C(66)	0.3827(6)	0.1239(4)	0.6922(8)	5.2(3)
C(67)	0.7364(5)	-0.0463(4)	0.7484(5)	2.9(2)
C(68)	0.6853(6)	-0.1202(4)	0.6675(6)	4.1(3)

Positional Parameters and B(eq) for **B2b** (cont'd).

atom	x	y	z	B(eq)
C(69)	0.6256(6)	-0.1666(4)	0.6555(6)	3.4(3)
C(70)	0.5665(7)	-0.1755(4)	0.7054(5)	3.8(3)
C(71)	0.5121(6)	-0.2192(5)	0.6903(7)	5.0(3)
C(72)	0.5152(8)	-0.2539(5)	0.6271(8)	5.8(4)
C(73)	0.5740(8)	-0.2442(5)	0.5768(7)	5.6(4)
C(74)	0.6279(6)	-0.2018(5)	0.5912(5)	4.0(3)
C(75)	0.6540(7)	0.0972(4)	1.1618(6)	6.0(3)

Positional Parameters and B(eq) for Compound **B2b** (cont'd)

Positional Parameters and B(eq) for **B2b** (cont'd).

atom	x	y	z	B(eq)
H(1)	0.827641	0.0740389	1.088642	3.236
H(2)	0.857022	0.0876220	1.283689	3.236
H(3)	0.929926	0.0834729	1.351109	3.236
H(4)	1.074532	0.0026330	1.228844	3.236
H(5)	1.063053121	0.023819012	1.32651423	3.236
H(6)	0.977034986	-0.019122001	1.414391041	3.236
H(7)	0.908097982	-0.077468000	1.374544978	3.236
H(8)	0.663681984	0.108158000	0.954675972	3.236
H(9)	0.647094011	0.112788998	0.856812000	3.236
H(10)	0.838958979	0.022699000	0.821241021	3.236
H(11)	0.754957020	0.054159999	0.762148976	3.236
H(12)	0.598863006	-0.038573999	0.820016980	3.236
H(13)	0.604902029	0.030833000	0.777176023	3.236
H(14)	1.056787014	0.106372997	1.216876030	3.449
H(15)	0.978810012	0.139163002	1.229454994	3.449
H(16)	1.045503974	0.205935001	1.304877996	4.066
H(17)	1.130233049	0.179829001	1.300426960	4.066
H(18)	1.088947058	0.280286998	1.394600987	4.743
H(19)	1.125583053	0.308513999	1.519580960	6.989
H(20)	1.167701006	0.242161006	1.615342021	6.421
H(21)	1.175042987	0.148747995	1.579126954	5.366
H(22)	1.138705969	0.121329002	1.453333020	4.009
H(23)	0.773562014	0.046495002	1.379029036	3.311
H(24)	0.845607996	0.035277002	1.441596031	3.311
H(25)	0.717571974	-0.058848001	1.502550960	5.243
H(26)	0.772221029	-0.008243000	1.527693987	5.243
H(27)	0.635441005	0.010805000	1.363201022	6.149
H(28)	0.523446023	0.068172000	1.355527043	7.943
H(29)	0.478814006	0.104969002	1.465700984	8.954
H(30)	0.547437012	0.084726997	1.585466981	8.889
H(31)	0.663712025	0.031785000	1.594027042	6.648
H(32)	1.086475968	-0.095688000	1.285913944	3.773
H(33)	1.085585952	-0.074711002	1.370798945	3.773
H(34)	1.104701042	-0.185753003	1.322566986	5.499
H(35)	1.040619016	-0.217161000	1.365123987	5.499
H(36)	1.225708008	-0.161430001	1.390133977	5.481
H(37)	1.308197021	-0.155787006	1.504696012	8.110
H(38)	1.254778028	-0.167809993	1.620463014	9.841
H(39)	1.116659045	-0.186010003	1.620901942	8.662
H(40)	1.034973979	-0.193761006	1.505877018	5.368
H(41)	0.853613973	0.135199994	0.860500991	3.630
H(42)	0.788098991	0.164623007	0.903550029	3.630
H(43)	0.736504018	0.229442999	0.828486025	4.092
H(44)	0.806218028	0.226540998	0.775510013	4.092

Positional Parameters and B(eq) for **B2b** (cont'd).

atom	x	y	z	B(eq)
H(45)	0.755416989	0.297482997	0.681469977	4.436
H(46)	0.663675010	0.321449012	0.575056016	6.259
H(47)	0.548829019	0.269670993	0.545459986	7.134
H(48)	0.525469005	0.191269994	0.615944982	6.158
H(49)	0.616212010	0.166246995	0.725606024	4.515
H(50)	0.503059030	0.018782999	0.898908973	3.287
H(51)	0.530283988	0.071644001	0.946322024	3.287
H(52)	0.395437002	0.070304997	0.828088999	7.297
H(53)	0.422930986	0.119657002	0.882568002	7.297
H(54)	0.422751009	0.214473993	0.831200004	5.551
H(55)	0.380409986	0.275110006	0.730639994	6.316
H(56)	0.344119012	0.243136004	0.605379999	7.293
H(57)	0.345111996	0.149201006	0.582781017	7.685
H(58)	0.381799012	0.084997997	0.680854023	6.136
H(59)	0.727288008	-0.023221999	0.703795016	3.468
H(60)	0.790789008	-0.059215002	0.753389001	3.468
H(61)	0.737891972	-0.135014996	0.665033996	4.888
H(62)	0.673744023	-0.093657002	0.627102971	4.888
H(63)	0.563444972	-0.151969001	0.749280989	4.569
H(64)	0.471846998	-0.225315005	0.724668980	5.914
H(65)	0.477988005	-0.283805013	0.618058980	6.897
H(66)	0.576564014	-0.267060995	0.532375991	6.719
H(67)	0.668290019	-0.195996001	0.556837022	4.718
H(68)	0.796460986	-0.011614000	1.087090015	1.965
H(69)	0.727645993	-0.200939998	1.089946985	2.996
H(70)	0.871740997	-0.178259999	1.230185032	3.859
H(71)	0.795880973	-0.159586996	1.268612027	3.859
H(72)	0.792222023	-0.212279007	1.216279984	3.859
H(73)	0.684749007	-0.186469004	0.939234018	3.946
H(74)	0.610539019	-0.170514002	0.982074022	3.946
H(75)	0.641763985	-0.129725993	0.922222972	3.946
H(76)	0.941758990	-0.095146999	1.079434991	3.236
H(77)	0.887619972	-0.095250003	0.983576000	3.236
H(78)	0.678092003	0.091251001	1.114977002	7.190
H(79)	0.661062002	0.064955004	1.193707943	7.190

Table F3. Anisotropic Displacement Parameters for **B2b**.

atom	U11	U22	U33	U12	U13	U23
Ca(1)	0.021(2)	0.030(2)	0.030(2)	0.004(1)	0.003(1)	0.000(1)
Cl(1)	0.093(3)	0.093(3)	0.121(3)	0.022(2)	-0.036(2)	-0.041(2)
Cl(2)	0.061(1)	0.093(6)	0.139(1)	0.001(1)	0.027(7)	-0.027(2)
O(1)	0.030(4)	0.047(4)	0.024(4)	0.011(3)	-0.004(3)	-0.002(3)
O(2)	0.040(4)	0.041(4)	0.024(4)	0.005(3)	0.009(3)	-0.005(3)
O(3)	0.023(4)	0.039(4)	0.039(4)	0.008(4)	-0.001(3)	0.005(3)
O(4)	0.037(4)	0.047(4)	0.023(4)	0.011(3)	0.005(3)	-0.003(3)
O(5)	0.024(4)	0.041(4)	0.041(4)	0.007(3)	0.004(3)	-0.005(3)
O(6)	0.033(4)	0.027(4)	0.037(4)	0.004(3)	0.010(3)	-0.008(3)
O(7)	0.037(4)	0.047(4)	0.030(4)	0.008(3)	0.016(3)	0.003(3)
O(8)	0.032(4)	0.027(4)	0.041(4)	0.004(3)	0.006(3)	0.001(3)
O(9)	0.050(4)	0.026(4)	0.040(4)	-0.017(3)	-0.006(3)	0.003(3)
O(10)	0.052(4)	0.043(4)	0.051(4)	0.001(4)	0.032(4)	0.013(4)
O(11)	0.045(4)	0.032(4)	0.059(4)	-0.001(4)	-0.008(3)	0.011(3)
O(12)	0.057(4)	0.014(4)	0.050(4)	-0.001(3)	-0.003(4)	0.010(3)
O(13)	0.013(4)	0.057(4)	0.050(4)	0.012(3)	0.005(3)	0.019(4)
O(14)	0.047(4)	0.034(4)	0.027(4)	-0.007(3)	0.006(3)	-0.007(3)
O(15)	0.030(4)	0.040(4)	0.036(4)	-0.002(3)	0.002(3)	-0.005(3)
N(1)	0.026(5)	0.026(5)	0.018(4)	-0.008(4)	0.002(4)	-0.002(4)
N(2)	0.030(5)	0.025(5)	0.009(4)	-0.006(4)	-0.002(4)	0.011(4)
C(1)	0.030(7)	0.033(6)	0.021(6)	-0.020(6)	-0.002(5)	0.003(5)
C(2)	0.038(7)	0.025(6)	0.022(6)	-0.001(5)	0.014(6)	0.014(5)
C(3)	0.015(7)	0.022(6)	0.038(7)	0.002(5)	0.000(5)	0.010(5)
C(4)	0.026(6)	0.019(6)	0.035(6)	-0.003(5)	0.003(5)	-0.003(4)
C(5)	0.026(6)	0.033(6)	0.034(6)	0.000(5)	0.005(5)	-0.005(5)
C(6)	0.029(6)	0.031(6)	0.015(5)	-0.004(5)	-0.003(5)	-0.005(5)
C(7)	0.028(6)	0.034(6)	0.029(6)	-0.003(5)	-0.005(5)	0.004(5)
C(8)	0.018(5)	0.030(6)	0.034(6)	0.003(5)	-0.007(5)	0.005(5)
C(9)	0.030(6)	0.031(6)	0.030(5)	-0.009(5)	0.003(4)	-0.002(5)
C(10)	0.018(6)	0.014(6)	0.038(7)	-0.007(5)	-0.004(5)	0.009(5)
C(11)	0.010(5)	0.023(6)	0.037(7)	0.004(5)	-0.005(5)	0.004(5)
C(12)	0.028(6)	0.025(6)	0.036(7)	-0.005(5)	0.001(6)	0.006(5)
C(13)	0.025(6)	0.021(6)	0.028(6)	-0.002(5)	0.006(5)	0.007(5)
C(14)	0.025(5)	0.025(6)	0.031(6)	-0.007(4)	0.000(4)	0.005(5)
C(15)	0.034(6)	0.030(6)	0.018(6)	0.001(5)	0.003(4)	-0.012(5)
C(16)	0.019(6)	0.026(5)	0.037(6)	0.003(4)	0.002(4)	0.004(5)
C(17)	0.012(5)	0.038(6)	0.024(6)	0.010(5)	0.000(4)	0.007(5)
C(18)	0.030(6)	0.024(6)	0.030(5)	-0.001(5)	0.004(4)	0.005(4)
C(19)	0.016(5)	0.021(6)	0.044(7)	0.001(5)	0.012(5)	0.003(6)
C(20)	0.026(5)	0.020(5)	0.020(6)	0.003(5)	0.008(5)	0.003(5)
C(21)	0.026(6)	0.018(6)	0.035(7)	-0.003(5)	0.012(5)	0.001(5)
C(22)	0.020(5)	0.037(7)	0.020(6)	0.001(5)	0.001(4)	0.001(5)
C(23)	0.031(6)	0.026(6)	0.040(7)	-0.013(5)	0.000(5)	-0.004(6)

Anisotropic Displacement Parameters for **B2b** (cont'd).

atom	U11	U22	U33	U12	U13	U23
C(24)	0.031(6)	0.026(7)	0.024(6)	0.005(5)	0.010(5)	0.019(5)
C(25)	0.042(6)	0.030(6)	0.053(7)	-0.006(5)	0.005(5)	-0.002(5)
C(26)	0.040(6)	0.042(6)	0.042(6)	-0.008(5)	-0.005(5)	0.003(5)
C(27)	0.039(6)	0.036(6)	0.033(6)	0.000(5)	-0.001(5)	-0.002(5)
C(28)	0.033(6)	0.039(7)	0.056(8)	0.003(5)	0.001(5)	0.006(6)
C(29)	0.029(6)	0.044(8)	0.034(7)	-0.013(5)	0.002(5)	-0.001(6)
C(30)	0.069(8)	0.021(7)	0.059(8)	-0.007(5)	0.006(6)	-0.005(6)
C(31)	0.13(1)	0.039(8)	0.047(8)	-0.028(7)	0.005(8)	-0.008(7)
C(32)	0.11(1)	0.047(8)	0.048(8)	-0.027(7)	0.005(7)	-0.017(7)
C(33)	0.064(8)	0.08(1)	0.023(7)	-0.022(7)	-0.003(6)	0.014(6)
C(34)	0.038(6)	0.034(6)	0.057(8)	-0.002(5)	0.009(6)	0.008(7)
C(35)	0.043(6)	0.045(7)	0.019(5)	-0.010(5)	0.009(5)	-0.004(5)
C(36)	0.071(8)	0.053(7)	0.044(7)	-0.002(6)	0.021(6)	0.016(6)
C(37)	0.051(8)	0.033(7)	0.056(8)	0.014(6)	0.018(7)	0.016(6)
C(38)	0.054(8)	0.069(9)	0.08(1)	-0.005(7)	0.021(7)	-0.007(7)
C(39)	0.059(10)	0.09(1)	0.10(1)	0.020(8)	-0.011(8)	0.011(9)
C(40)	0.059(10)	0.10(1)	0.13(1)	0.021(8)	0.03(1)	0.00(1)
C(41)	0.13(1)	0.075(10)	0.09(1)	0.043(10)	0.05(1)	-0.001(8)
C(42)	0.090(10)	0.063(8)	0.062(9)	0.028(8)	0.026(7)	0.010(7)
C(43)	0.026(6)	0.052(7)	0.039(6)	0.005(6)	-0.002(5)	-0.004(5)
C(44)	0.078(8)	0.027(7)	0.069(8)	0.016(6)	0.002(7)	0.006(6)
C(45)	0.035(8)	0.028(6)	0.036(8)	0.014(5)	-0.001(6)	0.003(5)
C(46)	0.079(9)	0.048(7)	0.048(8)	0.007(6)	0.029(8)	0.003(7)
C(47)	0.21(2)	0.027(7)	0.036(10)	0.00(1)	0.04(1)	0.001(6)
C(48)	0.16(2)	0.034(9)	0.10(1)	0.02(1)	-0.07(1)	-0.015(9)
C(49)	0.07(1)	0.073(10)	0.11(1)	0.004(7)	-0.01(1)	-0.03(1)
C(50)	0.055(9)	0.058(8)	0.061(9)	0.010(6)	0.014(7)	-0.008(6)
C(51)	0.031(6)	0.044(7)	0.038(6)	0.002(5)	-0.007(5)	0.013(5)
C(52)	0.035(6)	0.041(8)	0.055(7)	-0.001(5)	0.009(5)	0.002(5)
C(53)	0.029(6)	0.026(6)	0.033(6)	0.007(5)	0.003(5)	-0.003(5)
C(54)	0.070(8)	0.022(7)	0.051(7)	-0.007(5)	0.015(7)	0.008(6)
C(55)	0.11(1)	0.050(8)	0.036(7)	-0.001(8)	-0.023(7)	0.019(6)
C(56)	0.078(10)	0.061(9)	0.078(9)	-0.005(8)	-0.036(7)	0.016(8)
C(57)	0.056(8)	0.051(8)	0.083(9)	-0.015(6)	-0.019(7)	0.007(7)
C(58)	0.049(7)	0.046(7)	0.049(7)	-0.008(6)	0.004(6)	0.011(6)
C(59)	0.035(6)	0.039(6)	0.029(6)	0.006(5)	-0.007(5)	0.016(5)
C(60)	0.043(8)	0.083(9)	0.106(10)	0.011(7)	0.010(7)	0.049(8)
C(61)	0.013(6)	0.066(9)	0.051(8)	0.003(5)	0.011(5)	0.014(7)
C(62)	0.030(7)	0.055(9)	0.090(10)	-0.007(6)	0.002(6)	-0.021(8)
C(63)	0.050(8)	0.047(8)	0.10(1)	0.002(6)	0.002(8)	0.027(9)
C(64)	0.055(9)	0.08(1)	0.10(1)	0.011(8)	0.001(8)	0.039(10)
C(65)	0.062(9)	0.13(1)	0.046(8)	-0.012(9)	-0.013(6)	0.035(10)
C(66)	0.058(8)	0.046(8)	0.091(10)	-0.009(6)	0.003(7)	-0.007(8)
C(67)	0.025(6)	0.035(6)	0.048(7)	-0.005(5)	-0.001(5)	0.015(5)

Anisotropic Displacement Parameters for **B2b** (cont'd).

atom	U11	U22	U33	U12	U13	U23
C(68)	0.058(7)	0.048(7)	0.052(7)	-0.001(6)	0.017(6)	-0.007(6)
C(69)	0.051(7)	0.038(7)	0.038(7)	0.004(6)	-0.004(6)	0.005(6)
C(70)	0.053(7)	0.052(8)	0.039(7)	0.002(6)	-0.008(6)	0.000(6)
C(71)	0.049(8)	0.055(8)	0.082(9)	-0.016(7)	-0.001(7)	0.008(7)
C(72)	0.076(10)	0.045(8)	0.09(1)	-0.014(7)	-0.024(8)	-0.027(8)
C(73)	0.066(9)	0.064(9)	0.076(9)	0.005(8)	-0.027(8)	-0.023(7)
C(74)	0.060(8)	0.057(8)	0.031(7)	0.003(7)	-0.014(6)	-0.013(6)
C(75)	0.079(9)	0.057(8)	0.089(9)	0.025(7)	-0.010(7)	-0.009(7)

Table F4. Intramolecular Distances for **B2b**.

atom	atom	distance	atom	atom	distance	ADC(*)
Ca1	O2	2.274(6)	O13	C59	1.428(9)	
Ca1	O2	2.274(6)	O13	C60	1.41(1)	
Ca1	O3	2.299(6)	O14	C67	1.431(9)	
Ca1	O3	2.299(6)	O14	C68	1.41(1)	
Ca1	O15	2.382(5)	O15	H76	1.165	
Ca1	O15	2.382(5)	O15	H77	1.035	
CL1	C75	1.72(1)	N1	C2	1.45(1)	
CL2	C75	1.74(1)	N1	C3	1.39(1)	
O1	C1	1.27(1)	N1	C19	1.46(1)	
O1	H1	1.189	N2	C11	1.42(1)	
O2	C1	1.24(1)	N2	C12	1.41(1)	
O3	C10	1.245(9)	N2	C21	1.44(1)	
O4	C10	1.267(9)	C1	C4	1.55(1)	
O4	H1	1.260	C2	C6	1.50(1)	
O5	C2	1.212(9)	C3	C8	1.53(1)	
O6	C3	1.202(9)	C4	C5	1.53(1)	
O7	C11	1.200(9)	C4	C9	1.54(1)	
O8	C12	1.221(9)	C4	C27	1.53(1)	
O9	C27	1.417(9)	C5	C6	1.54(1)	
O9	C28	1.41(1)	C5	H2	1.066	
O10	C35	1.417(9)	C5	H3	0.956	
O10	C36	1.42(1)	C6	C7	1.53(1)	
O11	C43	1.42(1)	C6	C35	1.54(1)	
O11	C44	1.43(1)	C7	C8	1.54(1)	
O12	C51	1.415(9)	C7	H6	1.137	
O12	C52	1.40(1)	C7	H7	1.127	
C8	C9	1.55(1)	C21	C22	1.39(1)	
C8	C43	1.52(1)	C22	C23	1.39(1)	
C9	H4	1.183	C22	C26	1.51(1)	
C9	H5	1.059	C23	C24	1.38(1)	
C10	C13	1.52(1)	C23	H69	0.961	
C11	C17	1.51(1)	C24	C25	1.52(1)	
C12	C15	1.51(1)	C25	H70	0.950	
C13	C14	1.52(1)	C25	H71	0.946	
C13	C18	1.53(1)	C25	H72	0.949	
C13	C51	1.53(1)	C26	H73	0.950	
C14	C15	1.55(1)	C26	H74	0.948	
C14	H10	1.172	C26	H75	0.949	
C14	H11	1.046	C27	H14	0.950	
C15	C16	1.52(1)	C27	H15	0.949	
C15	C67	1.52(1)	C28	C29	1.51(1)	
C16	C17	1.53(1)	C28	H16	0.950	
C16	H12	1.136	C28	H17	0.950	
C16	H13	1.085	C29	C30	1.37(1)	

Intramolecular Distances for **B2b** (cont'd).

atom	atom	distance	atom	atom	distance	ADC(*)
C17	C18	1.53(1)	C29	C34	1.38(1)	
C17	C59	1.53(1)	C30	C31	1.35(1)	
C18	H8	1.121	C30	H18	0.949	
C18	H9	0.971	C31	C32	1.38(1)	
C19	C20	1.39(1)	C31	H19	0.949	
C19	C24	1.40(1)	C32	C33	1.38(1)	
C20	C21	1.39(1)	C32	H20	0.949	
C20	H68	0.971	C33	C34	1.35(1)	
C33	H21	0.949	C46	H40	0.952	
C34	H22	0.952	C47	C48	1.39(2)	
C35	H23	0.949	C47	H39	0.949	
C35	H24	0.949	C48	C49	1.33(2)	
C36	C37	1.51(1)	C48	H38	0.948	
C36	H25	0.951	C49	C50	1.35(2)	
C36	H26	0.949	C49	H37	0.951	
C37	C38	1.36(1)	C50	H36	0.951	
C37	C42	1.38(1)	C51	H41	0.949	
C38	C39	1.37(2)	C51	H42	0.949	
C38	H27	0.953	C52	C53	1.52(1)	
C39	C40	1.34(2)	C52	H43	0.950	
C39	H28	0.953	C52	H44	0.950	
C40	C41	1.35(2)	C53	C54	1.37(1)	
C40	H29	0.951	C53	C58	1.38(1)	
C41	C42	1.37(2)	C54	C55	1.39(1)	
C41	H30	0.950	C54	H45	0.951	
C42	H31	0.949	C55	C56	1.35(1)	
C43	H32	0.949	C55	H46	0.951	
C43	H33	0.950	C56	C57	1.35(1)	
C44	C45	1.47(1)	C56	H47	0.950	
C44	H34	0.950	C57	C58	1.41(1)	
C44	H35	0.950	C57	H48	0.951	
C45	C46	1.35(1)	C58	H49	0.950	
C45	C50	1.37(1)	C59	H50	0.950	
C46	C47	1.35(2)	C59	H51	0.950	
C60	C61	1.52(1)	C72	H65	0.950	
C60	H52	0.952	C73	C74	1.36(1)	
C60	H53	0.948	C73	H66	0.948	
C61	C62	1.39(1)	C74	H67	0.951	
C61	C66	1.41(1)	C75	H78	0.950	
C62	C63	1.38(1)	C75	H79	0.950	
C62	H54	0.949	C63	C64	1.36(2)	
C63	H55	0.946	C64	C65	1.35(2)	
C64	H56	0.951	C65	C66	1.39(1)	
C65	H57	0.949	C66	H58	0.953	

Intramolecular Distances for **B2b** (cont'd).

atom	atom	distance	atom	atom	distance	ADC(*)
C67	H59	0.949	C67	H60	0.951	
C68	C69	1.49(1)	C68	H61	0.950	
C68	H62	0.949	C69	C70	1.39(1)	
C69	C74	1.40(1)	C70	C71	1.39(1)	
C70	H63	0.951	C71	C72	1.38(1)	
C71	H64	0.951	C72	C73	1.39(2)	

Distances are in angstroms.
Estimated standard deviations in the least significant figure are given in parentheses.

Table F5. Intramolecular Bond Angles for **B2b**.

atom	atom	atom	angle	atom	atom	atom	angle
O2	Ca1	O2	180.00	Ca1	O15	H77	113.23
O2	Ca1	O3	85.8(2)	H76	O15	H77	109.74
O2	Ca1	O3	94.2(2)	C2	N1	C3	125.8(7)
O2	Ca1	O15	91.3(2)	C2	N1	C19	116.4(7)
O2	Ca1	O15	88.7(2)	C3	N1	C19	117.7(7)
O2	Ca1	O3	94.2(2)	C11	N2	C12	125.1(7)
O2	Ca1	O3	85.8(2)	C11	N2	C21	118.3(7)
O2	Ca1	O15	88.7(2)	C12	N2	C21	116.5(7)
O2	Ca1	O15	91.3(2)	O1	C1	O2	125.8(8)
O3	Ca1	O3	180.00	O1	C1	C4	114.7(8)
O3	Ca1	O15	91.8(2)	O2	C1	C4	119.4(9)
O3	Ca1	O15	88.2(2)	O5	C2	N1	119.2(8)
O3	Ca1	O15	88.2(2)	O5	C2	C6	124.8(8)
O3	Ca1	O15	91.8(2)	N1	C2	C6	115.9(8)
O15	Ca1	O15	180.00(1)	O6	C3	N1	120.4(8)
C1	O1	H1	123.79	O6	C3	C8	122.8(8)
Ca1	O2	C1	153.7(6)	N1	C3	C8	116.8(8)
Ca1	O3	C10	154.8(6)	C1	C4	C5	112.9(7)
C10	O4	H1	122.24	C1	C4	C9	111.0(7)
C27	O9	C28	113.8(6)	C1	C4	C27	100.5(6)
C35	O10	C36	113.2(7)	C5	C4	C9	112.2(6)
C43	O11	C44	112.9(7)	C5	C4	C27	110.0(7)
C51	O12	C52	113.3(7)	C9	C4	C27	109.5(6)
C59	O13	C60	111.0(7)	C4	C5	C6	115.1(7)
C67	O14	C68	112.2(7)	C4	C5	H2	108.39
Ca1	O15	H76	103.31	C4	C5	H3	103.42
C6	C5	H2	109.12	H4	C9	H5	105.90
C6	C5	H3	116.05	O3	C10	O4	124.7(8)
H2	C5	H3	103.95	O3	C10	C13	118.6(8)
C2	C6	C5	110.6(6)	O4	C10	C13	116.6(8)
C2	C6	C7	109.9(7)	O7	C11	N2	119.1(7)
C2	C6	C35	109.1(7)	O7	C11	C17	124.9(8)
C5	C6	C7	110.5(6)	N2	C11	C17	115.9(8)
C5	C6	C35	106.1(7)	O8	C12	N2	120.0(8)
C7	C6	C35	110.5(6)	O8	C12	C15	122.9(8)
C6	C7	C8	109.2(6)	N2	C12	C15	117.1(8)
C6	C7	H6	115.41	C10	C13	C14	113.4(7)
C6	C7	H7	111.27	C10	C13	C18	112.7(7)
C8	C7	H6	103.82	C10	C13	C51	102.6(6)
C8	C7	H7	102.50	C14	C13	C18	111.2(6)
H6	C7	H7	113.43	C14	C13	C51	108.7(6)
C3	C8	C7	110.3(7)	C18	C13	C51	107.6(7)
C3	C8	C9	108.7(6)	C13	C14	C15	114.4(6)
C3	C8	C43	107.8(7)	C13	C14	H10	112.60

Intramolecular Bond Angles for **B2b** (cont'd).

atom	atom	atom	angle	atom	atom	atom	angle
C7	C8	C9	109.6(7)	C13	C14	H11	117.91
C7	C8	C43	110.5(7)	C15	C14	H10	101.76
C9	C8	C43	109.9(7)	C15	C14	H11	99.19
C4	C9	C8	114.5(6)	H10	C14	H11	109.07
C4	C9	H4	111.09	C12	C15	C14	109.1(6)
C4	C9	H5	103.56	C12	C15	C16	110.9(7)
C8	C9	H4	113.66	C12	C15	C67	108.5(7)
C8	C9	H5	107.10	C14	C15	C16	109.9(7)
C14	C15	C67	106.9(7)	N2	C21	C20	118.9(7)
C16	C15	C67	111.5(7)	N2	C21	C22	120.1(8)
C15	C16	C17	107.8(6)	C20	C21	C22	121.0(8)
C15	C16	H12	106.12	C21	C22	C23	117.7(7)
C15	C16	H13	119.88	C21	C22	C26	123.4(8)
C17	C16	H12	111.63	C23	C22	C26	118.9(8)
C17	C16	H13	100.45	C22	C23	C24	122.8(8)
H12	C16	H13	110.88	C22	C23	H69	118.76
C11	C17	C16	110.2(7)	C24	C23	H69	118.39
C11	C17	C18	111.1(6)	C19	C24	C23	118.1(7)
C11	C17	C59	105.5(7)	C19	C24	C25	120.7(8)
C16	C17	C18	110.9(6)	C23	C24	C25	121.2(8)
C16	C17	C59	110.5(6)	C24	C25	H70	109.02
C18	C17	C59	108.5(7)	C24	C25	H71	109.26
C13	C18	C17	115.1(7)	C24	C25	H72	109.25
C13	C18	H8	114.52	H70	C25	H71	109.80
C13	C18	H9	111.31	H70	C25	H72	109.56
C17	C18	H8	102.82	H71	C25	H72	109.93
C17	C18	H9	104.82	C22	C26	H73	109.30
H8	C18	H9	107.34	C22	C26	H74	109.40
N1	C19	C20	119.4(7)	C22	C26	H75	109.31
N1	C19	C24	120.3(8)	H73	C26	H74	109.63
C20	C19	C24	120.2(8)	H73	C26	H75	109.53
C19	C20	C21	120.0(8)	H74	C26	H75	109.67
C19	C20	H68	119.71	O9	C27	C4	110.4(7)
C21	C20	H68	120.26	O9	C27	H14	109.09
O9	C27	H15	109.14	C29	C34	H22	119.72
C4	C27	H14	109.32	C33	C34	H22	120.04
C4	C27	H15	109.34	O10	C35	C6	108.4(7)
H14	C27	H15	109.51	O10	C35	H23	109.76
O9	C28	H29	112.1(7)	O10	C35	H24	109.79
O9	C28	H16	108.85	C6	C35	H23	109.63
O9	C28	H17	108.83	C6	C35	H24	109.67
C29	C28	H16	108.79	H23	C35	H24	109.59
C29	C28	H17	108.77	O10	C36	C37	115.7(8)
H16	C28	H17	109.51	O10	C36	H25	107.76

Intramolecular Bond Angles for **B2b** (cont'd).

atom	atom	atom	angle	atom	atom	atom	angle
C28	C29	C30	121.7(9)	O10	C36	H26	107.83
C28	C29	C34	120.2(9)	C37	C36	H25	107.98
C30	C29	C34	118.1(8)	C37	C36	H26	108.01
C29	C30	C31	122.4(9)	H25	C36	H26	109.44
C29	C30	H18	118.87	C36	C37	C38	124(1)
C31	C30	H18	118.69	C36	C37	C42	120(1)
C30	C31	C32	119.6(9)	C38	C37	C42	116.8(9)
C30	C31	H19	120.40	C37	C38	C39	121(1)
C32	C31	H19	120.04	C37	C38	H27	118.99
C31	C32	C33	118.4(9)	C39	C38	H27	119.67
C31	C32	H20	121.04	C38	C39	C40	121(1)
C33	C32	H20	120.52	C38	C39	H28	119.35
C32	C33	C34	121.3(9)	C40	C39	H28	119.68
C32	C33	H21	119.63	C39	C40	C41	119(1)
C34	C33	H21	119.11	C39	C40	H29	120.23
C29	C34	C33	120.2(9)	C41	C40	H29	120.72
C40	C41	C42	121(1)	C48	C47	H39	120.26
C40	C41	H30	119.67	C47	C48	C49	120(1)
C42	C41	H30	119.58	C47	C48	H38	119.73
C37	C42	C41	121(1)	C49	C48	H38	120.48
C37	C42	H31	119.31	C48	C49	C50	120(1)
C41	C42	H31	119.69	C48	C49	H37	120.38
O11	C43	C8	108.6(7)	C50	C49	H37	120.02
O11	C43	H32	109.67	C45	C50	C49	122(1)
O11	C43	H33	109.65	C45	C50	H36	119.18
C8	C43	H32	109.67	C49	C50	H36	119.31
C8	C43	H33	109.69	O12	C51	C13	108.3(7)
H32	C43	H33	109.51	O12	C51	H41	109.72
O11	C44	C45	115.2(8)	O12	C51	H42	109.82
O11	C44	H34	108.02	C13	C51	H41	109.65
O11	C44	H35	108.06	C13	C51	H42	109.73
C45	C44	H34	107.90	H41	C51	H42	109.62
C45	C44	H35	108.08	O12	C52	C53	111.0(7)
H34	C44	H35	109.45	O12	C52	H43	109.16
C44	C45	C46	120(1)	O12	C52	H44	109.18
C44	C45	C50	121(1)	C53	C52	H43	109.02
C46	C45	C50	119.1(9)	C53	C52	H44	109.02
C45	C46	C47	120(1)	H43	C52	H44	109.46
C45	C46	H40	120.12	C52	C53	C54	121.3(9)
C47	C46	H40	120.27	C52	C53	C58	119.0(8)
C46	C47	C48	120(1)	C54	C53	C58	119.6(8)
C46	C47	H39	119.33	C53	C54	C55	120.4(9)
C53	C54	H45	119.89	C60	C61	C62	121(1)
C55	C54	H45	119.67	C60	C61	C66	121(1)

Intramolecular Bond Angles for **B2b** (cont'd).

atom	atom	atom	angle	atom	atom	atom	angle
C54	C55	C56	120(1)	C62	C61	C66	117.6(9)
C54	C55	H46	120.07	C61	C62	C63	120(1)
C56	C55	H46	119.81	C61	C62	H54	119.77
C55	C56	C57	121(1)	C63	C62	H54	119.75
C55	C56	H47	119.57	C62	C63	C64	122(1)
C57	C56	H47	119.80	C62	C63	H55	119.25
C56	C57	C58	120.4(9)	C64	C63	H55	118.91
C56	C57	H48	119.74	C63	C64	C65	118(1)
C58	C57	H48	119.88	C63	C64	H56	121.22
C53	C58	C57	118.8(9)	C65	C64	H56	120.97
C53	C58	H49	120.56	C64	C65	C66	123(1)
C57	C58	H49	120.67	C64	C65	H57	118.26
O13	C59	C17	107.5(6)	C66	C65	H57	118.60
O13	C59	H50	109.86	C61	C66	C65	119(1)
O13	C59	H51	109.92	C61	C66	H58	120.45
C17	C59	H50	110.10	C65	C66	H58	120.40
C17	C59	H51	110.00	O14	C67	C15	110.5(7)
H50	C59	H51	109.42	O14	C67	H59	109.29
O13	C60	C61	110.2(8)	O14	C67	H60	109.14
O13	C60	H52	109.10	C15	C67	H59	109.21
O13	C60	H53	109.41	C15	C67	H60	109.20
C61	C60	H52	109.23	H59	C67	H60	109.52
C61	C60	H53	109.45	O14	C68	C69	112.8(8)
H52	C60	H53	109.45	O14	C68	H61	108.71
O14	C68	H62	108.77	CL2	C75	H79	108.94
C69	C68	H61	108.47	H78	C75	H79	109.48
C69	C68	H62	108.53	H61	C68	H62	109.58
C68	C69	C70	122(1)	C68	C69	C74	119(1)
C70	C69	C74	118.7(9)	C69	C70	C71	119.2(9)
C69	C70	H63	120.20	C71	C70	H63	120.59
C70	C71	C72	122(1)	C70	C71	H64	119.07
C72	C71	H64	119.19	C71	C72	C73	119(1)
C71	C72	H65	120.68	C73	C72	H65	120.66
C72	C73	C74	120(1)	C72	C73	H66	120.14
C74	C73	H66	119.70	C69	C74	C73	122(1)
C69	C74	H67	119.19	C73	C74	H67	119.27
CL1	C75	CL2	112.1(6)	CL1	C75	H78	108.64
CL1	C75	H79	108.62	CL2	C75	H78	109.01

Angles are in degrees.
Estimated standard deviations in the least significant figure are given in parentheses.

Table F6. Torsion or Conformation Angles for **B2b**.

(1)	(2)	(3)	(4)	angle	(1)	(2)	(3)	(4)	angle
CA1	O2	C1	O1	18(2)	O5	C2	C6	C5	-86(1)
CA1	O2	C1	C4	-159.3(8)	O5	C2	C6	C7	151.4(8)
CA1	O2	C1	O1	-18(2)	O5	C2	C6	C35	30(1)
CA1	O2	C1	C4	159.3(8)	O6	C3	N1	C2	-172.1(7)
CA1	O3	C10	O4	-21(2)	O6	C3	N1	C19	4(1)
CA1	O3	C10	C13	157.2(9)	O6	C3	C8	C7	-156.5(7)
CA1	O3	C10	O4	21(2)	O6	C3	C8	C9	83.3(9)
CA1	O3	C10	C13	-157.2(9)	O6	C3	C8	C43	-36(1)
O1	C1	C4	C5	32.6(9)	O7	C11	N2	C12	-175.7(7)
O1	C1	C4	C9	159.6(7)	O7	C11	N2	C21	1(1)
O1	C1	C4	C27	-84.6(8)	O7	C11	C17	C16	-149.4(8)
O2	CA1	O3	C10	25(1)	O7	C11	C17	C18	87(1)
O2	CA1	O3	C10	155(1)	O7	C11	C17	C59	-30(1)
O2	C1	C4	C5	-150.1(7)	O8	C12	N2	C11	172.6(7)
O2	C1	C4	C9	-23(1)	O8	C12	N2	C21	-4(1)
O2	C1	C4	C27	92.8(8)	O8	C12	C15	C14	-83.1(9)
O3	CA1	O2	C1	-21(1)	O8	C12	C15	C16	155.7(8)
O3	CA1	O2	C1	-159(1)	O8	C12	C15	C67	33(1)
O3	C10	C13	C14	21(1)	O9	C27	C4	C1	175.9(7)
O3	C10	C13	C18	148.4(7)	O9	C27	C4	C5	56.7(9)
O3	C10	C13	C51	-96.1(8)	O9	C27	C4	C9	-67.1(8)
O4	C10	C13	C14	-160.7(7)	O9	C28	C29	C30	-147.4(8)
O4	C10	C13	C18	-33.2(9)	O9	C28	C29	C34	32(1)
O4	C10	C13	C51	82.3(8)	O10	C35	C6	C2	58.5(8)
O5	C2	N1	C3	174.0(7)	O10	C35	C6	C5	177.8(6)
O5	C2	N1	C19	-3(1)	O10	C35	C6	C7	-62.4(8)
O10	C36	C37	C38	23(1)	N1	C2	C6	C5	91.2(8)
O10	C36	C37	C42	-158.9(9)	N1	C2	C6	C7	-31.1(9)
O11	C43	C8	C3	-60.8(8)	N1	C2	C6	C35	-152.4(7)
O11	C43	C8	C7	59.7(8)	N1	C3	C8	C7	24.4(9)
O11	C43	C8	C9	-179.2(6)	N1	C3	C8	C9	-95.7(8)
O11	C44	C45	C46	73(1)	N1	C3	C8	C43	145.2(7)
O11	C44	C45	C50	-109(1)	N1	C19	C20	C21	179.6(7)
O12	C51	C13	C10	176.3(7)	N1	C19	C24	C23	-179.8(7)
O12	C51	C13	C14	56.0(8)	N1	C19	C24	C25	3(1)
O12	C51	C13	C18	-64.6(8)	N2	C11	C17	C16	32.5(9)
O12	C52	C53	C54	-147.1(8)	N2	C11	C17	C18	-90.9(8)
O12	C52	C53	C58	34(1)	N2	C11	C17	C59	151.7(7)
O13	C59	C17	C11	179.8(6)	N2	C12	C15	C14	95.9(8)
O13	C59	C17	C16	-61.1(8)	N2	C12	C15	C16	-25(1)
O13	C59	C17	C18	60.7(8)	N2	C12	C15	C67	-148.0(7)
O13	C60	C61	C62	-99(1)	N2	C21	C20	C19	-179.8(7)
O13	C60	C61	C66	83(1)	N2	C21	C22	C23	177.7(7)

Torsion or Conformation Angles for **B2b** (cont'd).

(1)	(2)	(3)	(4)	angle	(1)	(2)	(3)	(4)	angle
O14	C67	C15	C12	69.9(8)	N2	C21	C22	C26	-4(1)
O14	C67	C15	C14	-172.5(6)	C1	C4	C5	C6	82.5(8)
O14	C67	C15	C16	-52.4(9)	C1	C4	C9	C8	-82.6(8)
O14	C68	C69	C70	10(1)	C2	N1	C3	C8	7(1)
O14	C68	C69	C74	-171.8(8)	C2	N1	C19	C20	71.9(9)
O15	CA1	O2	C1	-113(1)	C2	N1	C19	C24	-110.0(8)
O15	CA1	O2	C1	-67(1)	C2	C6	C5	C4	-69.4(9)
O15	CA1	O3	C10	116(1)	C2	C6	C7	C8	62.0(8)
O15	CA1	O3	C10	64(1)	C3	N1	C2	C6	-4(1)
C3	N1	C19	C20	-105.1(8)	C11	C17	C16	C15	-62.7(8)
C3	N1	C19	C24	73.1(9)	C11	C17	C18	C13	70.0(9)
C3	C8	C7	C6	-58.5(8)	C12	N2	C11	C17	3(1)
C3	C8	C9	C4	66.6(9)	C12	N2	C21	C20	104.0(8)
C4	C5	C6	C7	52.5(9)	C12	N2	C21	C22	-76.8(9)
C4	C5	C6	C35	172.3(6)	C12	C15	C14	C13	-65.5(9)
C4	C9	C8	C7	-54.0(9)	C12	C15	C16	C17	58.7(8)
C4	C9	C8	C43	-175.6(7)	C13	C14	C15	C16	56.3(9)
C4	C27	O9	C28	-172.2(7)	C13	C14	C15	C67	177.4(6)
C5	C4	C9	C8	44.7(9)	C13	C18	C17	C16	-52.9(9)
C5	C6	C7	C8	-60.4(8)	C13	C18	C17	C59	-174.5(6)
C6	C2	N1	C19	179.7(7)	C13	C51	O12	C52	152.9(7)
C6	C5	C4	C9	-43.8(9)	C14	C13	C18	C17	44.1(9)
C6	C5	C4	C27	-166.0(7)	C14	C15	C16	C17	-62.0(8)
C6	C7	C8	C9	61.1(8)	C15	C12	N2	C21	176.8(7)
C6	C7	C8	C43	-177.7(7)	C15	C14	C13	C18	-45.6(9)
C6	C35	O10	C36	170.4(7)	C15	C14	C13	C51	-163.9(6)
C8	C3	N1	C19	-176.4(7)	C15	C16	C17	C18	60.7(8)
C8	C7	C6	C35	-177.6(6)	C15	C16	C17	C59	-178.9(7)
C8	C9	C4	C27	167.3(7)	C15	C67	O14	C68	170.4(7)
C8	C43	O11	C44	172.8(7)	C17	C11	N2	C21	179.2(7)
C10	C13	C14	C15	82.6(8)	C17	C16	C15	C67	179.8(7)
C10	C13	C18	C17	-84.5(8)	C17	C18	C13	C51	163.1(7)
C11	N2	C12	C15	-6(1)	C17	C59	O13	C60	-179.2(8)
C11	N2	C21	C20	-73.0(9)	C19	C20	C21	C22	1(1)
C11	N2	C21	C22	106.2(8)	C19	C24	C23	C22	-1(1)
C20	C19	C24	C23	-2(1)	C43	O11	C44	C45	71(1)
C20	C19	C24	C25	-178.8(7)	C44	C45	C46	C47	179.0(9)
C20	C21	C22	C23	-3(1)	C44	C45	C50	C49	-178(1)
C20	C21	C22	C26	175.4(7)	C45	C46	C47	C48	-1(2)
C21	C20	C19	C24	1(1)	C45	C50	C49	C48	-1(2)
C21	C22	C23	C24	3(1)	C46	C45	C50	C49	1(2)
C22	C23	C24	C25	176.5(7)	C46	C47	C48	C49	1(2)
C24	C23	C22	C26	-175.6(7)	C47	C46	C45	C50	0(1)
C27	O9	C28	C29	171.9(7)	C47	C48	C49	C50	0(2)

Torsion or Conformation Angles for **B2b** (cont'd).

(1)	(2)	(3)	(4)	angle	(1)	(2)	(3)	(4)	angle
C28	C29	C30	C31	179(1)	C51	O12	C52	C53	-167.8(7)
C28	C29	C34	C33	-179.1(8)	C52	C53	C54	C55	-179.4(9)
C29	C30	C31	C32	-1(2)	C52	C53	C58	C57	179.9(9)
C29	C34	C33	C32	0(2)	C53	C54	C55	C56	1(2)
C30	C29	C34	C33	1(1)	C53	C58	C57	C56	-2(2)
C30	C31	C32	C33	1(2)	C54	C53	C58	C57	1(1)
C31	C30	C29	C34	0(1)	C54	C55	C56	C57	-2(2)
C31	C32	C33	C34	-1(2)	C55	C54	C53	C58	-1(1)
C35	O10	C36	C37	67(1)	C55	C56	C57	C58	2(2)
C36	C37	C38	C39	179(1)	C59	O13	C60	C61	174.4(8)
C36	C37	C42	C41	-177(1)	C60	C61	C62	C63	-177.4(9)
C37	C38	C39	C40	-2(2)	C60	C61	C66	C65	178.5(9)
C37	C42	C41	C40	-3(2)	C61	C62	C63	C64	-2(2)
C38	C37	C42	C41	1(2)	C61	C66	C65	C64	-1(2)
C38	C39	C40	C41	0(2)	C62	C61	C66	C65	0(1)
C39	C38	C37	C42	1(2)	C62	C63	C64	C65	1(2)
C39	C40	C41	C42	1(2)	C63	C62	C61	C66	1(1)
C63	C64	C65	C66	0(2)	C67	O14	C68	C69	-175.9(7)
C68	C69	C70	C71	179.2(9)	C68	C69	C74	C73	-178.9(9)
C69	C70	C71	C72	0(2)	C69	C74	C73	C72	-1(2)
C70	C69	C74	C73	0(1)	C70	C71	C72	C73	-1(2)
C71	C70	C69	C74	1(1)	C71	C72	C73	C74	1(2)

The sign is positive if when looking from atom 2 to atom 3 a clock-wise motion of atom 1 would superimpose it on atom 4.

4538-41